Recent Advances in Nanostructured Materials for Application as Gas Sensors

Pravas Kumar Panigrahi,* Basavaiah Chandu, and Nagaprasad Puvvada*

Read Online

ACCESS | Metrics & More | Article Recommendations

ABSTRACT: Many different industries, including the pharmaceutical, medical engineering, clinical diagnostic, public safety, and food monitoring industries, use gas sensors. The inherent qualities of nanomaterials, such as their capacity to chemically or physically adsorb gas, and their great ratio of surface to volume make them excellent candidates for use in gas sensing technology. Additionally, the nanomaterial-based gas sensors have excellent selectivity, reproducibility, durability, and cost-effectiveness. This Review article offers a summary of the research on gas sensor devices based on nanomaterials of various sizes. The numerous nanomaterial-based gas sensors, their manufacturing procedures and sensing mechanisms, and most recent advancements are all covered in detail. In addition, evaluations and comparisons of the key characteristics of gas sensing systems made from various dimensional nanomaterials were done.
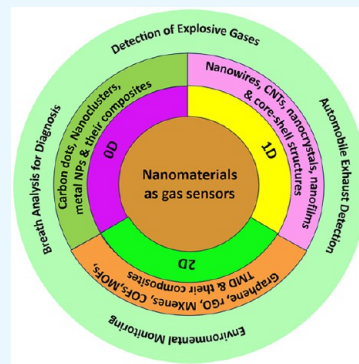
1. INTRODUCTION

The recent rise in atmospheric pollution is the result of a number of factors, such as the use of motor vehicles, population growth, industrialization, and urbanization. These elements have increased the amount of toxic, flammable, and hazardous gases released into the environment. High levels of gas emissions have a negative effect on people's social and public lives. For instance, carbon monoxide (CO) can result in fatalities,[1] and itchy eyes, respiratory problems, and even cancer can result from exposure to volatile organic compounds (VOCs).[2−4] Throat discomfort, inflammation of the eyes, fatigue, and nausea can all be brought on by exposure to too much nitrogen dioxide (NO_2).[5] Similarly, exposure to carbon dioxide (CO_2) can cause suffocation and, in extreme cases, death.[6] Hydrogen sulfide (H_2S) exposure can cause serious harm to the central nervous system (CNS).[7] Chlorine (Cl_2) can cause respiratory illnesses and even death, and other chemicals can also cause respiratory illnesses.[8] These harmful and flammable gases cause significant problems for both developing and developed countries. In order to more easily detect and alert the public to such poisonous, explosive, and volatile gases, it is imperative to develop a system. Gas sensor technology is employed to achieve this. Electronic devices called "gas sensors" are used to measure a gas' composition or concentration.[9] Monitoring and regulating these gases will raise living standards, lower health problem and mortality rates, and make workplaces safer. Numerous industries, including manufacturing, the food and beverage industry, the automobile and aerospace industries, environmental quality assessment, public safety industries, and factories, to mention a few, use gas

sensors extensively. The dimensions, sensing powers, levels of selectivity, mobility (portable and fixed), and ranges of gas sensors are all different. This is predicated on the notion that intricate physical and chemical processes can transform electrical signals by converting the content and concentration of different gases. The sensor processes the input signal—physical, chemical, or biological—using optics, conductivity, acoustics, etc. Gas sensing devices utilize various materials like metals (Pd, Pt, Ag, and Ni), semiconductors (Si, GaAs, GaN, and ZnS), ionic compounds (CaF_2, Ag_2S, and Na_2CO_3), and polymers (polyether, polyurethane, and Nafion). However, there are a number of disadvantages to these materials, including low selectivity, protracted drift, toxic exposure, and sophisticated technology. Another drawback is that interference from other gases can cause problems in complex sensing scenarios. A gas sensor should have the following qualities in order to function optimally: a long life cycle, strong selectivity, reliability, low detection boundaries, outstanding repeatability, and high sensitivity. To improve sensor performance, materials with a higher surface-to-volume ratio must be developed in order for the testing gas to interact with an active layer and affect its behavior. This has led to a great deal of interest in

nanostructured materials or nanomaterials as a methodology among the scientific community involved in gas sensing.

The development of gas detectors of the future with enhanced sensor effectiveness is possible with the development of nanotechnology, which opens up a wide range of possibilities, including low power consumption, exceptionally high sensitivity at very low gas concentrations, high accuracy, rapid reaction, large load carrier concentrations, many surface-active sites, and great reversibility at room temperature (RT).[10,11] Due to the fascinating characteristics of the nanostructured materials mentioned above, there has recently been a huge interest in researching the potential of using various nanostructures of different sizes and shapes for sensing applications.[12−14] Numerous nanostructured materials were tested and evaluated for use as sensing materials.[15−20] The surface-to-volume ratio is possibly the most important factor influencing the sensitivity of gas sensors. For nanodesigned gas sensors, the surface area for absorbing the target gas is improved, and greater efficiency is obtained than with traditional bulk-designed gas sensors.[12,21−23]

The production of effective sensors for many different applications is made possible by nanotechnology. Modern manufacturing techniques enable the miniaturization of sensors while maintaining the sensing performance of nanosized gas sensor arrays. The positions of the active surface, surface area, and electronic properties vary depending on the morphologies of the nanomaterials, which has an impact on the operation of the nanomaterial-based gas sensor.[24] Several nanomaterials have been investigated for use as gas sensing materials based on the interactions they have with the target analyte to produce certain properties. Different nanostructured variants of SnO_2,[25,26] In_2O_3,[15] ZnO,[17,27] graphene,[28−30] reduced graphene oxide,[31] Cu_2O,[18] Co_3O_4,[19] and TiO_2[20] have been studied. The nanomaterial needs to be created first with binders or solvents before it can be used to make the sensor. Following the preparation of the slurry, the sensor electrode's surface is assembled using drop-casting, screen-printing, or spin coating techniques.[32−36] Among the numerous technologies that are employed on a daily basis, nanosized gas sensors have a significant role to play in a number of ways. Some of them are as follows: Gas sensors are used to quantify and keep track of the trace gases including CO and NO_2, along with greenhouse gases, that are present when the environment is being monitored.[14,37] In the medical field, exhaled breath analysis is used for diagnostic and patient monitoring purposes.[38] The gas sensors are also useful in the food and beverage industries, managing fermentation procedures and keeping an eye on food spoilage,[39] and are employed to find explosive remnants in both the military and the civilian security fields.[12,40] The gas sensor is also needed for the home that can detect combustible gases, liquefied petroleum gas (LPG) leaks,[41] humidity, smoke, and CO in heating and cooking appliances. In factories and warehouses, gas sensors are used to sound an alarm if there is a gas leak. By using gas sensors, it is possible to detect toxic gases like NO_x, O_2, SO_2, O_3, hydrocarbons, or CO_2 in exhaust for environmental protection while keeping track of the amount of oxygen in fuel mixtures used in engines in the automotive and aerospace industries.[42] For the sake of everyone's safety, toxic and flammable gas detection is essential.[43]

The nanostructured materials were recently found to exhibit superior gas sensing capabilities comparable to their bulk counterparts. The size and properties of nanostructures used in gas sensors have a significant impact on their performance, influencing sensitivity, selectivity, and other sensing parameters. The size reduction from microscale to nanoscale rapidly enhances the active surface area of sensors and henceforth the performance. Smaller nanostructures often have a higher surface-to-volume ratio, which can enhance their sensitivity to gas molecules.[44] Nanomaterials can be divided into four groups based on their dimensions, including zero-dimensional (0D) nanomaterials (nanoparticles), one-dimensional (1D) nanomaterials (nanorods, nanotubes, and nanowires), two-dimensional (2D) nanomaterials (nanosheets), and three-dimensional (3D) nanomaterials (nanocrystals). The dimensions have been found to have an impact on the sensing behavior of the nanomaterial-based gas sensor. In contrast to 1D nanomaterials, which allow for the delocalization of electrons, 2D nanomaterials keep their electrons inside. Additionally, the electrons delocalize along the nanomaterial's axis, as opposed to 2D nanomaterials, which conduct electrons across their thickness.[45] Despite the homogeneity of the surfaces in all dimensions, this results in the development of an electron depletion region on the nanomaterials.[46] Metal oxides like ZnO[44] and TiO_2[47] exhibit varied gas-sensing performance based on their nanostructure dimensions and properties. The morphology and structure of nanostructures also play a crucial role in the performance of oxide-based gas sensors.[48] Using strategic synthesis routes, it is possible to modify the size, morphology and crystallographic structures of nanostructures and thereby enhance the sensor's response. In fact, comprehensive analyses of the synthesis and size of nanomaterials, such as ZnO,[44] TiO_2,[47] and metal oxide nanostructures in general,[49] are available in the literature. It is known that resistive components provide an elevated sensor response, vertical devices (such as a metal−insulator−semiconductor and a metal−insulator−metal) enable rapid response, and thin-film transistors (TFTs) devices can effectively sense at room temperature.[48] Capacitive sensors exhibit heightened selectivity for particular gases depending on the operating frequency. To expedite the recovery issues linked with room temperature, sensing using TFT technology, frequent UV exposure, or light irradiation can be employed. The performance of gas sensors can also be improved through modification with metal materials, electron sensitization, and chemical sensitization, especially in the case of metal oxide−semiconductor (MOS) gas sensors.[50] Comprehending the correlation between the structure and performance of gas sensors, it is vital for fine-tuning their design and functionality to suit specific applications. Nanostructured materials, like hierarchical ZnO structures, have exhibited enhanced gas sensing capabilities owing to their extensive surface area and reactivity.[51,52] Furthermore, the selection of materials plays a pivotal role in determining sensitivity and selectivity. Metal oxide semiconductor sensors are frequently employed and possess distinctive parameters that impact their performance.[53] Gas sensors featuring high aspect ratio configurations, such as nanowires, can bolster the detection of particular gases at room temperature.[54] Gas sensors operate on the principle of adsorption between semiconductor materials and gas molecules, and comprehending this mechanism can lead to performance enhancements.[55] The electronic structure of sensor materials, encompassing the energy levels of conjugated materials, can closely correlate with sensor performance.[56] Again, employing fractal geometry in the design of gas sensors at both the macroscale and the microscale can augment their
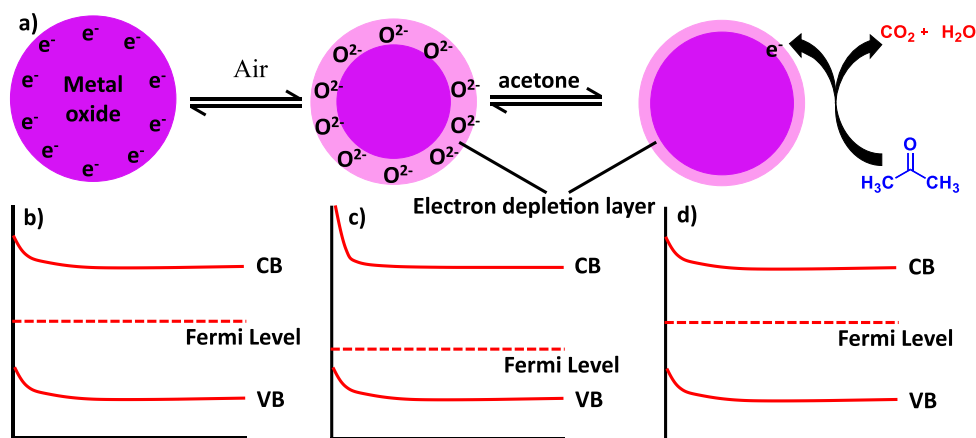
Figure 1. (a) Mechanistic representation of acetone sensing by a metal oxide gas sensor. (b) Initial electronic levels. Changes in the electronic levels of MOS upon exposure to (c) oxygen and (d) target gases.

performance.[57] Therefore, in this report the discussion is mainly focused on the gas sensing performances of various types of surface modified/functionalized nanomaterials or their composites.
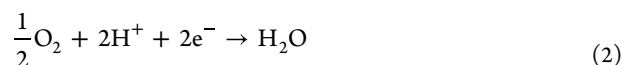
2. MECHANISMS OF GAS SENSING

The mechanism of sensing target gas molecules by nanomaterial-based gas sensors is different depending on the type of sensor materials and the nature of the target gas. A brief summary of some of the mechanisms, including catalytic combustion, thermal and electrical conductivity, electrochemical, and optical gas sensing mechanisms, is given in this section.

2.1. Catalytic Combustion Mechanism. The catalytic combustion mechanism is based on the principle that the combustible gas mixtures, on contact with a specific chemical, start burning even at low temperatures and produce heat. For almost a century, this approach has been used in sensors to identify flammable gases. In 1923, Jones discovered the first kind of sensor based on catalytic combustion to detect methane in mines.[58] A Wheatstone bridge is used in this type of sensing mechanism. The heat generated due to combustion increases the temperature as well as the resistance of the coil in the Wheatstone bridge and thereby disturbs its voltage, giving a signal corresponding to the concentration of gas.[59] Here, the sensing material acts as a heater. Although this gas sensing technology is simple and inexpensive, measuring the flammability of gases, it needs oxygen for its operation and may get poisoned by the presence of substances like Si, Pb, and Cl_2.

2.2. Thermal Conductivity Mechanism. The sensor compares the target gas's thermal conductivity to air in order to calculate the amount of heat lost from a body with a higher temperature to one with a lower temperature. Gases with higher thermal conductivities than air (like H_2 and CH_4) can usually be detected using the sensors involving a thermal conductivity measurement mechanism. This method of sensing is not useful for detecting the gases like NH_3, CO, CO_2, butane, etc., which have thermal conductivities close to or lower than air. This method is inexpensive and involves simple and strong construction with wide range of measurement at RT. However, its main drawbacks include possible reaction due to wire heating and its sensitivity toward humidity and temperature.[59]

2.3. Electrochemical Mechanism. The sensor involving an electrochemical mechanism is based on the working principle of measuring an electric current produced in the electrochemical cell containing a sensing electrode and a counter electrode. The target gas, after diffusing across a porous membrane, get oxidized or reduced at the surface of the detecting electrode, and the electrical signal generated in the electrochemical cell is in a direct proportion to the concentration of the gas. As a result of this electrochemical reaction, flow of current between the electrodes take place.[59] For instance, in detecting hydrogen gas, hydrogen is allowed to undergo the oxidation reaction at the anode (sensing electrode), and a simultaneous reduction reaction involving oxygen takes place at the other electrode, as per eqs 1 and 2.

$$H_2 \rightarrow 2H^+ + 2e^- \tag{1}$$

$$\frac{1}{2}O_2 + 2H^+ + 2e^- \rightarrow H_2O \tag{2}$$

This method of gas sensing can be used for detection of a wide range of gases, including toxic gases, even at low concentrations, but it needs modern techniques for monitoring.

2.4. Optical Sensing Mechanism. The light absorption/emission and scattering behaviors of different gases are different. This variation in the optical properties is utilized in gas sensors involving an optical sensing mechanism. Light-emitting, photodetecting, and gas-sensing components are all present in this kind of sensor, which responds to light including phosphorescence and fluorescence and convert it into electrical signals. Here a gas is detected based on the concentration proportionated signal resulting from its specific optical property.[60] The approach generally makes use of optical fibers coated with small layers of palladium or chemochromic oxides as sensors. These materials are easy to employ in an oxygen-free environment and are not affected by electromagnetic interference, but they are affected by surrounding light.[59]

2.5. Electrical Conductivity/Resistivity Mechanism. This type of sensing mechanism is generally observed in case of metal oxide semiconductor (MOS) materials. The gas sensing mechanism involving MOS nanomaterials is not governed by a single, unified process. Instead, it relies on intricate interactions that transpire at the interfaces between the gas and solid phases when the target gas is adsorbed onto

the catalyst's surface. In the 1930s, scientists observed alterations in the conductance and work function of a MOS when it came into contact with gases like O_2 and CO.[61] Indeed, the adsorption/desorption model is the major gas sensing mechanism reported now-a-days. This model primarily relies on the process of chemical or physical adsorption/ desorption of gas on a material's surface, leading to a modification in resistance attributable to fluctuations in the charge carrier concentration. A general oxygen adsorption model with illustrations that explain the reactions on the sensor surface and the corresponding changes in the energy levels is depicted in Figure 1. The oxygen gas undergoes adsorption on the surface of the sensor and accepts the electrons from its conduction band to generate negatively charged oxygen species, as presented in eqs 4−6, and an electron depletion layer is created on the surface of the sensor material, as presented in Figure 1a.[61] This electron depletion layer increases the resistance in the case of an n-type MOS sensor, such as ZnO, TiO_2, or SnO_2 (Figure 2a). When this
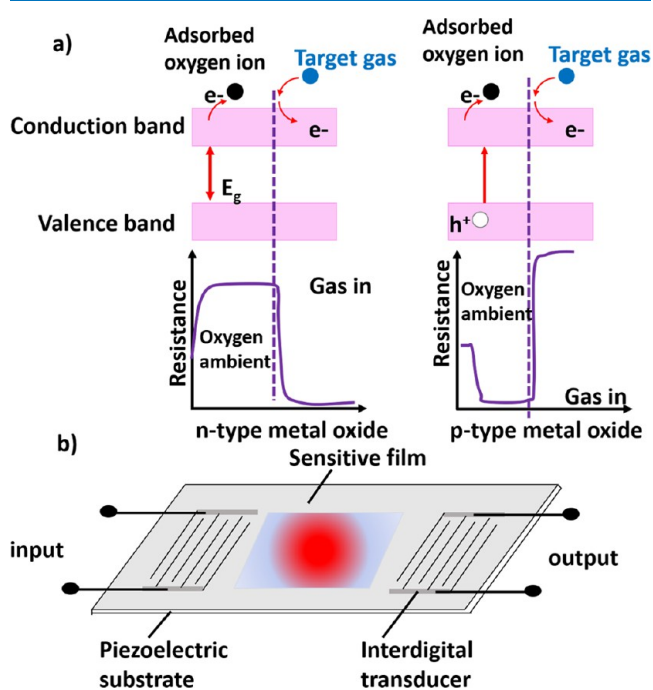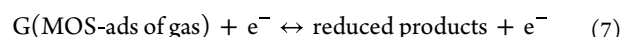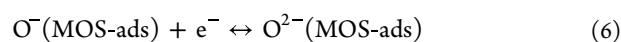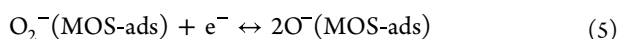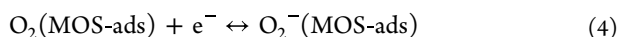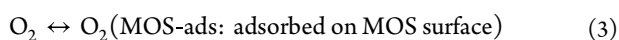

Figure 2. (a) Schematic illustration of resistance changes in the MOS sensors (n-type and p-type) in the presence of oxygen (air) and the target gas. (b) Schematic representation of gas sensing principle of a SAW device.

surface is exposed to target gas, the later undergoes a redox reaction with oxygen anions, and the electrons are given back to the conduction band. As a consequence, the electron depletion layer shrinks and the resistance decreases. Interestingly, the resistance of the p-type MOS sensor (such as NiO or CoO) decreases during the adsorption of oxygen and increases after the exposure to the target gas, exactly the reverse process compared to the n-type MOS sensor (Figure 2a).

$$O_2 \leftrightarrow O_2 \text{(MOS-ads: adsorbed on MOS surface)} \quad (3)$$

$$O_2\text{(MOS-ads)} + e^- \leftrightarrow O_2^-\text{(MOS-ads)} \quad (4)$$

$$O_2^-\text{(MOS-ads)} + e^- \leftrightarrow 2O^-\text{(MOS-ads)} \quad (5)$$

$$O^-\text{(MOS-ads)} + e^- \leftrightarrow O^{2-}\text{(MOS-ads)} \quad (6)$$

$$G\text{(MOS-ads of gas)} + e^- \leftrightarrow \text{reduced products} + e^- \quad (7)$$

The changes in the electronic energy levels due to the adsorption of oxygen and target gases on the MOS sensor surface are presented in Figure 1b−d. The Fermi level shifts to lower energy, and the conduction band bends upward due to the initial adsorption of oxygen gas, thus causing an increase in the resistance. Upon the adsorption of the target gas, electrons are given back to the conduction band and hence the electron depletion layer gets reduced. As a consequence, the conduction band and Fermi level revert back to their original positions, decreasing the resistance. The sensors with this type of mechanism exhibits quick response and recovery time and remain unaffected under a highly humid atmosphere. However, they are affected by the presence of contaminants and need high operating temperatures.

2.6. Surface Acoustic Wave (SAW) Sensing Mechanism. SAW is based on the principle of transduction, employing an interdigitated transducer that makes advantage of the piezoelectric effect to transform an electrical signal input into a mechanical wave and back again into an electrical signal. The target gas is selectively adsorbed onto a thin polymer to enable gas detection. Due to the adsorption of gas, there is an increase in the mass, resulting in an alteration in the electrical signal (Figure 2b). A sensor involving this method could be used for wireless applications and exhibits good response time. However, during its fabrication, it has handling difficulties due to its miniature size.[62,63]

3. GAS SENSORS BASED ON ZERO-DIMENSIONAL NANOMATERIALS

3.1. Gas Sensors Based on Carbon Dots. The advantages of carbon dots (CDs) include their exceptional optical qualities, high degree of water solubility, minimal toxicity, environmental friendliness, variety of raw materials, sources, low price, and excellent biocompatibility.[64] CDs, a 0D carbonaceous nanomaterial, have a number of peculiar properties, including high conductivity, a high number of functional groups, a large number of edges, and a quantum size. They are the perfect component for a gas sensor, because they significantly influence the growth of the nanofield, which enhances the gas sensing efficiency. Using a green one-pot technique, Hu et al. created reduced graphene oxide−carbon dots (rGO-CDs) hybrid materials, where tiny particles of carbon dots are produced on the surfaces while reducing GO.[65] The schematic of the synthesis method and TEM micrographs of GO and rGO-CDs are shown in Figure 3. The detection of gases by rGO is significantly improved by the addition of CDs. Composite structures are able to sense even an extremely low amount of NO_2 (10 ppb) at RT. After being exposed, the rGO-CDs that had been made displayed excellent levels of selectivity, sensitivity, stability, and reproducibility for NO_2 gas at RT. The tremendous improvements in rGO's capacity to sense gases can be attributed to the inclusion of CDs and the creation of an all-carbon nanoheterojunction. The addition of CDs to rGO, which results in a higher hole density on the rGO surface with just minor nitrogen defects promoting significant charge transfer, has been suggested as the cause for its enhanced gas sensing characteristics. The sensor performs better in terms of sensing when compared to the recognition of bare rGO. The production of chemically adsorbed oxygen
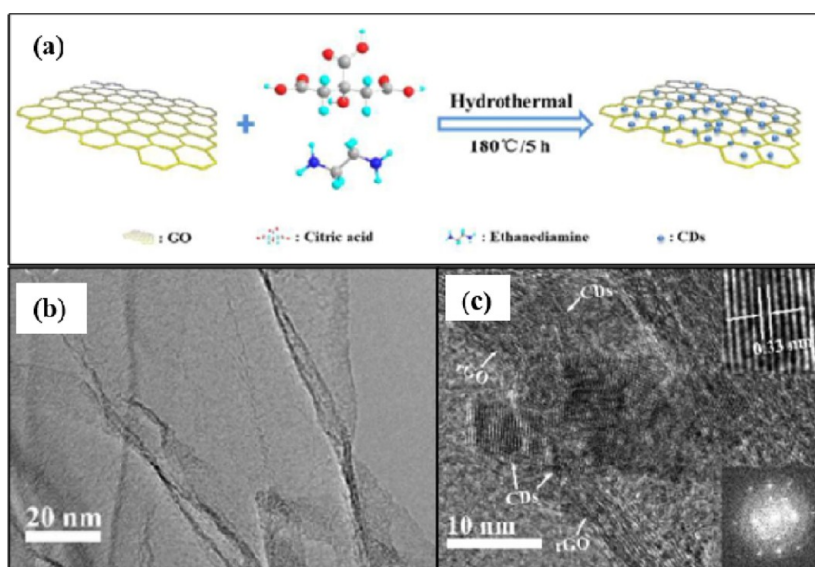
Figure 3. (a) Schematic representation of the synthesis of rGO-CDs hybrids, (b) TEM image of GO, and (c) HRTEM images of rGO-CDs. Reproduced with permission from ref 65. Copyright 2017 Royal Society of Chemistry.
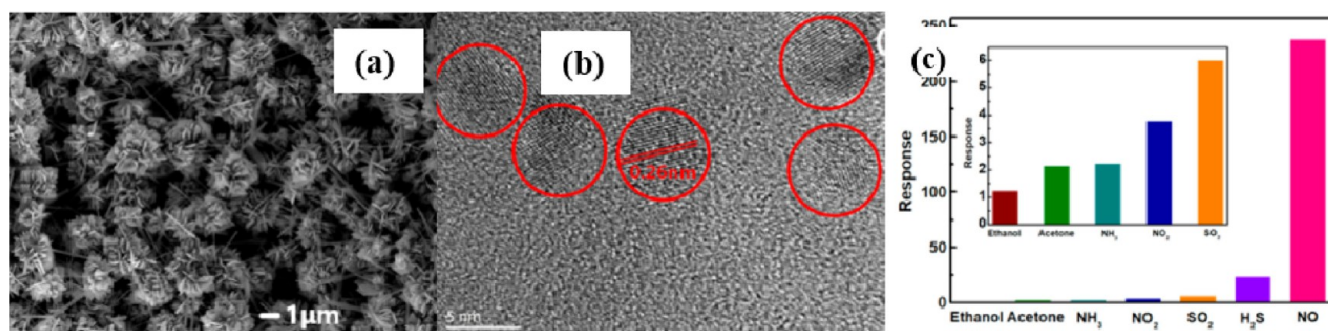

Figure 4. (a) SEM image of ZnO microspheres. (b) TEM images of the CDs. (c) Representative graph indicating the selectivity of the ZnO/CDs (1 equiv) composite toward 100 ppm of different gases. Reproduced with permission from ref 70. Copyright 2020 MDPI.

species, such as O_2^-, O^{2-}, and O^-, might occur as a result of the adsorbed oxygen molecules on the sensor drawing electrons from the semiconductor when exposed to air. This causes the rGO-CDs' surface to develop a depletion layer. On contact with NO_2 gas, its selective adsorption occurs on the numerous active sites available at the grain boundaries and the all-carbon nanoscale interfaces of the rGO-CDs hybrid material.[66] Charge transmission is considerably accelerated in the depletion layer of nanomaterials by the existence of all-carbon nanoheterostructures and a modest degree of N-doping. The very intense interface electron exchange of the sensor with NO_2 gas due to its lone pair electrons will result in dramatic changes in the sensor's resistance. The electrical properties of the system are impacted by each of these factors and significantly improve the sensor's sensitivity.

The focus of Cheng Ming's investigation is carbon dot-based gas sensors. He employed a straightforward green hydrothermal technique, followed by annealing treatment, to synthesize uniform and hierarchical In_2O_3/carbon-like nanospheres and investigated their gas detection capabilities.[67] In this method, gas sensors are produced by utilizing the excellent properties of In_2O_3. Oxygen molecules will stick to the surface of indium oxide (In_2O_3) when it comes into contact with air. This adhesion causes the oxygen molecules to grab electrons in the indium oxide conduction band, resulting in chemically

adsorbed oxygen species (O^{2-}). An electron depletion layer forms as a result of this action close to the In_2O_3 surface, thereby reducing the electron concentration and increasing the resistance. When in contact with oxidized gases like NO_2, NO_2^- species will be formed by obtaining electrons from In_2O_3, causing the resistance to increase. After combining with the CDs, the resultant In_2O_3−CDs hybrid materials become excellent NO_2 gas sensors compared to pristine In_2O_3. The creation of an In_2O_3−CDs heterojunction, which results in electron transport from In_2O_3 to CDs, is responsible for the increased sensing capability of this hybrid nanostructured material. The electron depletion layer enlarges as a result, increasing the resistance. In addition, the introduction of carbon dots provides a highly active surface effect that facilitates the adsorption of oxygen and NO_2 gas, accelerating the reaction and enhancing the gas sensing ability. The actual nuclear charge decreases due to the shielding effect caused by the addition of CDs. As a result, the NO_2 molecules will absorb the released electrons easily and enhance the sensing capability. The proportion of oxygen vacancies (O_v) and adsorbed oxygen (O_s) in In_2O_3−CDs hybrid also increases with the addition of CDs. Increases in the O_s percentage are essential for enhancing sensing, because surface adsorbed oxygen has high activity. The higher percentage of O_v in the crystal structure can increase the number of free electrons for
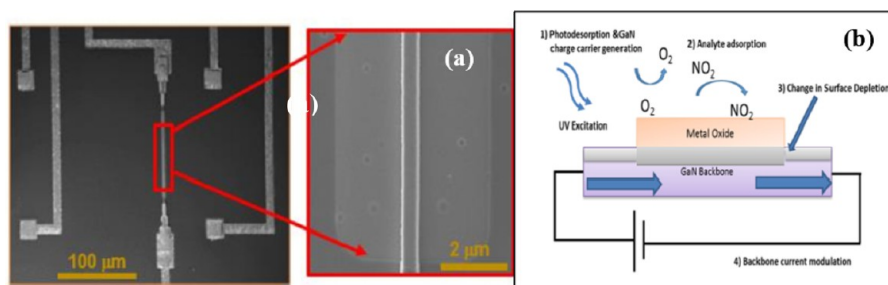
Figure 5. (a) FESEM image of the TiO_2/GaN sensor device with a top view of the GaN sub-micrometer wire (zoomed). (b) Schematic diagram (not to scale) to describe the gas sensing mechanism using GaN-TiO_2 nanoclusters toward the detection of NO_2 under UV excitation. Reproduced with permission from ref 71. Copyright 2020 IOP Publishing.

the interaction of adsorbed oxygen with NO_2 gas, improving the performance of the sensing system.[68,69] Thus, the gas sensor's distinct structure and properties enable it to significantly enhance its sensing efficiency.

Yu et al. investigated the hydrothermal method for synthesizing ZnO and carbon dots (CDs).[70] He doped the CDs into the ZnO using a grinding technique to create ZnO/CDs composites. The enormous surface area of ZnO for the adsorption of gases may be discovered by analyses employing optical sheet diffraction and scanning electron microscopy (SEM) (Figure 4a and b). High gas sensitivity is demonstrated by the ZnO/CDs combination in contrast to ZnO microspheres. The ZnO/CDs composite sensor's high NO response is revealed by the gas sensitivity test (Figure 4c). In contrast to conventional techniques, ZnO/CDs composites react with NO much more quickly, and the NO is significantly influenced by the active functional groups of the CDs. The main distinction of this work is that doping CDs into ZnO has considerable influence on the greater gas responsiveness of NO gas. One distinguishing characteristic of NO gas is the spontaneous formation of free radicals. Active functional groups bind to CD surfaces by taking up free electrons in the composites' ZnO conduction band. Therefore, when the concentration of the carrier increases, the material's conductivity similarly decreases. The measured resistance value increases, indicating an enhancement in the ZnO/CDs composite's gas sensing response. The inclusion of CDs in the composite alerts the gas adsorption process and the solid-phase contact reaction undergoes an electron transfer more frequently. Large surfaces can test more target gas molecules and adsorb more oxygen molecules, as in the case of materials with porous micromorphologies. The improved gas sensing reaction will result from the increased surface contact. ZnO/CDs composites can interact with NO gases more intensely because their sheet assemblies are in the shape of microspheres and have large specific surface areas. With more NO gas-sensing reaction sites made available by the various functional groups on CDs in the composite, this technique can increase the material's gas sensitivity and boost the effectiveness of the gas sensor.

3.2. Gas Sensors Based on Nanoclusters. In the field of nanotechnology, nanoclusters have recently emerged as a novel material. Since gold nanoclusters are thought to be the most typical representative of metal nanoclusters and have received the most attention, researchers have become increasingly interested in them. Using organic molecules as templates, molecular aggregates exhibiting fluorescence characteristics are called gold nanoclusters. They can distinguish between particular energy levels and have a size similar to a Fermi wavelength. As a result, when excited at a particular

wavelength, they release fluorescence. Gold nanoclusters are superior materials for gas sensors compared to conventional luminous materials like organic fluorescent dyes and nanoparticles because of their straightforward fabrication processes and distinctive physicochemical characteristics. Because of their many beneficial properties, including excellent biocompatibility, light-induced and light-stabilized fluorescence, and superior sensing performance, nanoclusters have made significant progress in the study and production of gas sensors.

In order to functionalize GaN submicrometer wires with titanium dioxide (TiO_2), Khan et al. investigated a very sensitive and specific technique for detecting NO_2. The authors used nanoclusters and a top-down method to fabricate dual-terminal GaN/TiO_2 sensor devices. The FESEM image of the cross section of the devise is shown in Figure 5a. The sensor's ability to function at RT is made possible by gas sensing.[71] After the study, it was discovered that the sensor was highly selective for NO_2 and capable of withstanding other obstructing agents. The sensor device performed well over an extended period of time at RT and humidity, and it is generally reliable and stable in a variety of environments. In this study, GaN sensors that were functionalized with metal oxide nanoclusters were used to detect NO_2 molecules. The sensing mechanism, as schematically represented in Figure 5b, involves the creation of surface defects, active sites, and an electron–hole pair framework on the GaN as a result of the photodesorption of water and oxygen by metal nanoclusters upon UV irradiation. Chemisorption of NO_2 molecules (analyte) at these active sites actively absorbs and releases charge carriers for alterations to the surface potential of GaN main chains, adjusting sensor currents in proportion to analyte concentrations. Chemisorption of oxygen molecules in Ti^{3+} vacancies on the TiO_2 surface creates negative charges.[72] Additionally, molecular adsorption or dissociation adsorption of water molecules on the TiO_2 cluster surfaces generates OH^- compounds at the Ti^{3+} defect sites, which have numerous advantages as sensors.[73] Clusters of TiO_2 and GaN exhibit activated electron–hole pairs when exposed to UV illumination with energy greater than the bandgap energies of these materials. The photocurrent in the GaN submicrometer wire increases because of the diffusion of photogenic holes toward the GaN surface, brought on by bending with a surface energy band and carrier lifetime. Oxygen and water molecules that have been chemisorbed on TiO_2 nanoclusters get desorbed after receiving these photogenerated holes. Due to the high electrophilicity, NO_2 is directly adsorbable on these newly created sites. On the surface of nanoclusters, certain NO_2 molecules engage in chemical reactions with chemisorbed oxygen that result in their chemical adsorption. The charge
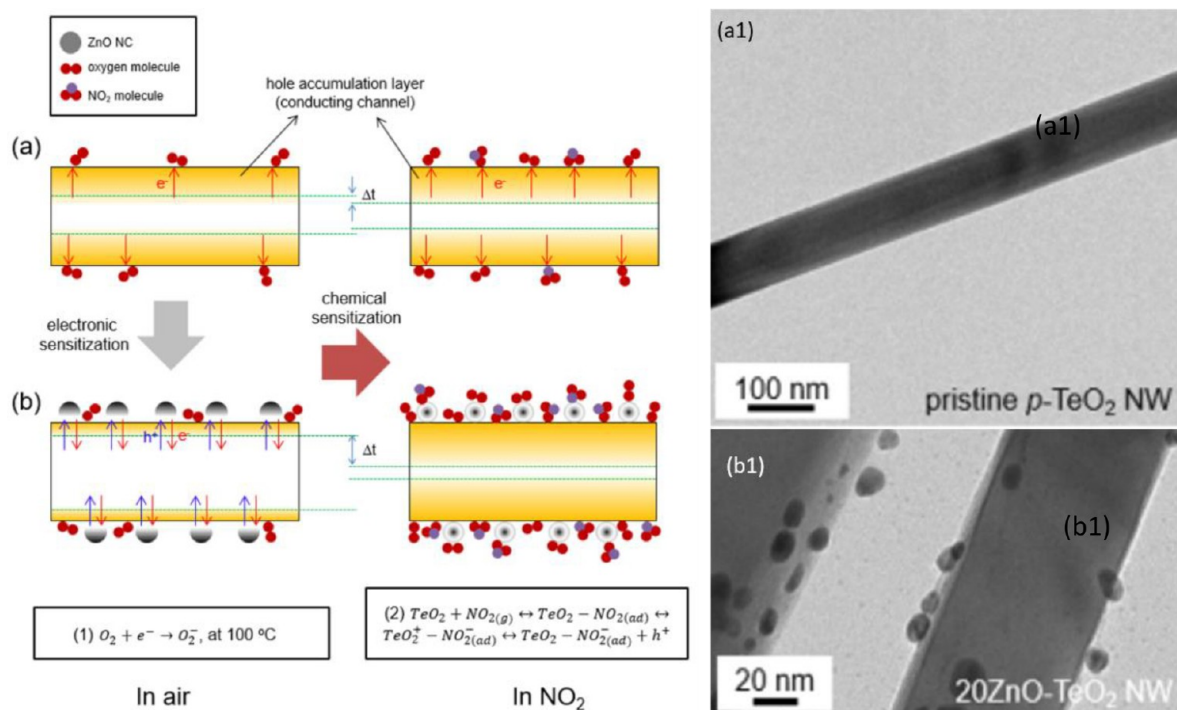
Figure 6. Schematic diagram depicting the sensing mechanism for NO_2 in (a) bare TeO_2 NWs and (b) TeO_2NWs-ZnO NCs heterostructures (a1) and (b1) TEM images of bare TeO_2 NW and TeO_2NWs-ZnO NCs, respectively. Reproduced with permission from ref 75. Copyright 2020 Elsevier.

transfer between TiO_2 nanoclusters and NO_2 molecules widens the depletion region inside the GaN, reducing the sensor's sensitivity current. High-performance NO_2 gas sensing is made possible by the regulation of the depletion area width in GaN, caused by the light-induced desorption of oxygen and the charge transfer between NO_2 molecules and TiO_2 nanoclusters.

Silver nanoclusters and phosphorene were combined in a gas nanosensor system that was studied theoretically by Wang et al.[74] The Ag_N nanoclusters ($1 \leq N \leq 13$) have different structural characteristics and can successfully slow down the breakdown of phosphorene and hypophosphorous in the catalyst. A more active adsorbent interaction, which can effectively serve an adsorption function, can significantly increase the system's selectivity and sensitivity to adsorbed molecules. Phosphorene's sensitivity can be increased by the presence of valence electrons of silver atoms, which can also control how charges are distributed among the atoms of adsorbed molecules and phosphorene. The work function changes dramatically as the amount of NO_2 molecules that adsorb on Ag_1 phosphorene increases significantly. In comparison to Ag_1 phosphorene, NO_2 adsorption also needs a higher bias voltage. The detection of NO_2 gas is then accomplished. In order to lessen the deterioration and passivation of phosphorene by metals, as well as the aggregation of silver nanoclusters, this work proposes a composite system of silver-trimmed phosphorene for gas sensing. This composite system has stronger interactions than the original system. Adjusting the adsorption energy and temperature increased the selectivity and sensitivity. The reagent used in this study is stable and has good selectivity.

This study shows that the sensitivity of all four molecules (CO, CH_4, NO, and NO_2) to Ag_1 phosphorene is considerably enhanced due to the surface alteration of phosphorene/silver nanoclusters, as the Ag atoms increase the energy difference as well as the adsorption energy. The amount of NO_2 molecules that get adsorbed, as well as the sensitivity and selectivity of NO_2 molecules, can all be boosted with Ag_1 phosphorene, making it the perfect substance for gas sensors. The fact that phosphorene is a better scattering substrate compared to MoS_2 and graphene makes this experiment exceptional. Silver nanoclusters are effectively scattered by strengthening the silver–phosphorene bond and decreasing the binding of silver–silver. In comparison to a single silver-modified phosphorene, NO_2 adsorption requires a higher bias voltage. With more Ag nanoclusters present, Ag_N nanoclusters become more responsive to the adsorption energy of four gas molecules, giving rise to a range of methods for the selective adsorption of gas molecules. Thus, the phosphorene surface's sensitivity and selection properties as a gas sensing element can be improved by adjusting the adsorption strength and electronic properties by adding silver decoration that produce new synergistic effects.

In order to detect NO_2 gas molecules, Byoun's team synthesized heterostructured nanomaterials made up of discrete n-type ZnO nanoclusters (n-ZnO NCs) and p-type TeO_2 nanowires (p-TeO_2 NWs).[75] The formation of TeO_2 NWs and its clusters with n-ZnO is confirmed by TEM study of the samples (Figure 6a1 and b1). A thorough investigation of NO_2's capabilities with respect to its response, selectivity, and operating temperature has been conducted following the atomic layer deposition and heat evaporation processes that formed these nanomaterials. The report suggests that there is great improvement in the p-TeO_2 nanowire sensor's reaction to NO_2 by combining it with discrete n-type ZnO nanoclusters. The synthesized sensors exhibit strong NO_2 selectivity when compared to SO_2, C_2H_5OH, and other interfering gases. ZnO-TeO_2 heterostructures have effective electron sensitiza-
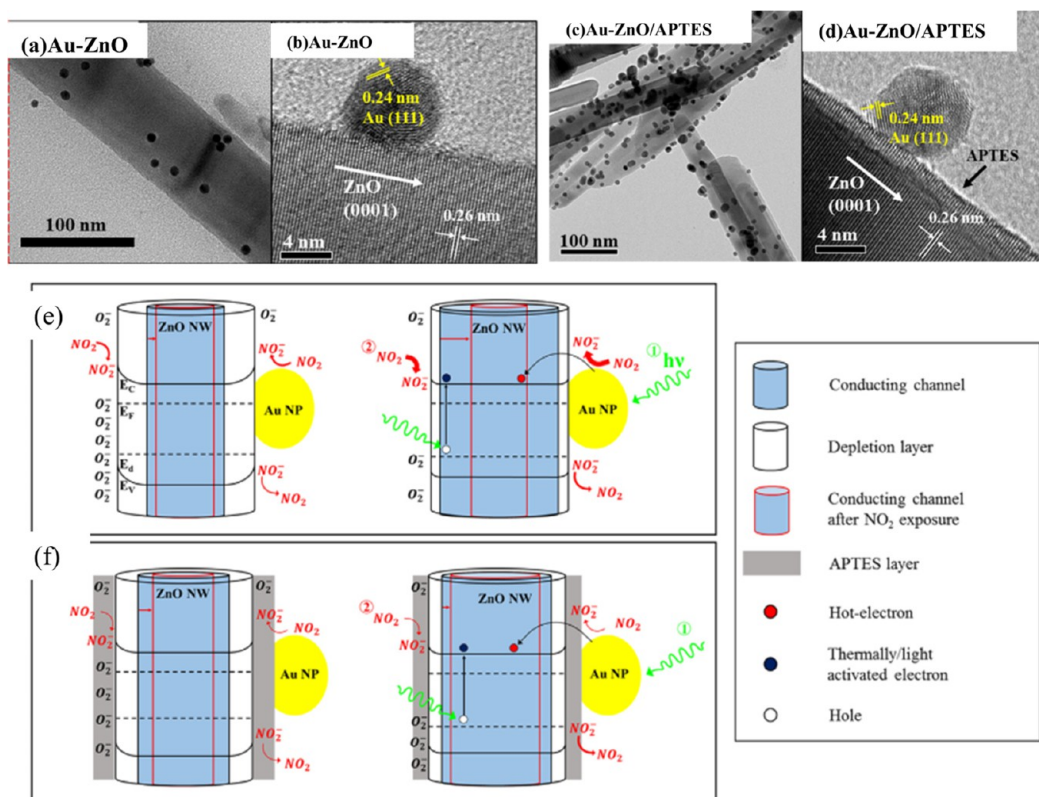
Figure 7. TEM and HRTEM images respectively for (a and b) Au−ZnO and (c and d) Au−ZnO/APTES. Schematic illustration of the sensing mechanisms for NO$_2$ gas using (e) Au−ZnO and (f) Au−ZnO/APTES in absence of any light (left) and in the presence of green light (right). The adsorption and desorption processes of NO$_2$ gas are represented by the red curved arrows, and the thick arrows and thin arrows indicate acceleration and deceleration of the processes, respectively. The intrinsic conduction (E_C), valence (E_V), and Fermi (E_F) levels are indicated by solid lines, and defect (E_d) levels are indicated by dotted lines, respectively. Reproduced with permission from ref 79. Copyright 2020 Elsevier.

tion for NO$_2$ gas detection. When n-ZnO and p-TeO$_2$ come into contact, electron flow occurs from n-ZnO to p-TeO$_2$, which is then transmitted back to n-ZnO to balance the Fermi level, which creates a barrier with band bending. In addition to improving p-TeO$_2$ nanowire resistance, oxidizing gas detection may be done with the help of heterojunction nanowires functionalized by n-ZnO nanoclusters. Because of this, oxidant adsorption and desorption cause a greater relative change in hole-accumulation layer volume than reductive gas. The surface of ZnO-TeO$_2$NW heterostructure nanocrystals can adsorb NO$_2$ molecules more easily than SO$_2$ molecules. Thus, there is a notable improvement in the response to NO$_2$. The schematic representation in Figure 6a and b describes the sensing mechanism of the bare TeO$_2$ NWs and ZnO-TeO$_2$ NW heterostructure in the presence of air as well as NO$_2$ gas. The ability to create heterostructures like p-TeO$_2$ and continuously functionalize them with n-ZnO nanoclusters by adopting atomic layer deposition and thermal evaporation methods is the main benefit of this study. Fabricated sensors outperform the original sensors in terms of their ability to detect NO$_2$. The NO$_2$ gas sensing is specifically influenced favorably by functionalizing the surface of the p-TeO$_2$ nanowires with n-ZnO nanocrystals.

3.3. Gas Sensors Based on Metal Nanoparticles. Gold nanoparticles (Au-NPs) have a tremendous amount of potential for use in gas detection technology, and this potential has long been recognized, thanks to developments in the study of nanomaterials. Nanostructured gas probes and the associated detection technology have received a lot of praise.

In recent years, gas molecule−Au−NPs hybrid systems have gained popularity and shown promising results in a number of biological analyses. Au-NPs were used to create gas sensors that could identify specific gases because of their ability to be easily prepared and biochemically modified, to have a high density, and to have a high dielectric constant. The effects of Au-NPs on CO gas sensing sensor performance were studied by Nasresfahani et al.[76] They created Au/PAni nanocomposites by ultrasound mixing the colloidal solution of Au-NP and polyaniline and thoroughly investigated the properties of polyaniline and the Au/PAni composite at RT. Additionally, using FESEM and energy dispersive X-ray (EDX) analysis, it is confirmed that the fiber surface is modified as a result of electrostatic interaction and hydrogen bonding of Au-NP with PAni. The study then examined the gas sensitivity to a limited range of carbon monoxide gases by employing different Au/PAni sensors containing various amounts of Au-NP. The Au/PAni sensor's excellent responsiveness, low noise, rapid reaction time, wide variable range, and strong stability have all been demonstrated through experiments. The sensor's selectivity and high sensing capacity are both influenced by the catalytic performance of Au-NPs. The positive charge on the carbon atom of the CO molecule is transferred to the nitrogen on the amine functional groups in PAni, increasing both the positive charge and the conductivity of polyaniline.[77] However, the sensitivity of the p-type semiconductor PAni to CO gas increased with the introduction of Au nanoparticles. Au-NPs with negative charges were deposited on the positively charged polyaniline surface to form the Au/PAni composite by

physical mixing of the two components. The produced Au/PAni sensors display superior gas detecting characteristics over a range of CO concentrations at RT because of the high surface energy of the Au-NPs, which create adsorption sites for CO gas molecules and transmit the positive charges to polyaniline.[78]

Kim et al. suggested a NO_2 gas sensor based on Au nanoparticle-modified ZnO nanowires (Au-ZnO) that is highly sensitive and quick to react.[79] The surface of ZnO nanowires (NWs) with and without a (3-aminopropyl)triethoxysilane (APTES) layer was altered with Au-NPs, as depicted by TEM images in Figure 7a−d. Because of the local surface plasmon resonance (LSPR) of the Au-NPs, the model without the APTES layer is highly sensitive to NO_2 gas. Surprisingly, compared to bare ZnO nanowires, the model without the APTES layer (i.e., Au-ZnO) exhibited a three times faster NO_2 gas response and an 86% lower response time. The APTES surface layer facilitates better Au-NP attachment, and the LSPR effect can significantly boost gas sensor performance. The absorption and desorption mechanisms for NO_2 gas response by Au-ZnO and Au-ZnO/APTES in the dark and under green light illumination is clearly illustrated by Figure 7e and f. The ZnO surface should be the only place where the NO_2^- ions suction emerges. By causing the Au-NPs to produce plasmon-mediated hot electrons, the adhesion of Au-NPs to ZnO should improve NO_2 gas adsorption when illuminated with green light. To be more precise, under green light illumination, hot electron afflux and light-stimulated electrons from defect sites of ZnO NWs cause the conducting channel of the ZnO NWs to become wider. As more electrons are added, more NO_2 gas then adsorbed on the surface of ZnO by trapping these electrons, thereby causing the depletion region to be extended and decreasing ZnO NW's electric channel. Au-ZnO consequently attained the highest improvement ratio and NO_2 gas response. Although the creation of ZnO NW holes under green illumination also improved the removal of the adsorbed NO_2 and O_2 ions, improvements were also observed in the hot electron-associated gas adsorption method. On the other hand, Au-ZnO/APTES's ability to adsorb NO_2 gas is obstructed by the APTES layer attached on the ZnO NW surface.

As evidenced by the relatively thin NO_2 arrows in Figure 7f, the APTES layer prevented NO_2 gas from adhering to the ZnO NW. In contrast, compared to the absorption process, the suction of the NO_2 gas was significantly less hampered by the APTES layer once it had been adsorbed on the ZnO NW surface of Au-ZnO/APTES. Due to the hot electron afflux and light-induced electron stimulation, Au-ZnO/APTES demonstrated a ZnO NW electric channel that widened upon exposure to green light.[80,81] However, the narrowing of ZnO NW's electric channel was less than that of the Au-ZnO case because the APTES layer's interference prevented the NO_2 gas adsorption process from being abundantly accelerated on the surface of the ZnO NW. This could explain why, despite the Au NPs' LSPR effect, the Au-ZnO/APTES response to NO_2 gas was less than that of Au-ZnO upon exposure to green light. Additionally, for all three samples (bare ZnO, Au-ZnO, and Au-ZnO/APTES) except Au-ZnO, where the LSPR effect was particularly strong, both red and green illumination accelerated the process of desorption of NO_2 gas more quickly than the process of adsorption did. The hot electron generation from the Au NPs by LSPR and the reduction in gas adsorption by

the APTES layer might therefore be the basis for the NO_2 gas sensing mechanism of the synthesized materials in this report.

In this study, Li proposed the fabrication of microgas sensors by assembling and depositing Au-NPs functionalized with 11-mercaptoundecanoic acid (MUA) between two electrodes using laser writing technology.[82] It predicted how conductivity would change in response to volatile organic compounds (VOCs) using interparticle characteristics, such as a dielectric constant. The microsensor's responses to seven different VOCs were studied. This microsensor exhibited increased sensitivity while cutting down the response time for all the VOCs analytes compared to other conventional sensors. This Au-NP-based gas sensor, however, responds more strongly to o-xylene. The larger surface-to-volume ratio, resulting from surface abrasion and device miniaturization, is proposed to be the reason for the higher response and the shorter time for the gas to precipitate. Gas sensors are becoming smaller, which increases response time and speed.[83] The sensing mechanism of this Au-NP-based microsensor is based on a particle-to-particle electron technique.[84] Unlike a metal oxide semiconductor, the gas molecules and nanoparticles do not interact chemically. The physical characteristics of the Au-NP-based sensor change when it is exposed to analytes due to the VOCs' ability to adsorb on its surface. As the polar gas molecules (VOCs) diffuse in the Au-NP-based microsensor, the dielectric constant and the distance between particles are increased accordingly, which changes the conductivity and gives rise to an appropriate signal to sense the gas.

PbS nanocrystals were the subject of research by Mosahebfard et al., and this material recently demonstrated RT gas sensing capability for a particular gas (i.e., CH_4).[85] Another typical noble metal that is added to device to enhance performance is gold. The CH_4-sensing capabilities can be enhanced by adding Au-NPs.[86] The conductivity, sensor response, and sensor speed of PbS-NCs for CH_4 sensing have all been investigated and analyzed. PbS-NCs show that the addition of the right amount of Au-NPs can improve the sensing properties for methane. The impact of Au-NPs on the electrical characteristics of PbS was investigated in this study using a variety of properties. It is possible to lower the electrical conductivity of the PbS-NCs by modifying their surface with Au-NPs, which results in higher sensing performance. The main reason is that Au-NPs have the capacity to boost the quantity of oxygen adsorbed on the PbS-NCs surface, and methane molecules find more adsorbed oxygen to interact, in comparison to pure PbS NCs, under the same environment and methane concentration.[85] Compared to the conventional method, this increases the sensor's efficiency and sensitivity. The improvement of the adsorption of oxygen onto gold can enhance the sensor's performance, which is because O_2 and CH_4 molecules are competing for the gold's attention. At low methane concentrations and a high percentage of Au-NPs on PbS NCs, methane molecules find more oxygen molecules that are adsorbed, thus causing the conduction of the PbS-NCs to vary significantly. On the contrary, at high methane concentrations and a high percentage of Au-NP on PbS NC, the interaction with the adsorbed oxygen involves an interaction between Au-NPs and CH_4 molecules. The quantity of Au-NPs on PbS NCs has an impact on the increase of the sensor's characteristics, and it is discovered that the sensor performs at its best when 1 wt % Au-NPs are added to the surface of the PbS NCs.
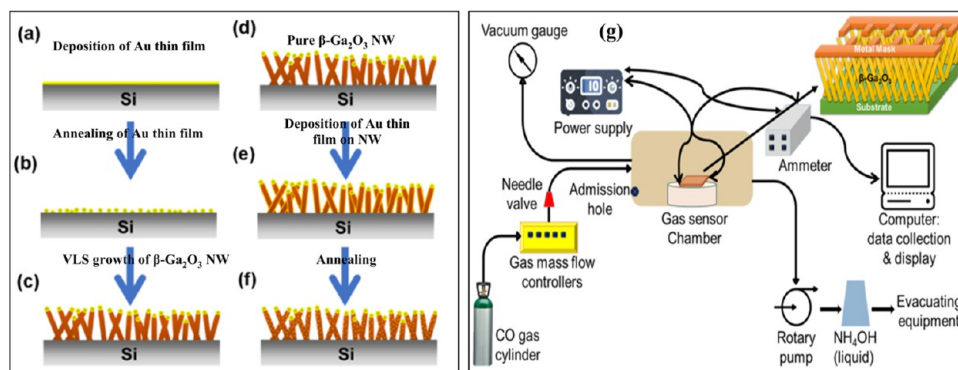
Figure 8. (a−f) Schematic representation of the growth mechanism for pure and Au decorated β-Ga$_2$O$_3$ nanowires. (g) Schematic representation of the CO gas sensing measuring unit. Reproduced with permission from ref 91. Copyright 2020 Elsevier.

4. GAS SENSOR BASED ON ONE-DIMENSIONAL NANOMATERIALS

4.1. Gas Sensors Based on Nanowire. In addition to raising production and living standards, the ongoing global industrialization process also damages the surroundings to different degrees. These last several years have seen an increase in the diversity and complexity of hazardous gas components, posing serious risks to both production safety and human health. As a result, self-defense awareness among people has increased. Therefore, it is necessary to continuously monitor potentially dangerous and toxic gases in the environment. Nanowire materials have flourished and assumed a crucial role in the market due to their benefits of great sensitivity, easy preparation, and affordability. The result has been a steady improvement in the performance of devices using a nanowire material as the carrier. By modifying the structure and morphology and investigating synergistic recombination, the sensor's performance can be improved.

Lin et al. investigated a hydrogen detection SnO$_2$ nanowire Hall effect gas sensor.[87] It generated SnO$_2$ nanowires by employing a horizontal electric furnace to produce stainless steel mesh, and the authors used XRD and XPS to determine its crystal structure, morphology, and electron binding energy. A discussion of the SnO$_2$ nanowire Hall effect gas sensor's detecting process was also included in the review. Responses to H$_2$ gas were displayed by the synthesized SnO$_2$ NW sensor at various operating temperatures and H$_2$ concentrations. In comparison to pure SnO$_2$ gas sensors, the Hall effect sensors' response characteristics are shown to be superior. The target gas sensing mechanism is related to the Hall effect principle and the reactions of adsorbed H$_2$ and O$_2$ on the surface of SnO$_2$ nanowires. As the adsorbed oxygen molecules accepted the electron from the conduction band of the SnO$_2$ nanowires, the density of electrons on the exterior surface of n-type SnO$_2$ semiconductor nanowires decreased.[88] Upon exposure to hydrogen gas, the carrier concentration increased over time. The interaction between adsorbed hydrogen and oxygen ions released electrons when water was formed; hence, the carrier concentration increased along with the increase in hydrogen concentration. The Hall voltage and Hall coefficient therefore saw a drop in their absolute values. Increases in H$_2$ gas concentration were shown to cause a further drop in Hall voltage. Therefore, this type of gas sensor has enormous potential to be used for hydrogen gas in real life applications.

In order to create highly selective and sensitive nanowire based hydrogen sensors, Cai et al. synthesized SnO$_2$ nanowires modified by Pd nanoparticles.[89] The vapor−liquid−solid method was used to prepare a SnO$_2$ nanowire, which was subsequently subjected to UV irradiation using 1 mM PdCl$_2$ solution to modify its surface with Pd nanoparticles. SnO$_2$ nanowires modified with Pd nanoparticles perform electrochemically well compared to the bare SnO$_2$ nanowires and show a range of hydrogen sensitivity as the Pd nanoparticle concentration increases. The selectivity of this nanowire-based sensor also gets better as the amount of Pd nanoparticle increases. After surface modifications with Pd nanoparticles, SnO$_2$ NWs display significantly improved hydrogen detection sensitivity, in comparison to other gases.

Another unique feature of this discovery is that, when exposed to air, oxygen from the air is adsorbed on the surface of the SnO$_2$ nanowires due to the attraction of static charge. By removing electrons from the surface of the SnO$_2$ nanowires, adsorbed oxygen is transformed into oxygen ions. As a result, the resistance increases and the nanowires' surface depletion layer grows. In the presence of hydrogen gas, hydrogen gas adsorbs on the surface of the SnO$_2$ nanowires and subsequently, reacts with the already adsorbed oxygen ions to form H$_2$O.[90] Through this reaction, oxygen ions that had taken electrons from the SnO$_2$ nanowires return to them, restoring the nanowires' surface area, resistance, and carrier concentration to their initial values. However, upon the modification of the surface of the SnO$_2$ nanowires with the Pd nanoparticle, the concentration of adsorbed oxygen and hydrogen increases significantly due to the catalytic effect of metal NPs. The initial depletion layer on the surface of the SnO$_2$ nanowires was produced as a result, which also changed the electrical band structure. The resistivity of such nanowires in a hydrogen environment was greatly decreased as a result of SnO$_2$ using electrons as electrical carriers on nanowire surfaces. Thus, in the presence of hydrogen and air, the behavior of this SnO$_2$ nanowire with respect to gas-sensing capabilities became more apparent after the modification by Pd nanoparticles.

Weng team used multinetwork arrays and single nanowire devices made up of pure β-Ga$_2$O$_3$ nanowires and nanowires that had been modified with gold to study the sensing behavior toward CO gas at RT.[91] High-density Ga$_2$O$_3$ single crystal nanowires were grown on silicon substrate using the vapor−liquid−solid growth technique. The detailed growth mechanism is depicted schematically in Figure 8a−f. Through the use of FESEM and TEM, the authors examined the morphology of the synthesized nanowires. Using the focused ion beam technique, they created single-nanowire gas sensors. With the help of the Au modification to the β-Ga$_2$O$_3$ nanowire, a single
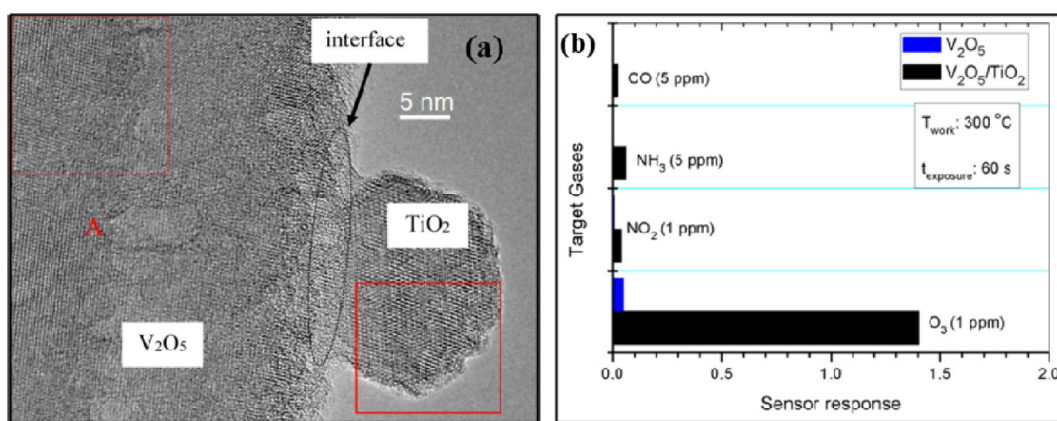
Figure 9. (a) HRTEM image of V_2O_5/TiO_2 heterostructures. (b) Comparison of responses for pristine V_2O_5 and V_2O_5/TiO_2 heterostructures exposed to various gases. Reproduced with permission from ref 94. Copyright 2019 American Chemical Society.

CO gas-detecting nanowire was proposed to detect CO gas at RT with amazing sensitivity. The purpose of this study was to determine how altered Ga_2O_3 nanowire devices performed when exposed to various gas concentrations with Au-NPs, which have improved and reliable RT gas sensing properties. Various gas sensors were used to measure the CO gas concentration and produced a range of results. In those cases, as gas concentrations fall, response and recovery times gradually get shorter and longer, respectively. The modification of the surface of the β-Ga_2O_3 nanowire with Au-NPs facilitates the availability of free electrons on β-Ga_2O_3 nanowire lattices, which subsequently enhance the electronic conduction through the formation of oxygen ions from the adsorbed oxygen molecules. Depending on how much oxygen has been deposited sensor's surface, the response and recovery time change. The performance of the sensor is also improved when there are more oxygen vacancies in the Ga_2O_3 nanowire lattices, since this causes trapped oxygen molecules to be under more pressure. It helped the CO-gas sensor via adsorption, and as the reducing agent reacts with the material's surface, the resistance drops. Increased conductivity is the result of the free electron after the reduced gas has chemically reacted with absorbed the oxygen in semiconductor. This also explains why Au-modified β-Ga_2O_3 has excellent gas sensing capabilities.[92] A schematic diagram for CO gas sensing measuring unit is shown in Figure 8g.

A ZnO/Si nanowire sensor for NO gas based on a heterojunction array with a very high response, operating at RT, was studied by Samanta et al.[93] The sensor is very selective for NO gas, and there is also little variation in the sensing response in the presence of moisture. The sensor was fabricated by combining Si nanowires and ZnO nanostructures, which were prepared by electroless etching, followed by chemical solution deposition and spin coating. Because of the synergistic effect, the heterostructures resulting from combining p-Si nanowires with n-ZnO exhibited greater sensing response than the sum of their individual contributions. One distinguishing quality of this gas sensor is its selectivity for a specific compound. In order to ascertain NO gas sensing using the ZnO/p-Si nanowire sensor, various types of gases were tested on it. High NO gas selectivity is achieved using this sensor. In addition, this ZnO/p-Si nanowire sensor's response toward the detection of gases improves, as the amount of environmental moisture decreases. A study on the changes in gas reaction at various temperatures is also included in the

review. Temperature-dependent reactions between NO gases and ZnO/Si nanowire devices are observed to increase, thereby increasing their response with temperature. The main reasons behind the high sensitivity of this device toward NO gas are the strong oxidizing nature of NO gas and the combination of p-type SiO_2 nanowires and n-type ZnO to produce a p−n heterojunction.

Avansi et al. synthesized the TiO_2 nanoparticles and V_2O_5 nanowires by the hydrothermal reaction of metal peroxide complexes and studied the chemiresistive sensing ability of the prepared V_2O_5/TiO_2 heterostructure.[94] Heterostructures are generally created by combining different nanostructured semiconductors with varying band energies. By using TEM (Figure 9a), X-ray diffraction (XRD), and X-ray photoelectron spectroscopy (XPS) measurements, the formation of V_2O_5/TiO_2 heterostructures was investigated. Compared to bare V_2O_5, this 1D V_2O_5/TiO_2 heterostructure is suggested to have good detection capabilities as well as ozone sensing qualities (Figure 9b) that are strongly correlated with repeatability and selectivity. Here, the V_2O_5/TiO_2 heterojunction that results from n-type V_2O_5 and n-type TiO_2 semiconductors exhibits a distinct electron affinity, work function, and band gap. An n−n type heterojunction is produced, which causes a change in the resistance at the interface and the formation of an energy barrier and depletion layer at the junction. When these two semiconductors reach equilibrium, electrons move from TiO_2 to the V_2O_5 semiconductor's low-energy conduction band until they have identical Fermi levels. As a result of this, bending of the band occurs at the junction, and more electron conduction bands are present in the TiO_2. The heterostructure of V_2O_5/TiO_2 exhibits a variety of kinetic curves for the sensor's response, indicating that the formation of the heterojunction results in the creation of additional active sites. Thus, the enhanced response of this V_2O_5/TiO_2 heterostructure towards ozone gas can be correlated to the synergistic effect resulting from the creation of an effective heterojunction at the biphase interface of V_2O_5 nanowires and TiO_2 nanoparticles, which alters the resistance and subsequently enhances the response to the gas.[95,96]

4.2. Gas Sensors Based on Carbon Nanotubes. The potential to create energy-efficient, extremely sensitive, affordable, and portable sensors has greatly increased with the development of nanotechnology. Emerging nanomaterials known as carbon nanotubes make excellent candidates for gas molecule adsorption due to their superior electrical con-
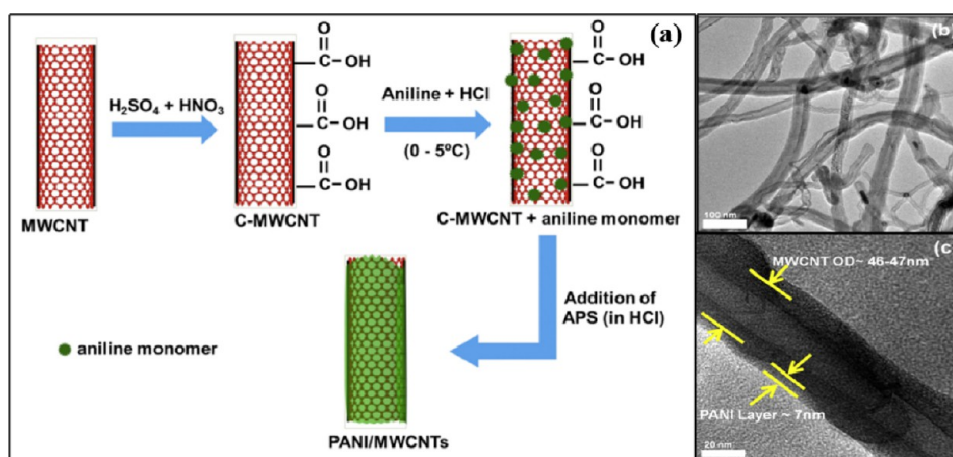
Figure 10. (a) Schematic illustration of the synthesis of polyaniline-functionalized MWCNTs. (b and c) HRTEM images of the PANI/MWCNT nanocomposite. Reproduced with permission from ref 99. Copyright 2015 Elsevier.

ductivity, substantial surface area, and distinctive hollow structure. The frequently used semiconductor metal oxide gas sensing materials often need to operate at a higher temperature and display semiconductor properties.[97] The incorporation of CNTs affects semiconductor oxides' ability to detect gases, and as a result, the obtained composite gas sensing materials have effective gas detection capabilities. Kumar et al. investigated gas sensors based on single-walled carbon nanotubes (SWCNTs) to more effectively detect one of the toxic greenhouse gases, namely NO_2.[98] In this study, a SiO_2 substrate was used to fabricate a thin-film of SWCNTs sensors via the thermal CVD method that was then functionalized with polyethylenimine (PEI). The great sensitivity of the PEI-functionalized SWCNTs to potent electron-absorbing compounds was confirmed. In comparison to SWCNT gas sensing elements, SWCNTs with PEI functionalization have a sensitivity that is almost 50% higher at RT. Over the course of the entire concentration range of the study, the gas sensor displays a recurrent response. By functionalizing PEI, SWCNT's gas sensing components perform better compared to uncoated single-walled carbon nanotubes, as PEI-coated ones have a higher NO_2 adhesion coefficient, which absorbs electrons. The chemiresistive PEI-SWCNT gas sensor performs well and reacts quickly in terms of NO_2 sensing at RT. The improved sensitivity of PEI-SWCNTs, compared to bare SWCNTs, can be attributed to the creation of additional defect sites on the surface of SWCNTs, which helps in the adsorption of more NO_2 gas molecules. The increased charge transfer between SWCNTs and PEI leads to variations in the sensor's resistance. It was possible to achieve complete sensor recovery with careful heat treatment process selection. The sensing ability of the SWCNT can be enhanced with longer functionalization times with PEI. PEI-SWCNTs sensors can be used in a variety of industries depending on the type of chemical situations they are exposed to, by adjusting the alkalinity and degree of modification of SWCNTs networks.

Abdulla et al. investigated how thin films with effective polyaniline (PAni) arrangements were created.[99] Langmuir–Blodgett (LB) technology was used to obtain highly directional arrangement of multiwalled carbon nanotubes (MWCNTs), which also enhances ammonia sensing capabilities. The coating of the PAni is carried out by polymerization process as depicted schematically in Figure 10a, and TEM analysis was done to confirm the formation of PAni/MWCNT nanocomposite (Figure 10b and c). At the gas–water interface, polyaniline-MWCNTs gradually organize into ordered small blocks during the interfacial assembly process, and they then continue to assemble into a directed, globally defined monolayer. In order to analyze the gas sensor properties, the PAni@MWCNT LB films were spin coated onto the double electrodes that had been previously cleaned with gold sputter. The p-type polyaniline's orientation and uniform coating on the surface of the MWCNTs are what allow for its great sensitivity and quick response to NH_3 at RT. In constract, the surface-functionalized polyaniline-modified MWCNTs, used in this study, have the ability to make up for surface imperfections caused by the 3D aggregation of CNTs. In addition, the thin layer of PAni coating on MWCNT enables effective NH_3 molecule adsorption by providing a high surface area and active sites. Compared to a random network, the sensitivity to ammonia is higher with this aligned assembled polyaniline-coated MWCNT sensor due to directional electron transport in the presence of NH_3 at RT.[100] Because of adequate molecular regulation, ultrathin LB membranes permit quick analyte diffusion and active sensing layer assembly.

A carbon nanotubes (CNT)-based transparent gas sensor was studied by Loghin et al. for the detection of NH_3 and CO.[101] Using the spray deposition technique, a CNT-based electrode and sensing layer were created. The sensing properties of NH_3 and CO_2 have been investigated using transparent sensor electrodes with high transmittance (>60%), and the results have been compared against a reference sensor that was created with the same sensing layer but an evaporated gold electrode. Both the transparent sensor and the reference sensor exhibited the same response for NH_3. However, in comparison to the reference electrode, the transparent sensor device was found to be more sensitive to CO_2. The study also indicated that the spacing between consecutive electrodes affects the sensitivity of the sensors. A transparent sensor with wider spacing between electrodes exhibits enhanced sensitivity due to its higher sensing resistance, whereas reference electrodes did not exhibit this effect due to their minimal resistance in comparison to CNTs. However, this study uses an electrode distance that is larger, which will have an impact on the sensor's overall resistance and enhance the performance of the translucent CO_2 sensor significantly. The sensor's sensitivity is greater at higher concentrations for transparent

sensors than for the reference gold gas sensor.[102] This better sensitivity effect of the fully-CNT gas sensor can be attributed to the varied network densities. Again, CO_2 can significantly alter electrode resistance at higher concentrations, which increases distance-insensitive normalized resistance and enhances gas sensitivity. Thus, the transparent sensors perform better than other sensors, proving they have effective transparent gas sensing properties.

Rong et al. created high-performance acetone gas sensors made up of molecularly imprinted polymers of $Ag-LaFeO_3$, (ALFOMIPs) and multiwalled CNTs through the microwave-assisted sol−gel process.[103] Additionally, they investigated the functional groups, particle size, and surface morphology of synthesized materials using a variety of techniques, along with their responses to various sample gases. Through testing and analysis using acetone gas sensing, the CNT and ALFOMIP nanocomposites (CNT/ALFOMIP) were found to have greater thermal stability than the reactions of the ALFOMIPs models. The molecular imprinting process has provided the sensor with improved acetone vapor selectivity and sensing performance, which allows it to respond strongly to acetone at a range of temperatures. The change in electrical resistance of the CNT/ALFOMIP sensor can be correlated to the adsorption−desorption of the gases.[104] When CNT/ALFO-MIP gas-sensitive materials are exposed to air, oxygen atoms are chemisorbed and physically adsorbed on the surfaces of the sensors. Once the adsorbed O_2 molecules were transformed into different oxygen anions, depletion layers close to the sensor surface formed, causing the electron density to decrease and the sensor resistance to increase. On contact with acetone, the oxygen is chemically adsorbed onto the surface by evaporating in acetone, and the gas-sensitive CNT/ALFOMIP material lets go of its free electrons, which enter the conduction band. The electrical resistance of the CNTs is thus found to have significantly decreased. The CNTs are good conductors of electricity, and the presence of so many surface functional groups like −COOH or −OH can reduce the sensor's resistance. The operating temperature of CNT/ALFOMIP composites is low, and their response time is quick. The formation of a p−p homojunction between CNTs and metal ALFOMIP further increases the sensor's gas sensitivity to acetone vapor.

Struzzi et al. looked into how electronic properties could be altered on the surface of the film containing vertically aligned and randomly distributed CNTs.[105] They also optimized the sensing properties of these materials using the hydrophobic characteristics of CNTs after exposing them to plasmas of $Ar:F_2$, and CF_4. The resilience and sensitivity of these so-obtained fluorinated CNTs toward two chosen pollutants, namely NO_2 and NH_3, were investigated thoroughly. When a vertical carbon nanotube (vCNT) is used after fluorination to increase the surface hydrophobicity, it is possible to enhance the sensor's response and reproducibility toward NH_3, although fluorination does not change the high responsiveness toward NO_2. The higher sensitivity for NH_3 gas can be attributed to the higher degree of interactions of NH_3 with the fluorinated surface of CNTs due to hydrogen bond formation. This interaction facilitates the charge transfer process in the fluorinated CNT sensor.[106] Moreover, compared to randomly distributed CNT film, the improved sensing property of the vCNTs can be attributed to the significant role played by the tips of the vCNTs.

4.3. Gas Sensors Based on Other One-Dimensional Materials.
Yang et al. investigated a novel carbyne nanocrystalline system used in a visible-light-driven RT gas sensor. The carbyne nanocrystals (CNCs), synthesized by the laser ablation in liquid (LBL) method, were seen to be stacked flakes composed of rod-like crystals.[107] When exposed to light with a wavelength 447 nm, a CNC sensor can detect NO_2 molecules at concentrations as low as 2 ppb with a response and recovery time of under 100 s. It explained that the fluorescence emission of CNCs was what caused the light-driven sensing. The stability and selectivity of the device were found to be outstanding. In comparison to other gases, NO_2 molecules have high adsorption energy on the surface of CNCs, which enables highly sensitive NO_2 gas detection. When light with a suitable amount of energy (447 nm) is absorbed, the sensing process includes the creation of many electron−hole pairs in CNCs. In the presence of gold, Au-CNC Schottky junctions were created at RT due to the CNCs' lower work function compared to gold. As a result, electron transfer occurs from CNCs to Au, causing the development of an interface-proximate depletion zone. In the presence of NO_2 gas, chemisorption of the gas takes place by accepting these electrons to form NO_2^- ions. As the NO_2^- adsorption is not dissociated and is not influenced by thermal energy, the energy barrier height is the sole variable that influences the adsorption activation energy of NO_2. The CNCs have a greater adsorption energy barrier height, which decreases with the addition of Au at the Au-CNC Schottky junctions, thereby facilitating the adsorption of NO_2^- ions.[108,109] In addition, the energy barrier height of the photogenerated electrons from the bottom conduction band of the CNCs to NO_2 molecules is reduced in the presence of Au-NPs. Therefore, preferential adsorption of NO_2^- occurs at the Au-CNCs Schottky contacts. This behavior results in an increase in device resistance and a widening of the depletion region. In a dark nitrogen atmosphere, the gas exhibits high sensor resistance due to a small number of thin layer of electron−hole pairs on its exterior, and a high barrier height of the CNCs. These results demonstrate the capability of this gas sensor as a visible light driven NO_2 gas sensor at RT.

Pytlicek et al. examined sputtered-deposited anodized Nb_2O_5 nanocrystalline films on a silicon dioxide-coated Si wafer for the detection of gases.[110] The Nb_2O_5 nanorods are kept upright by the niobium layers in the nanofilm. Two types of nanofilms were prepared. A sophisticated 3D structure with a silicon chip with a multilayer structure and 33 microsensors was created using each of the films. In order to construct a Pt/NiCr top electrode and a multifunctional SiO_2 sandwich on a silicon wafer by etching, laser dicing, and ultrasonic wire-bonding, it was necessary to combine procedures of high temperature vacuum or air annealing, sputtering, and stripping lithography. The on-chip sensor system that is being suggested enables sensitive, quick, and highly selective hydrogen detection. The efficiency and capacity of 1D metal oxide nanomaterials for gas sensing can be improved by this technology for making chips and thin films. According to the study, completely depleted oxide nanorods exhibit a noticeable increase in resistance following patching, because air-annealed nanorods have lower oxygen vacancy concentrations deeper down the rods. This flat band condition is caused by the decreased oxygen vacancy concentrations. However, upon vacuum annealing, the oxygen vacancy concentrations increases, causing a greater electrical conductivity of the rods as well as a smaller depletion layer at the Schottky junction.
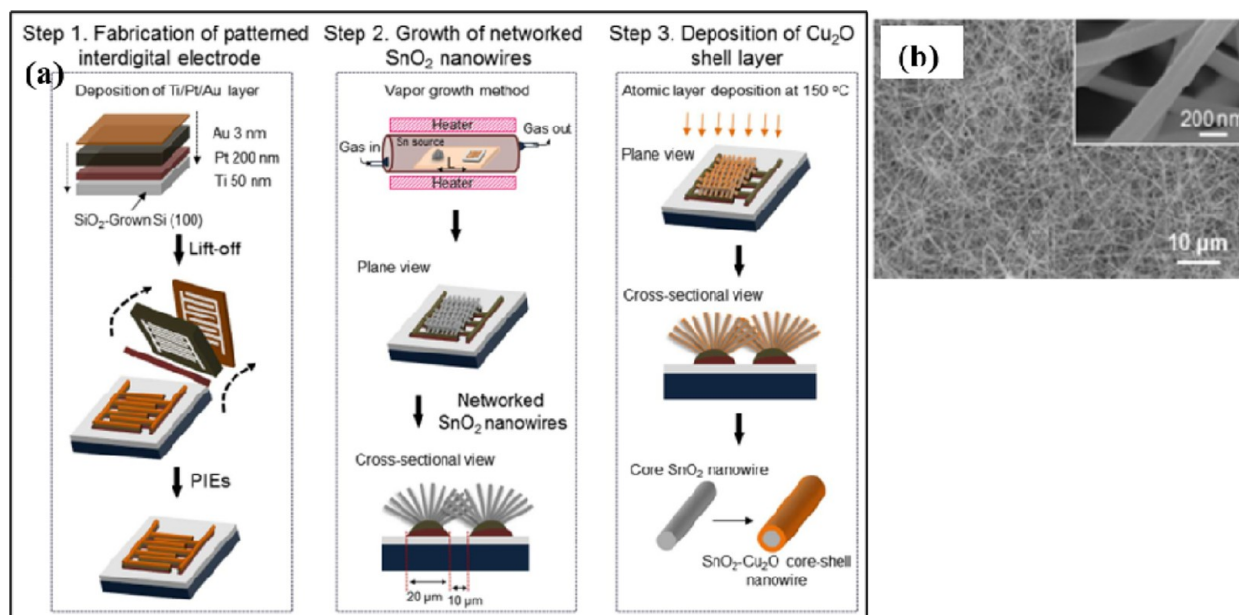
Figure 11. (a) Schematic illustration of the steps for the fabrication of SnO_2–Cu_2O C–S NWs sensors. (b) SEM image of SnO_2–Cu_2O C–S NWs with 30 nm thickness. Reproduced with permission from ref 111. Copyright 2015 American Chemical Society.
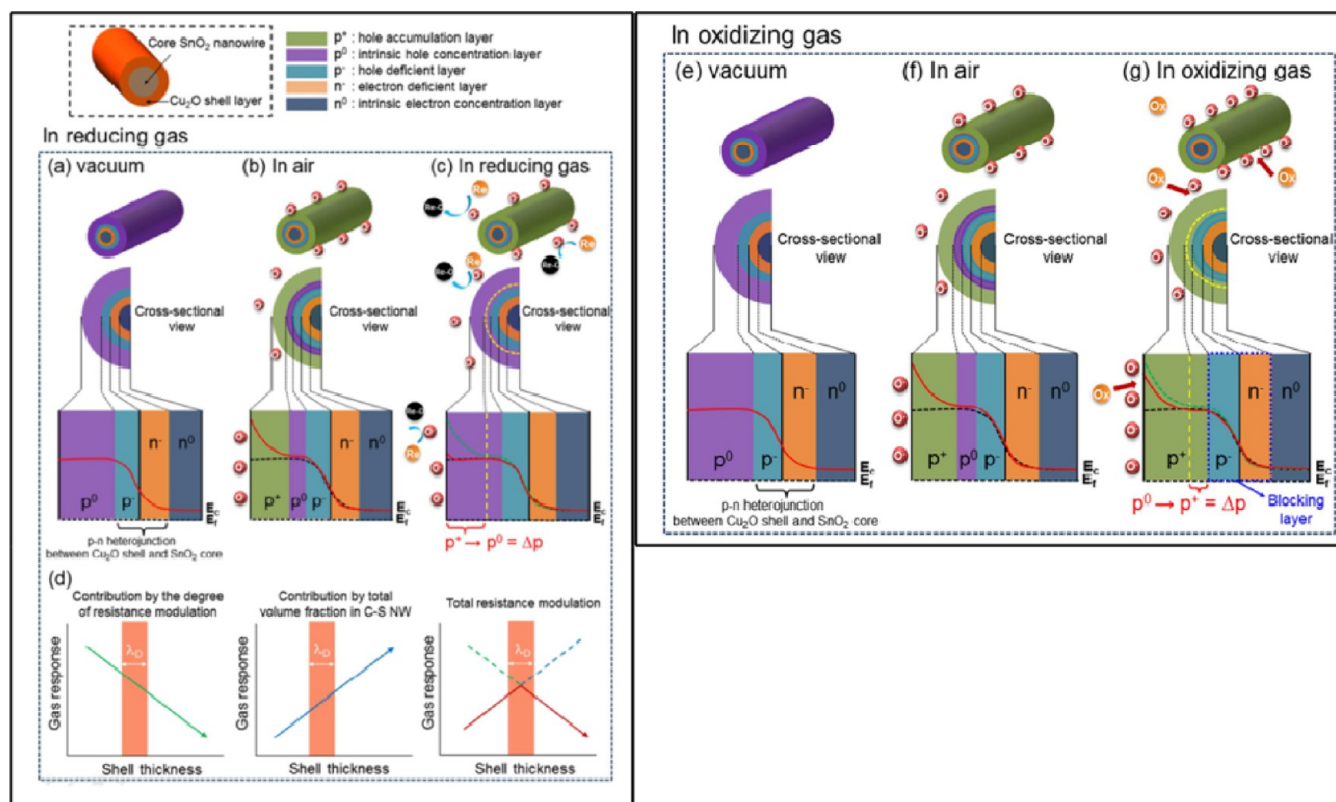

Figure 12. (a–d) An illustration showing the SnO_2–Cu_2O C–S NW sensor's detecting process for reducing gases in various environments, including hoover, air, reducing gases, and total resistance modulation of the C–S NWs. The three oxidizing gas detecting methods are (e) in the vacuum state, (f) in the air, and (g) in oxidizing gases. Reproduced with permission from ref 111. Copyright 2015 American Chemical Society.

The reaction to H_2 is then greatly enhanced as the resistance declines. As a result, the sensor on the high-capacity, low-power semiconductor chip performs noticeably better in terms of sensing.

In order to detect trace amounts of gases, Kim et al. synthesized SnO_2–Cu_2O core–shell nanowires (Figure 11).[111]

The variation of the resistances of the core–shell nanowires (C–S NWs) sensors with different shell thicknesses was examined in the presence of 10 ppm of C_7H_8, C_6H_6, and NO_2. At 300 °C, the C–S NW sensor demonstrated detection sensitivities of 11.7 and 12.5 to 10 ppm of C_7H_8 and C_6H_6, respectively. This was achieved by optimizing the shell

thickness to 30 nm. Additionally, for both gases, the response and recovery times were close to 4 s. However, the C−S NW sensor's ability to detect NO_2 was lowered by the presence of Cu_2O shell. Figure 12 depicts a proposed sensing mechanism through the schematic diagram by SnO_2−Cu_2O C−S NW sensor in the presence of reducing gases, oxidizing gases, and air and under vacuum conditions with total resistance modulation. Figure 12b shows the concentration profiles of holes in ambient air and vacuum conditions, respectively, as a red line and a black dotted line. In Figure 12c, the blue line represents the concentration profile of air holes traveling in the direction of the red line. Due to the oxygen absorption onto the Cu_2O shell and the development of core−shell heterojunctions, it is feasible to divide the concentration of holes into three zones while examining ambient air conditions. A hole-accumulated layer (HAL (p^+)) is created as the chemically adsorbed oxygen species remove electrons from the valence band of Cu_2O. The hole-deficient layer (p^-) is created when the electrons in the n−p heterojunction electrostatically react with the hole layer, while the intrinsic hole concentration layer (p_0), which is formed at a certain temperature, stays at the level of holes in Cu_2O that is at equilibrium. When exposed to reducing gas, the p-Cu_2O shell layer of the sensor becomes more resistant because the concentration of holes in the "p" shell layer is reduced. As a result of the weaker hole-accumulation layer, the detection capacity of pure Cu_2O NWs was lower than that of C−S NWs sensors. The resistance modulation of the p^+ layer shifts inversely with respect to the thickness of the shell. Therefore, a thicker shell suffers less resistance modulation as a result of being in a partial hole accumulation condition. Since the p^- | n^- interface acts as a blocking layer for the extension of p^+ layer, the existence of this interface further restricts the development of the p^+ layer, which contributes to the sensor's limited sensitivity to NO_2.

5. GAS SENSORS BASED ON TWO DIMENSIONAL NANOMATERIALS

5.1. Gas Sensors Based on Graphene. The applications of 2D nanomaterials in a wide range of devices, including gas sensing, storage, electronic devices, owing to their unusual physical and chemical properties have drawn remarkable research interest worldwide.[112−114] In industrial production and environmental monitoring, graphene gas sensors are crucial and widely used. The unique physical, chemical, and mechanical characteristics of graphene have made it a popular subject for academic research. The sensors consisting of graphene are capable of lowering the working temperature and enhancing recovery and also exhibit good gas sensitivity, making them capable of being used as gas sensors for a wide range of gases. Moreover, the graphene-based gas sensor with organic polymers can be prepared for use at ambient temperatures. Huang et al. investigated the use of flavin monocleotide sodium salt (FMNS) functionalized graphene as chemically resistive gas sensors for the detection of ammonia gas.[115] The thorough characterization shows the synthesis of well-structured graphene sheets with negligible defects. This sensor, under optimized conditions, exhibits an outstanding sensing ability and an extremely low detection limit when detecting gases. In regard to the role of FMNS in the fabrication of graphene-based sensors for NH_3 sensing, this is demonstrated through all-atomic molecular dynamics simulations. Ammonia molecules bind weakly to graphene surface when it is not functionalized with FMNS, and a very low

number of electrons are transferred from NH_3 molecules to graphene, resulting in a low sensing response even after contact with high NH_3 concentrations.[116] In the case of the FMNS-functionalized graphene sensor, more electrons are transported from NH_3 molecules to graphene, as the FMNS performs the dual role as p-type dopant to graphene and active sites for NH_3 molecule adsorption via forming hydrogen bonds. Thus, graphene-based sensors with FMNS provide excellent sensing response and gas sensing capability even in the presence of less concentration of NH_3. Again, the weak hydrogen bonding interaction of NH_3 molecules with FMNS facilitates the recovery process of FMNS functionalized graphene sensor.[117]

The possibility of utilizing graphene nanosheets to detect NH_3 gas was investigated by Ahmed et al.[118] The measurement was performed using a comparison of electrical resistance values obtained before and after the gas exposure. Upon gas exposure, the resistivity was found to increase considerably in response to the adsorption of gas molecules. This graphene-based gas sensor was inclined toward NO_2 and NH_3. When gases are detected by ultraviolet or heating sensors, graphene reacts quickly and provides enough energy for graphene sheet desorption.[115] Since graphene is a p-type semiconductor, the change in conductivity of graphene results from the carrier's predominant hole hybridization with coupled electrons on the material's surface following the weak gas molecule adsorption. This device demonstrated the superb sensing properties of particular gases as well as the sensor's performance.

meta-Toluic acid (MTA) functionalized graphene oxide (GO) films for RT gas sensors were prepared via chemical deposition using the Langmuir−Blodget (LB) technique by the research group of Kumar.[119] They made use of the thermal evaporation technology for the deposition of the aluminum contact to measure the resistance of the synthesized film. The MTA-functionalized GO was characterized using XRD, FTIR, Raman spectroscopy, and SEM. Studies on the selectivity of the sensor under various circumstances revealed that it was strongly selective for ammonia gas, demonstrating the gas's favorable sensing properties. The group investigated how the sensors responded to ammonia at various concentrations in the range of 100−2000 ppm. For 100 ppm of NH_3, the response was found to be highest with the 75 mM MTA-GO sensor. This improvement in the response to gas can be attributed to accelerated ester formation processes on the detecting film's surface, leading to its increased interaction with ammonia molecules. In addition, the flaws and carbon vacancies in the MTA functionalized GO promote interactions with NH_3 on the surface, leading to both high chemisorption and physical adsorption. The structural and electrical characteristics of functionalized GO surfaces are altered by the adsorption and dissociation of NH_3. As a result, charge transfer takes place from NH_3 to functionalized GO surfaces via the development of hydrogen bonding.[120] Alternatively, the sensing mechanism can be explained as follows. The surface characteristics of GO may be impacted by epoxide rings on its surface breaking during functionalization or NH_3 dissociation (NH_3 into NH_2 and H species). As a result of a reaction between free NH_2 and H species on carbon and oxygen sites, OH and NH_2 molecules may be chemisorbed. The sensor shows exceptional ammonia gas sensitivity and selectivity.

In order to develop a mass-type poisonous gas sensor, Van Cat et al. investigated GO nanosheets (GO-NSs) that were used with a quartz crystal microbalance (QCM) transducer.[121] Its working electrode, the QCM's surface, was treated with a

spray of GO-NS suspension. It was designed to study the concentration of toxic gases such as SO_2, CO, NO_2, and NH_3 using GO-NSs that have excellent adsorption capabilities and work well as sensors for identifying dangerous gases. Nanosheet-structured GO has a negatively charged large surface area with oxygen functional groups (such as hydroxyl and carboxylic) and is an excellent adsorbent for gases. The GO-coated QCM sensor showed an excellent sensitivity factor (S-factor) with SO_2 and NO_2 gases, according to the sensing findings. The working principle of this mass-type gas sensor is based on the layer of testing gas molecules that adsorb and desorb on the surface of the GO-coated QCM sensor.[122] The hydrogen bonding-type interaction between the polar analyte gas molecules on the sensor's surface is the key to the adsorption process. Therefore, the S-factor of the GO-NS-coated QCM sensor is influenced by the adsorption capacity and molecular weight of the analyte gas molecules. The sensor showed similar sensitivity factors for SO_2 and NO_2 but a comparatively lower value for CO. The higher value of the S-factor for NO_2, even though it has a weaker dipole−dipole interaction than CO, can be attributed to the fact that NO_2 generally exists in its dimer form, and the dimerization of NO_2 leads to the formation of a higher molecular weight, N_2O_4. For harmful gases like SO_2 and NO_2, the QCM sensor with GO-NS coating has very high gas sensitivity. Additionally, QCM sensors exhibit repeatability, long-term cycle stability, and excellent responsiveness.

On the other hand, the response of graphene, when made into nanocomposites with PAni via chemical oxidative polymerization, toward 100 ppm of NH_3 was found to be 11.33 with a 50 s response time and good repeatability at RT.[123] This performance may be attributed to the homogeneous distribution of PAni over graphene, which helps in creation of the p−n junction and a positively charged depletion layer.

Wang et al. investigated the application of borophene-based materials as nanogas sensors, taking into account gold electrodes, MoS_2 substrate, and gas molecules.[124] According to the study, CO, NO, NO_2, and NH_3 gas molecules may be detected and distinguished using borophene and borophene−MoS_2 heterostructures with gold electrodes. In contrast to systems without gold electrodes, the MoS_2 substrate produced nonlinear current−voltage behavior, while the gold electrodes decreased current levels.

5.2. Gas Sensors Based on MXenes. MXene-based nanomaterials are a unique family of materials that are stacked in two dimensions (2D) and have a morphology similar to that of graphene. When A-element layers from the MAX phase are etched with an appropriate etching agent, MXenes are created. A denotes elements from groups 13 or 14; early transition metal elements are represented by M; and C, N, or their mixtures are represented by X in the standard formula for the MAX phases, i.e., $M_{n+1}AX_n$.[125] $M_{n+1}X_nT_x$ is the chemical formula for MXenes, where T stands for surface terminal functional groups (fluorine, hydroxyl, and/or oxygen) that were added during etching. Various etching procedures can be used to tailor surface termination groups on MXenes.[126] Because of its high electronegativity and surface area, the MXene nanomaterial is perfect for surface reactions and gas sensing. Because of the reaction between the gas analyte and the MXene layer surface, its resistivity or conductivity changes. Charge transfer takes place when gas molecules come into contact with the MXene layer, changing the sensor layer's total

conductivity. MXene nanomaterials have an easy resistance-type sensing mechanism, making them a potential material for gas sensors. The electrons in MXene nanomaterials are taken out by oxidizing gas molecules and added by volatile organic chemicals. Adsorption and desorption processes are involved in charge transfer. Through surface functionalization and metal ion implantation, MXene-based gas sensors can have higher selectivity and sensitivity.[127]

Using MXene materials and their composites, researchers have created gas sensors for a variety of gases, including H_2,[128] methanol,[129] formaldehyde,[130,131] toluene,[132,133] NH_3,[134−137] and NO_2.[138,139] Due to their dependable portability, strong potential for integration, adaptability, and handling simplicity, MXene-based flexible piezoresistive sensors have potential applications in intelligent robot technology, touch displays, electronic skin, and human−computer interactions. For instance, a flexible pressure sensor constructed from poly(vinyl alcohol) (PVA) and MXene ($Ti_3C_2T_x$) has over 10 000 cycles of durability, ultrahigh sensitivity (2320.9 kPa^{-1}), a large sensing range (65.3 Pa to 294 kPa), a low detection limit (~6 Pa), and a short reaction time (~70 ms).[140] The review paper on MXene gas sensing by Deshmukh et al. is referred to interested readers.[141]

The increased hydrophilicity, high mechanical stability, and improved conductivity of $Ti_3C_2T_x$ MXene-based gas sensors are contributing to their growing popularity.[142,143] The surface of $Ti_3C_2T_x$ MXene is enhanced by the inclusion of functional groups, creating more active sites for gas adsorption.[144] Effective, inexpensive, and very sensitive gas sensors are essential for tracking trace volatile organic compounds (VOCs) in environmental and biological applications. The 2D $Ti_3C_2T_x$ MXene gas sensor created by Kim et al. outperforms the sensitivity of typical semiconductor channel materials thanks to its high metallic conductivity, low noise, and completely functionalized surface.[145] The MXene-based gas sensor outperforms the best gas sensors available today with a low VOC gas detection limit of 50−100 ppb at ambient temperature. Its robust association with the analyte is made possible by its metal conductivity and high functional group coverage. The sensor allows for early diagnosis and treatment, since it can detect different VOCs at a 100 ppm level without the need for pretreatment. The study's findings point to the creation of a high-sensitivity sensor with a highly functional metal sensor channel.

Kim et al. used interfacial self-assembly to produce an ultrathin Ti_3C_2 MXene sheet with a thickness of 10 nm, which they then deposited onto a variety of substrates.[146] At 100 ppm of ethanol, 100 ppm of acetone, and 5 ppm of ammonia, the gas response performance was evaluated. The films demonstrated exceptional performance in thin-film devices when employed as gas sensors. Because of its excellent conductivity, the Ti_3C_2 gas sensor has a low electrical noise of 0.0015%. Ammonia's signal-to-noise ratio reached 320, indicating its exceptional gas-detecting sensitivity. Wu et al. achieved great selectivity in the development of a Ti_3C_2 MXene-based sensor for room temperature NH_3 detection.[147] To detect a range of gases, such as ethanol, methanol, acetone, NH_3, CH_4, H_2S, and H_2O, the sensor was coated on ceramic tubes. The most selective gas was NH_3, with a response of 6.13%, four times more than that of the other gases. From 10 to 700 ppm of concentration, the sensor's linear response changed. The outstanding performance of the sensor for NH_3 detection at room temperature was validated by humidity and cycle testing.
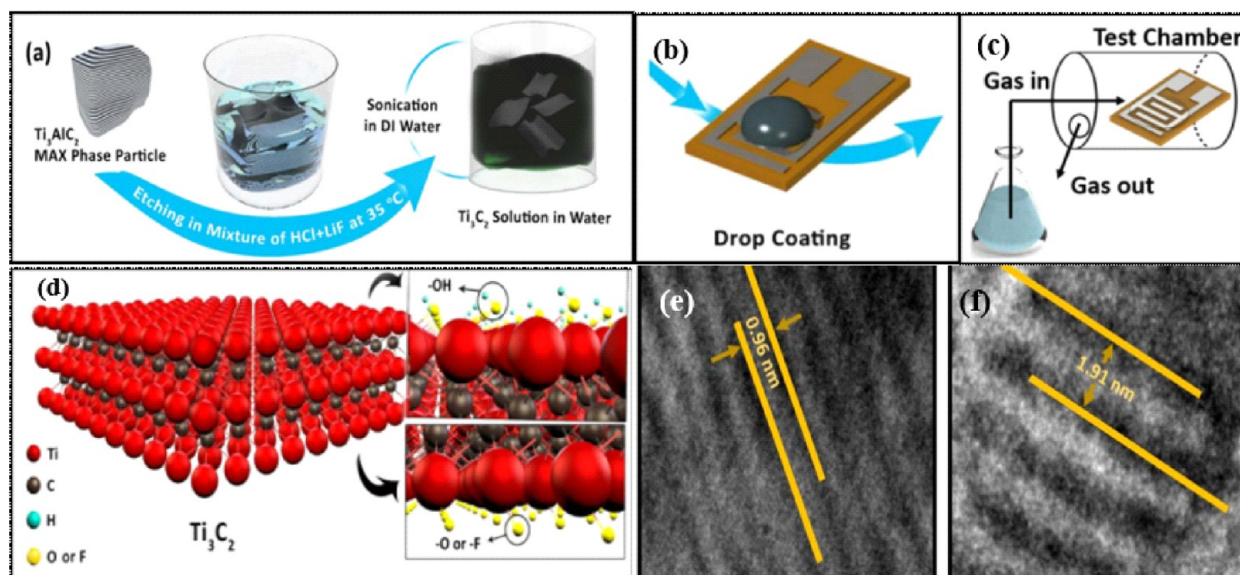
Figure 13. Schematic diagram of $Ti_3C_2T_x$ illustrating the following processes: (a) synthesis, (b) solution deposition, (c) gas sensing apparatus, and (d) structure and various functional groups on the surface of $Ti_3C_2T_x$ nanosheets. Reproduced with permission from ref 148. Copyright 2017 American Chemical Society. (e and f) High-resolution TEM pictures of the interlayer spacing of undoped and sulfur-doped $Ti_3C_2T_x$ MXenes, respectively. Reproduced with permission from ref 149. Copyright 2020 American Chemical Society.

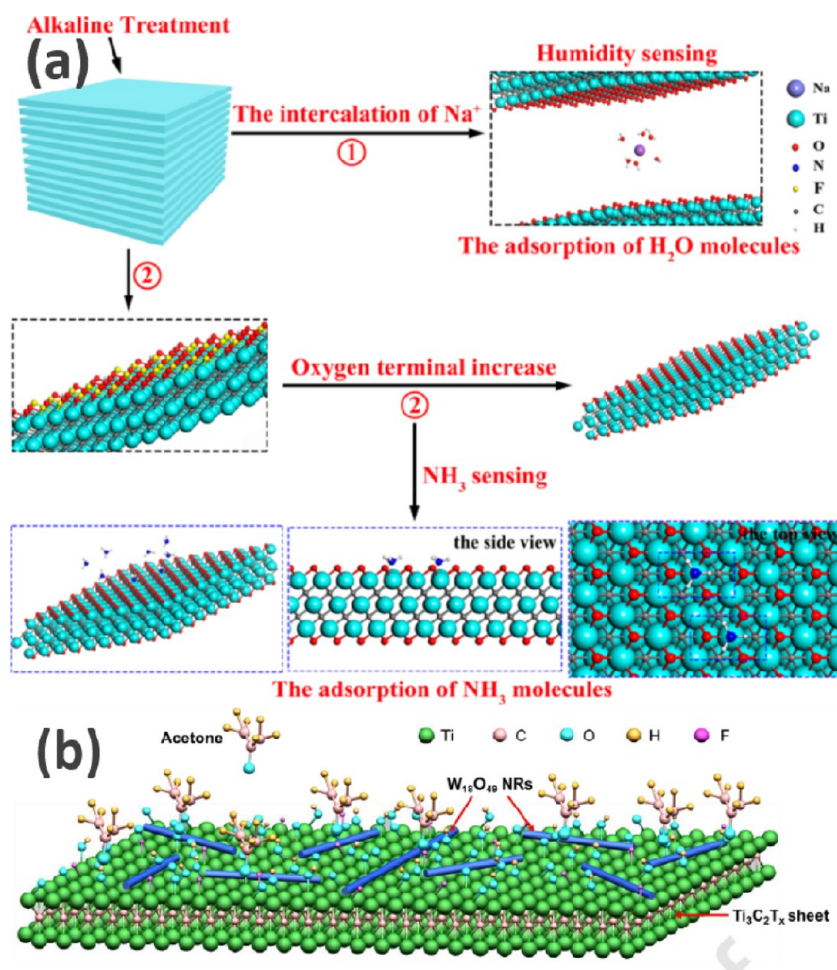**Figure 14.** (a) Schematic representation showing how NH_3 and H_2O molecules adsorb to the surface of alkalized $Ti_3C_2T_x$. Reproduced with permission from ref 152. Copyright 2019 American Chemical Society. (b) A schematic depicting the acetone-$W_{18}O_{49}/Ti_3C_2T_x$ composite reaction. Reproduced with permission from ref 153. Copyright 2020 Elsevier.
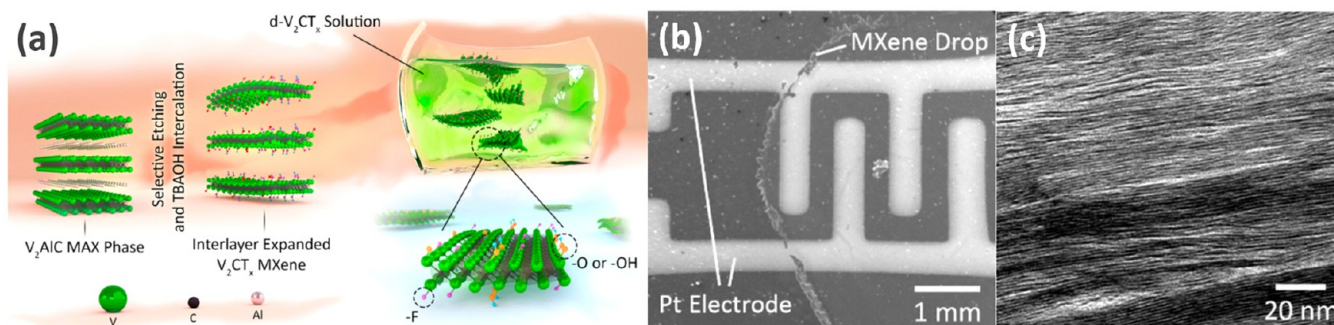
Figure 15. (a) A schematic diagram illustrating the structure of the final surface-functionalized V_2CT_xMXene produced via delamination and synthesis of V_2CT_xMXene. (b) SEM image of the interdigitated platinum electrodes with a drop-cast V_2CT_x film deposit. (c) A V_2CT_x film cross-sectional TEM image. Reproduced with permission from ref 144. Copyright 2019 American Chemical Society.

By synthesizing $Ti_3C_2T_x$ nanosheets by extracting Al atoms from Ti_3AlC_2, Lee et al. developed an RT gas sensor that was integrated into flexible polyimide substrates using an easy solution-based technique, as schematically depicted in Figure 13 a−d.[148] Room temperature ethanol, methanol, acetone, and ammonia gas levels are all detectable by the $Ti_3C_2T_x$ gas sensor. The sensing material's efficient adsorption/desorption on the surface of the $Ti_3C_2T_x$ sheet is the sensor's mechanism. The replacement of surface functional groups by gas molecules results in gas absorption, which modifies the resistance of the $Ti_3C_2T_x$ film significantly and facilitates carrier transfer. Certain sensing materials attach themselves to structural defects in the $Ti_3C_2T_x$ nanosheet, while other materials work by means of charge transfer with surface terminals such as hydroxyl and oxygen groups.[148]

The improved performance and distinct selectivity of toluene were shown in Shuvo's investigation on the gas sensing characteristics of volatile organic compounds utilizing sulfur-doped $Ti_3C_2T_x$ MXene.[149] In order to create conducto-metric gas sensors, the team synthesized a sensing material and used drop-casting to construct the electrodes (silver) on PET substrates. Volatile organic molecules with various functional groups were evaluated for their presence using the sensors. Unique toluene selectivity was demonstrated using sulfur-doped $Ti_3C_2T_x$ MXene sensors, which show improved responsiveness (from 214% at 1 ppm to 312% at 50 ppm). $Ti_3C_2T_x$ MXene sensors doped with sulfur exhibit exceptional stability over time and a unique reaction to 500 ppb of toluene. MXene nanoflakes come into contact with the reductive gas' molecules when toluene is added. Compared to other volatile organic compounds, sulfur-doped MXenes enhance the sensing response to toluene by releasing trapped electrons back into the conduction band.[150] Compared to nonaromatic VOCs, the benzene ring in toluene interacts more with preadsorbed sulfur species. The sensor's selectivity to toluene is determined by the methyl group's electron-donating action, which enhances hydrogen atom activity on the benzene ring. More active gas adsorption sites are made possible by the increased interlayer gap caused by the sulfur doping process. TEM (Figure 13e and f) investigations demonstrate the increased interlayer spacing. This resulted in enhanced interaction between sulfur species on MXene nanoflakes and toluene molecules and amplified the gas sensing response.

Using flexible wet spinning, Lee et al. created a $Ti_3C_2T_x$ MXene/graphene hybrid fiber for NH_3 sensing.[151] In comparison to MXene and graphene, the fibers show a considerably increased NH_3 sensing response and high NH_3

gas sensitivity at ambient temperature. The fiber also has outstanding mechanical flexibility, maintaining a low fluctuation of ±0.2% even after 2000 bending cycles with no resistance fluctuation. Using organ-like MXene, Yang et al. have created a gas/humidity sensor that can be treated with alkaline to enhance its detecting capabilities.[152] Increased −O terminals and Na^+ intercalation make the sensor to exhibit improved humidity and gas detection capabilities. Changes in electrical conductivity are brought about by the adsorption of NH_3 and H_2O molecules (Figure 14a) as well as electron transfer in the adsorption mechanism of the sensor. The NH_3 molecule's N atom adsorbed on the Ti atom in $Ti_3C_2T_x$ is made possible by strong chemical interactions between the titanium and nitrogen atoms (Figure 14a). The stretched Ti−C bond pulls the NH_3 that the Ti atom has adsorbed out a little bit, increasing the adsorption capacity. Alkaline treatment increases the number of −O terminals, which increases the number of N−Ti binding sites and improves NH_3 adsorption.

$W_{18}O_{49}$ nanorods were generated on the surface of 2D $Ti_3C_2T_x$-Mxene sheets by Sun et al. utilizing the solvothermal process to manufacture $W_{18}O_{49}/Ti_3C_2T_x$ composites.[153] The $W_{18}O_{49}/Ti_3C_2T_x$ composites show a low detection limit for 170 ppb of acetone, quick response and recovery times, long-term stability, strong selectivity, and great responsiveness to low acetone concentrations. This method offers significantly enhanced acetone sensing capability compared to $Ti_3C_2T_x$ and $W_{18}O_{49}$ nanorods alone. The even distribution of $W_{18}O_{49}$ nanorods on the surface of $Ti_3C_2T_x$, the elimination of fluorine-containing groups during solvothermal treatment, and the synergistic contact between $W_{18}O_{49}$ nanorods and $Ti_3C_2T_x$ are all responsible for this. The composite surface absorbs oxygen molecules from the air and uses the electrons it captures to create oxygen species. A new electron depletion layer arises on the $W_{18}O_{49}$ surface as a result of this decrease in electron concentration, which also causes the Schottky barrier at the interface to increase. Acetone and ionic oxygen react to liberate electrons (Figure 14b), which lowers the $W_{18}O_{49}/Ti_3C_2T_x$ sensor's resistance. Owing to the oxygen vacancies in $W_{18}O_{49}$ and facile acetone adsorption on the $Ti_3C_2T_x$ surface, the adsorption of oxygen in air and acetone molecules is enhanced, causing an increase resistance change and thereby a strong sensor response.

A very sensitive gas sensor based on 2D vanadium carbide MXene was also described by Lee et al. for the purpose of finding traces of nonpolar gas.[144] Multilayered V_2CT_x was produced by selectively etching Al atoms from the V_2AlC MAX phase using hydrofluoric acid. There is no direct delamination
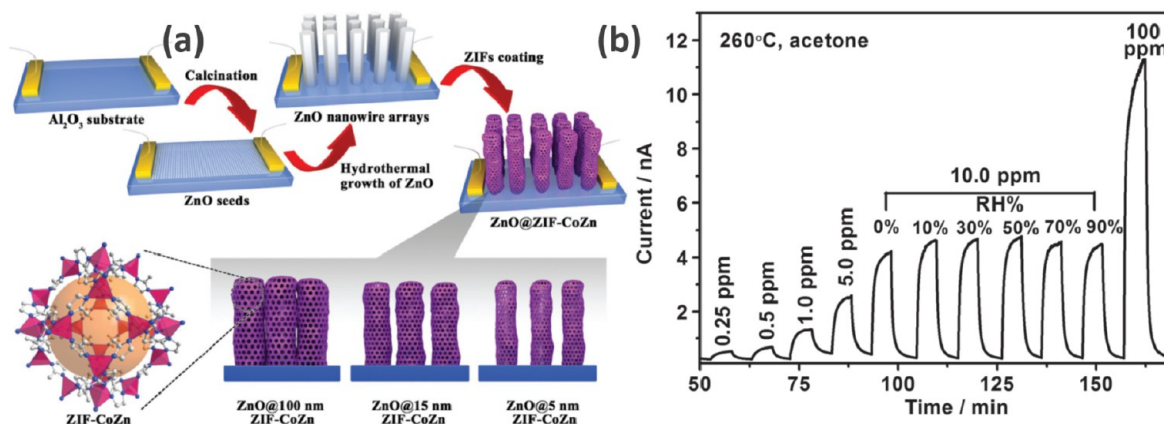
Figure 16. (a) Schematic depiction of ZIF-8-coated ZnO gas sensors. (b) Dynamic response/recovery curve for the sensor with a 5 nm ZIF-8 layer thickness when subjected to different acetone concentrations and humidity conditions. Reproduced with permission from ref 167. Copyright 2016 Wiley-VCH Verlag GmbH & Co.

of this powder into 2D MXene flakes. Tetra *n*-butyl ammonium ion intercalation and dispersion were used to delaminate the intercalated MXene particles and for device fabrication, as depicted in Figure 15. The V_2CT_x surface's oxygen terminal groups support the receptor's operation. The adsorption of ionic species on the hydrophilic surface is more advantageous as opposed to the hydrophobic surface. Research has been done on the gas sensing capabilities of the V_2CT_x gas sensor, which can detect a range of gases at ambient temperature with a 2 ppm detection limit for hydrogen. The nonpolar gas detection performance of this sensor is superior to that of most cutting edge 2D gas sensor materials.

Zhao et al. used cobalt and aluminum as catalysts to create MXene-based sensors with good selectivity for the detection of only acetone gas. The $V_4C_3T_x$ film offers a lot of potential for ultrasensitive and extremely selective gas sensing because of its enormous specific surface area and distinctive atomic structure.[154] The $V_4C_3T_x$ MXene sensor measures resistance from a $V_4C_3T_x$ film using DC voltages. A sealed chamber with varying quantities of acetone steam is allowed to be in contact with the sensors. The $V_4C_3T_x$ MXene changes from metal V_4AlC_3 to semiconductor after HF treatment. The contact performance of the $V_4C_3T_x$ film is impacted by the larger molecular size of acetone, which causes greater resistance changes for smaller water molecules. Despite this, the sensor performs well in detecting acetone, with a 1 ppm detection limit and at 25 °C operating temperature. MXene may find use in gas sensors as a result of being one of the few acetone sensors that can satisfy the parameters of low concentration, high sensitivity, and good selectivity for mixed gases.

5.3. Gas Sensor Based on Metal Organic Frameworks (MOFs). Inorganic secondary building blocks and organic ligands combine to generate crystalline nanoporous materials known as metal−organic frameworks (MOFs). They are interesting for gas sensing applications because of their distinctive qualities, which include strong crystallinity, structural diversity, high thermal and chemical durability, large specific surface area, tunable pore size/geometry (physiological interactions like host−guest interactions), and reversible gas absorption and release.[155] In 2014, Zhang and associates showed that formaldehyde and trimethylamine vapors could be detected with cobalt-based ZIFs [Co-$(mim)_2$],[156] (ZIF-67), and [Co-$(im)_2$],[157] (mim = 2-methylimidazolate; im = imidazolate), with detection limits

of 5 and 2 ppm, respectively. These materials do, however, have long response−recovery durations and poor conductivity at ambient temperature. Selectivity and sensitivity for a range of analytes have improved due to developments in the construction of semiconductive chemiresistive MOF-based RT sensors.[158] RT chemiresistive sensors were developed by Dincà and colleagues to detect ammonia concentrations as low as ppm utilizing pristine MOFs such as $Cu_3(HITP)_2$ (HITP = 2,3,6,7,10,11-hexaiminotriphenylene).[159] Using drop-casting onto gold electrodes, a MOF with 0.2 S cm^{-1} bulk conductivity was produced. In the range of 0.5−10 ppm, it showed linear responses to NH_3. The MOF was utilized to build a sensor array that could distinguish between five volatile organic compounds: amines, aliphatic hydrocarbons, aromatic hydrocarbons, ketones/ethers, and alcohols. It also included $Cu_3(HHTP)_2$ and $Ni_3(HITP)_2$ (HHTP = 2,3,6,7,10,11-hexahydroxytriphenylene).[160] The nature of the metal largely affects the response direction of this MOF-based chemiresistive sensor array, demonstrating a process of electron transport between metal centers and analyte molecules. On the other hand, the observed relationship on analyte concentration implies the presence of an additional active mechanism, which may be hydrogen bonding with organic linkers.

Xu et al. created a high-performance sensing device by fabricating thin $Cu_3(HHTP)_2$ films on various substrates patterned with gold IDEs using the spray layer-by-layer liquid-phase epitaxy process.[161] A number of performance characteristics for their bulk powder equivalents were exceeded by the resultant NH_3 gas sensors.[160,162] The gas sensors outperformed previous ones using Cu_3HHTP_2 powders, nanorods, or thick films, with a 129% response rate and faster recovery times. They also selectively detected ammonia from ten other reducing gases, including CO, H_2, acetone, ethanol, methane, methanol, *n*-hexane, toluene, benzene, and ethylbenzene.[161] Compared to the powder form, they also achieved a low detection limit of 0.5 ppm of NH_3 and outstanding long-term stability and repeatability.[160] By spray-coating flexible polycarbonate foils or glass slides with Cu_3HHTP_2 nanoplatelets, Behrens et al. developed a device that can detect methanol with strong, quick, and reversible responses by a chemiresistive mechanism.[163] In comparison to earlier studies, the coatings demonstrated excellent interparticle interactions and a conductivity of 0.045 S cm^{-1}. Owing to their superior chemical and thermal stability, zirconium MOFs have been

shown by Dmello et al. to be able to detect acidic gases like CO_2, SO_2, and NO_2.[164] For resistive detection, they employed UiO-66-NH$_2$, a zirconium-based compound functionalized with amine. Because of its poor electrical conductivity (i.e., about 3.8×10^{-8} S cm^{-1} at 300 K) and high working temperature requirement of 150 °C, UiO-66-NH$_2$ is not a good choice for most real-world applications.[165] The device displayed responses of 21.6%, 7.6%, and 11.4% for 10 ppm of SO_2, 10 ppm of NO_2, and 5000 ppm of CO_2, respectively. It also had rapid response−recovery durations and a low SO_2 detection limit. Lower sensitivity in UiO-66-OH and UiO-66-(OH,NH) and no resistance changes in nonfunctionalized UiO-66 were also seen in the research. The distinct sensing characteristics of MOFs functionalized with amines are assumed to be caused by efficient charge-transfer networks formed by acid−base interactions between NH$_2$ groups.

Chemiresistive sensor devices can be made by combining a composite of MOFs with an appropriate conducting component. The selectivity and sensitivity of the sensor are increased by the analyte receptor function of an electrically nonconducting MOF. Electrical transduction is carried out by the composite's conductive element, namely semiconductor metal oxide (SMO). Applications involving sensors can benefit from this strategy of making composites.[166]

Water-soluble ZIF-8/ZIF-67-coated zinc oxide (ZnO) sheath-core nanowires with hydrophobic properties were created by Xu and colleagues using a wet chemical method.[167] For the hydrophobic ZIF-8/ZIF-67 film (Figure 16a), the nanowired ZnO was used as template. Our ZIF-8/ZIF-67 shelled ZnO-based sensor's ability to sense gas was put to the test in a damp environment. In contrast to bare ZnO nanowire-based sensors, the sheath-core nanostructure's dynamic response/recovery curve demonstrated enhanced selectivity toward acetone (Figure 16b). Its usefulness was demonstrated by the fact that the MOF structure's hydrophobicity nullified the influence of moisture on the sensing performance.

ZIF-8/67@ZnO is the ZnO nanowire coated MOF used in the formaldehyde, acetone, and H$_2$ sensor series.[167−169] Later in 2017, using a thin, porous, and finely grained ZIF-8 coating on a glass substrate, Wu et al. produced a ZnO/ZIF-8 core−shell nanorod film. Good selectivity in detecting H$_2$ over CO was demonstrated by devices made from this material.[170] Utilizing a chemical solution deposition technique, the composite microstructure was manipulated to provide a 110 nm thick ZIF-8 shell, which thereby increased the number of oxygen vacancies. This added layer of oxygen vacancies increased the sensitivity of the ZIF-8@ZnO nanorod film to H$_2$ in comparison to the pure ZnO film. The ZIF-8 coating's tiny grain size (<140 nm) greatly improved its molecular sieving function and hence prevented CO molecules from interacting with it at 200 °C. Zhou et al. researched into the correlation between MOF pore size and gaseous analyte molecule size in a related study.[171] Through their methodical study, they were able to demonstrate MOF@ZnO nanorods' selective sensing by molecular sieving. Researchers used two types of coatings (ZIF-71 with 4.8 Å pores and ZIF-8 with 3.4 Å pores) and probe molecules of varied kinetic diameters (2.89−5.85 Å). Utilizing ZIF-8-coated In$_2$O$_3$ nanofibers, Liu et al. detected NO_2 at ppb levels chemiresistively in a different study.[172] According to their findings, the ZIF-8@In$_2$O$_3$ heterostructure's composition affected the resistive response. The device with the greatest resistance response of 16.4 to 1 ppm of NO_2 over air and a detection limit of 10 ppb for NO_2

was that with ZIF-8/In$_2$O$_3$ (1:4 Zn/In molar ratio). Comparing ZIF-8@In$_2$O$_3$ to prisitine In$_2$O$_3$, this composite also showed improved resilience to humidity.

In place of semiconductor nanorods, Kalidindi and colleagues employed SnO$_2$ nanoparticles to make a composite with ZIF-67 for investigating CO_2 sensing properties.[173] With a 16.5% response at 205 °C, the sensing behavior against CO_2 was found to increase up to 12 times at the 50% CO_2 level and twice at 5000 ppm of CO_2. XPS investigations indicated that the enhanced performance might be attributed to changes in the electrical structure at the ZIF-67 and SnO$_2$ interface. Ren et al. studied the ZIF-8 shell's ethanol-sensing behavior on the surface of ZnO microspheres.[174] When exposed to ethanol vapor at 160 °C, the synthesized ZIF-8@ZnO core−shell material demonstrated much higher sensor response (35.90), selectivity, and stability than pristine ZnO microspheres (R_{air}/R_{gas} = 14.54).

To improve the selectivity and sensitivity of the sensor, sophisticated heterostructures have been employed, bring novel transduction mechanisms including photoresponse. Weber et al. have shown that three-component composites made of metal oxide, nanoparticles, and a MOF may be used for gas sensing, improving the sensitivity and selectivity of hydrogen detection devices.[175] After growing ZnO nanowires on interdigitated electrodes (IDEs) and decorating them with Pd nanoparticles by atomic layer deposition, an outer molecular sieve layer known as a ZIF-8 nanomembrane was produced as a consequence of the partial solvothermal conversion of the ZnO surface. At 200 °C, the ZIF-8@Pd@ZnO gadget demonstrated strong responses (R_{air}/R_{gas} = 3.2, 4.7, 6.7) to VOCs such acetone, toluene, ethanol, and benzene. In another report, a Au@ZnO@ZIF-8 composite gadget was used to detect and remove formaldehyde simultaneously by oxidation.[176] Although acquiring photoresponses using this device needed powerful photoirradiation, it could detect formaldehyde concentrations (0.25−100 ppm) at RT even when there was toluene interference and humidity. The selectiveness of the analyte was increased by ZIF-8, and the visible light-driven charge carrier production on ZnO surfaces was improved due to plasmonic gold nanorods. However, there were challenges, as MOF@SMO development needed high temperatures. Wang et al. enhanced ZIF-8@ZnO's sensitivity and selectivity by adding polyoxometalate (POM) to the apparatus.[177] Under Xe lamp irradiation, improved form-aldehyde detection performance at room temperature air was achieved by the POM@ZIF-8@ZnO device. It demonstrated exceptional selectivity against ethanol and a 0.4 ppm detection limit. The POM component, which prevents electron−hole recombination in semiconducting materials, is responsible for improving the sensing capability.

Carbon nanoparticles, graphite oxides, and other semi-conductor materials have been mixed with MOFs. Cu-BTC/GO composites were developed by Travlou et al. for ammonia sensing; these composites had delayed reaction times (>10 min) but increased resistance ($\Delta R/R_0$) by 4% at 100 ppm.[178] Because of the MOF structure collapsing and the poor ammonia adsorption in the resulted amorphous phase, the NH$_3$ sensing was initially irreversible but later became reversible. Mirica et al. created ball-milled Cu$_3$HHTP$_2$, M-CAT-1 (M = Co, Ni), or Fe-HHTP MOF/graphite blends to construct chemiresistive sensors. These blends were then mechanically abraded onto paper substrates using IDEs.[179] At 80 ppm, a series of four chemiresistor devices identified and
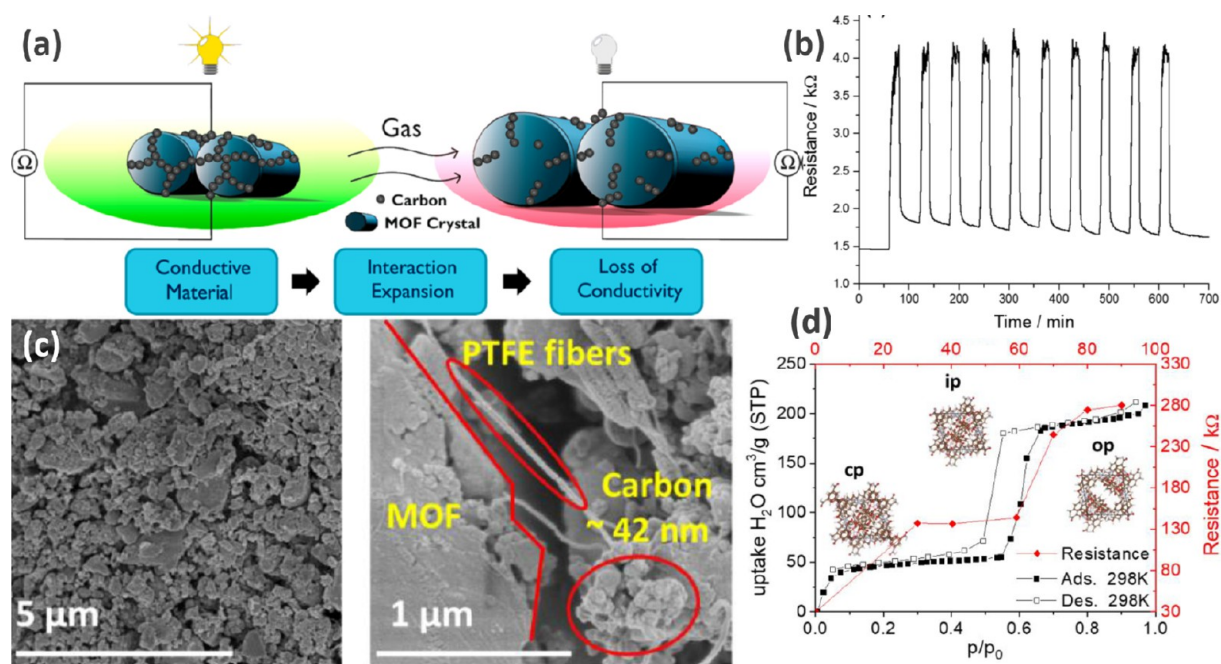
Figure 17. (a) Schematic representation of the threshold sensor's operating principle based on switchable MOF composites. (b) MIL-53/CNP/ PTFE resistance actions to *n*-butane during dry environment cycling. Reproduced with permission from ref 180. Copyright 2017 American Chemical Society. (c) SEM images. (d) In contrast to water vapor absorption at 298 K, the resistance responses of the JUK-8/CNP/PTFE to humidity. Reproduced with permission from ref 182. Copyright 2020Wiley-VCH Verlag GmbH & Co.

distinguished NH_3, NO, and H_2S from each other. The use of graphite improves the electrical contact between MOF and IDEs, and graphite-containing composites made it easier to integrate them with other materials and increased their detection ability. The high detection limit in ball-milled composites owing to pores that are blocked and limited surface areas for analyte interaction was overcome by Kaskel and colleagues with the development of the first MOF-based electrically transducing threshold sensors.[180] Using structurally flexible MOFs such as DUT-8(Ni), ELM-11(Cu), and MIL-53(Al) with CNPs and a PTFE binder, they were able to develop chemiresistive sensing composite membranes. The mechanism of operation of the sensors is based on the MOF particle volume change that occurs throughout the analyte adsorption procedure, which causes a considerable resistance change by disrupting the percolating carbon−-particle network (Figure 17a and b). For *n*-butane detection, the switchable DUT-8 MOF exhibits repeatable responses $(\Delta R/R_0)$ of 5000%, spanning a broad range of gas concentrations of 20−80%. This idea has been effectively applied to selective threshold sensing of CO_2 utilizing MIL-53 (Al) in mixtures including methane at high pressure[181] and moisture threshold sensing using JUK-8 composites (Figure 17c and d).[182]

5.4. Gas Sensors Based on Covalent Organic Frameworks (COFs). Planar building blocks are used to create 2D covalent organic frameworks (COFs), which are layer-stacked structures with periodic columnar π-arrays and extended planar networks. Because of their modest out-of-plane van der Waals force, high stability, porosity, and crystallinity, they are desirable for gas sensing.[166]

Even while MOF-based chemiresistive gas sensors have improved, the limited applicability for electrically transduced gas sensing by intrinsically conducting π-conjugated COFs are possibly related to their complicated synthesis process, along with difficulty in generating a stable electrode contact and

controlling the crystallinity of COF.[183,184] With liquid phases, COFs have become the principal sensing materials for luminescence-based sensing.[185] In ambient conditions, chemiresistive detection of 1−200 ppm of NH_3 is achieved using an amorphous heptazine-based organic framework (HMP-TAPB-1) in relative humidity ranges of 23−85%.[186]

The sensor's strong selectivity for ammonia was caused by electron-withdrawing heptazine units, which also led to higher responses with humidity and recovery durations. The interaction of 2,3,9,10,16,17,23,24-octaamino-phthalocyanine nickel(II) with pyrene-4,5,9,10-tetraone resulted in the production of a novel multilayer COF (COF-DC-8) with a macrocyclic metallic site.[187] According to the study, intrinsically conductive COFs have a tremendous bulk electrical conductivity, which can be increased by three orders of magnitude via iodine doping. It has good responses to NH_3, H_2S, NO, and NO_2 gases when incorporated into chemiresistors, having detection limits at the ppb level. The charge transfer interaction between the nickelphthalocyanine component present in the COF and the analytes and surface adsorption are responsible for the sensing process.

5.5. Gas Sensors Based on Other 2D Nanomaterials. Two-dimensional nanomaterials, particularly transition metal dichalcogenides (TMDs) have shown excellent capability to be used as gas sensing devices due to their layered structure.[188] Their naturally large surface-to-volume ratio and distinctive adjustable band gap, characteristics of a semiconductor, make them potential materials for sensing applications. The primary cause of the 2D TMDs' sensing process is the charge transfer that occurs between the surface of the sensing material and the gas molecule. Depending on whether the material used in 2D TMDs is acting as a charge acceptor or donor, the device's electrical resistance changes. When reactive gases and gas molecules interact, the gas molecules become electrostatically adsorbed on the surfaces of 2D materials. Depending on the
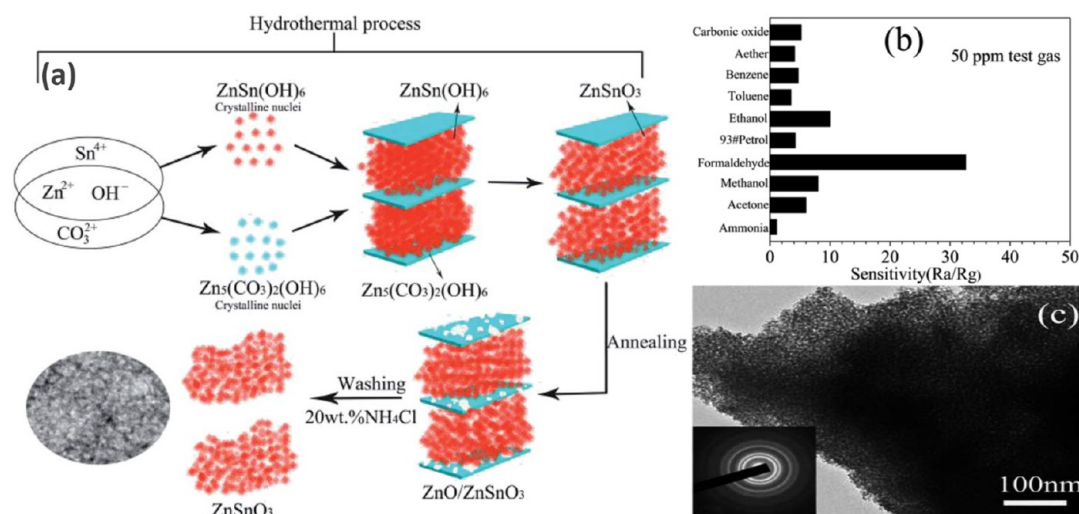
Figure 18. (a) Scheme for the systematic formation process of QTMZNS. (b) Selectivity of the QTMZNS-based sensor to various gases (50 ppm) at 210 °C. (c) HRTEM image and SAED pattern of QTMZNS. Reproduced with permission from ref 191. Copyright 2019 Royal Society of Chemistry.

nature of the adsorbed gases (whether reducing or oxidizing), the direction of electron charge transfer varies; hence, the degree of change in resistance modulation is decided by the electron-releasing or electron-withdrawing behavior of the adsorbed gases. The sensing material encounters resistance equal to its initial value after gas molecules have been removed from the surface. A p-type 2D sensing material's resistance usually increases as it is subjected to reduced gas. In contrast, when the electrons from the reducing gas are transferred to the metal oxide's conduction band, the resistance of the sensor falls in the case of metal oxide. However, the incorporation of the metal oxides into 2D TMDs can improve the gas-sensing capabilities resulted from the synergistic effect of the hybrid material. Researchers have widely studied the synergistic interactions of 2D-TMD and metal oxide hybrid materials, as well as their sensing mechanism.

Hydrothermally synthesized 2D-TMD, MoS_2 nanosheets with SnO_2 NPs, were found to be promising for the detection of NH_3 at RT.[189] This nanocomposite demonstrated responses of about 2080 towards 200 ppm of NH_3 with a quick response time and good reproducibility. The formation of nanocomposite facilitates the charge transfer process and the interaction with NH_3 gas molecules. Similarly, Kaur et al. prepared a RT NH_3 gas sensor by making thin film of consisting of a n-type MoS_2/p-type CuO nanoworm heterojucntion on a glass substrate coated with indium tin using the magnetic sputtering method.[190] The response (47%) and response time (17 s) with outstanding repeatability toward 100 ppm of NH_3 gas were shown by the resultant gas sensor device.

Wang et al. used a template-free hydrothermal method to synthesize quasi-2D mesoporous $ZnSnO_3$ nanomaterials (QTMZNS) (Figure 18a) for the detection of formaldehyde (Figure 18b).[191] A mixture of $Zn_5(OH)_6(CO_3)_2$ and $ZnSnO_3$ solutions was heated under hydrothermal conditions to create the high-purity QTMZNS, which was characterized by different techniques, such as XRD, TG/DTA, FTIR, SEM, and TEM (Figure 18c). The mechanism of quasi-crystal growth and its impact on the 2D mesoporous structure along with its gas-sensitivity characteristics were also discussed in the report. When exposed to the vapors of formaldehyde, the

sensor displayed strong gas sensitivity and detection capabilities.

The sensing mechanism of this QTMZNS material involves a change in electrical conductivity at the surface, which is due to a cyclic adsorption, oxidation, and desorption process.[192,193] The surface layer of the QTMZNS sensor becomes heavily adsorbed with oxygen when it is exposed to the air, causing significant oxygen adsorption by accepting electrons. At the working temperature, this adsorption process caused the oxygen species to change into oxygen ions and created a layer that was lacking in electrons. Consequently, the material's resistance increases. Interaction with formaldehyde vapor at the surface results in the release of oxygen and electrons into the sensor material, thereby decreasing its resistance. The large specific surface area of the material, $ZnSnO_3$, helps the conduction band, because it generates more voids and contact areas, as well as lower band gap energies and more chemically active sites. Adsorption is facilitated by special nanopores with perforations that shorten the path of gas diffusion. Thus, a high surface area, chemically adsorbed oxygen, and open nanoholes can enhance the sensing efficiency. Table 1 compares a few widely used nanomaterial-based gas sensors with various dimensional nanomaterials.

Hashtroudi et al. studied the impacts of 2D hybrid nanomaterial devices consisting of layered transition metal dichalcogenides (TMDs) and graphene on the sensing ability of gases at ambient temperature.[194] By functionalizing the surface with metals or polymers, increasing the surface area, making nanocomposites, or creating heterojunction layers, it is possible to improve the performance of sensing. The unique feature of this study is how the sensitivity, acceleration response, and recovery of the sensor are improved by the hybridization of several types of nanomaterials. The sensor's ability to detect gas is greatly enhanced by the interaction of the gas with the active surface of the sensor, which changes the resistance. The effectiveness of gas sensing is increased by the addition of new physical and electrical properties brought by gas molecules' interaction with the sensor device's surface. The thickness and quantity of reaction sites for interactions between gas molecules were modified through surface engineering. The electrical and heterojunction layers' con-

Table 1. Comparison of Some Commonly Used Nanomaterial-Based Gas Sensors

dimensions	sensing material	target gas	operating temp. (°C)	sensing conc. (ppm)	response	response time (s)	method of preparation	ref
0D	rGO−CD hybrid materials	NO_2	RT	25	120%	100	hydrothermal	65
	In_2O_3−CD	NO_2	50	500	130	9.6	hydrothermal	67
	ZnO−CD composite	NO	100	100	238	34	hydrothermal	70
	GaN−TiO_2	NO_2	RT	1	13.3	140	etching, sputtering	71
	ZnO−TeO_2 NW heterostructure	NO_2	RT	10	2.1	20	thermal evaporation, atomic layer deposition	75
	Au−PAni composite	CO	RT	6000	27%	180	ultrasound mixing	76
	ZnO−Au NPs	NO_2	RT	1	169%	100	ultrasonication	79
	Au NPs−MUA-coated electrode	o-xylene	RT	100		57	laser writing technology	82
	Au NPs−PbS NCs	CH_4	RT	10000	47.6%		drop-casting	85
1D	Pd−SnO_2 NWs	H_2	300	100	56	22	VLS growth	89
	Au NPs−Ga_2O_3 NWs	CO	RT	100	5%	21	VLS growth	91
	SnO_2 NWs	H_2	125	1000	7.8		gas-phase reaction	87
	ZnO − Si NWs	NO	RT	10	35%	130	chemical solution deposition	93
	V_2O_5 NW − TiO_2	Ozone	300	1.25	1.4	60	hydrothermal	94
	SWCNTs−PEI	NO_2	RT	20	37%	240	CVD process	98
	MWCNTs−PAni	NH_3	RT	2	15.5%	6	oxidative polymerization	99
	CNT−ALFOMIP	Acetone	86	5	59	58	MW-assisted sol−gel	103
	fluorinated CNT	NH_3	RT	10000	11%	600	catalytic CVD	105
	carbyne nanocrystal (flakes)	NO_2	RT	2	1.5	90	LBL technology	107
	SnO_2−Cu_2O core−shell structure	C_6H_6	300	10	12.5	4	atomic layer deposition	111
2D	graphene−FMNS	NH_3	RT	1000	18.5%	900	ultrasonication	115
	GO−MTA	NH_3	RT	100	12%	60	LB technology	119
	mesoporous $ZnSnO_3$	HCHO	210	100	45.8	4	hydrothermal	191
	graphene−PAni	NH_3	RT	100	11.3%	50	magnetron sputtering	123
	MoS_2 nanosheets−SnO_2	NH_3	RT	200	2080	23	hydrothermal	189
	MoS_2−CuO nanoworms	NH_3	RT	100	47%	17	magnetron sputtering	190
	$Ti_3C_2T_x$ MXene	acetone	RT	0.05	0.97		fully functionalized surface	145
		ammonia	RT	0.1	0.80			
		ethanol	RT	0.1	1.7			
	Ti_3C_2 MXene	acetone	RT/	100	0.22		self-assembly	146
		ammonia	RT/	5	0.46			
		ethanol	RT	100	0.18			
	$Ti_3C_2T_x$ MXene	acetone	RT/	100	0.115		solution casting	148
		ammonia	RT/	100	0.075			
		ethanol	RT	100	0.21			
	S-doped $Ti_3C_2T_x$ MXene	toluene	RT	1	214%		drop-casting	149
	$Ti_3C_2T_x$ MXene/graphene fiber	ammonia	RT	10	6.77		wet-spinning process	151
	alkalized organ-like $Ti_3C_2T_x$ MXene	ammonia	RT	100	0.288		alkaline treatment	152
	$W_{18}O_{49}$ NR/$Ti_3C_2T_x$ MXene composite	acetone	RT	0.17		5.6	solvothermal	153
	$V_2C_2T_x$ MXene	acetone	RT	5	0.022		oxygen-functionalized	144
		H2	RT	2	0.243	120		
		methane	RT	25	0.016	480		
	$V_4C_3T_x$ MXene	acetone	RT	1	0.6	40	Al and Co as catalysts	154
	$Cu_3(HITP)_2$ MOF	ammonia	RT	0.5	2.5%		drop-casting on IDEs	159
	$Cu_3(HITP)_2$ MOF	ammonia	RT	0.5	129%		spraying LbL liquid-phase epitaxy	161
	$Cu_3(HITP)_2$ MOF	methanol	RT		125%		spray-coating on glass slide	163
	UiO-66-NH_2 MOF	NO_2	150	10	7.6%		powder pellet between electrodes	164
	5 nm ZIF-8/ZIF-67 MOF coated ZnO NWs	acetone	260	10	27	43	solution casting	167
	ZIF-8 MOF-coated ZnO NRs	HCHO	300	100		16	hydrothermal	168
	110 nm ZIF-8-coated ZnO NRs	H_2	250	50	3.28		solution casting	170
	ZIF-8-coated In_2O_3 NFs	NO_2	140	1	16.4		electrospining	172
	ZIF-67-coated SnO_2 NPs	CO_2	205	5000	16.5		solution casting	173
	ZIf-8@Pd@ZnO NW core	H2	200	50	6.7		VLS-ALD-Solvothermal	175
	HMP-TAPB-1 COF	ammonia	RT	50	16.6	65	amine condensation	186
	COF-DC-8	ammonia	RT	40	39%		condensation reaction	187

ductivity, charge transfer, and Fermi properties at their interfaces modify the longitudinal energy disparities that govern the current carrying flow. Surface functionalization and special processing enhance selectivity, sensitivity, and particular sensing properties, as well as significantly enhancing the sensor's performance when utilized in a natural environment and its capacity to detect gases.

6. SUMMARY AND FUTURE SCOPE

The effectiveness of a gas sensor is decided by many parameters, such as low power consumption, exceptionally high sensitivity at very low gas concentrations, high accuracy, rapid reaction, selectivity, response time, stability, great reversibility, and other environmental conditions, as well as the cost of production of the sensor. In this Review, the fabrication of gas sensors made of nanomaterials with different dimensionalities, their sensing effectiveness, and their preparation methods, along with the sensing mechanism, were discussed. From the reported literature, it is found that the sensing behavior of the nanomaterial-based sensors exhibited varied degree of success toward a particular gas and was also influenced by the synthesis routes besides the nature of materials and their morphology. A comparison of different parameters for some widely used nanomaterial-based gas sensors with varying dimensionality and synthesis methods is presented in Table 1. The performance of the gas sensor device can be tuned as per requirement by controlling the morphologies of the nanomaterials used. Depending on the synthesis routes, nanomaterials with various types of surface morphologies can be obtained. A wide range of synthesis processes, such as hydrothermal, sol−gel, ultrasonication, solution-phase reaction, solid-state reaction, vapor-phase reaction, and etching processes, have been employed for the fabrication of nanomaterials. Again, processes like drop casting, sputtering, CVD, ALD, and LbL technology are used for the fabrication of sensor devices. All these synthesis processes have their own advantages and disadvantages. The mechanisms of gas sensing have also some impact on the gas sensing ability of different nanomaterials. The merits and demerits of different mechanisms are discussed in the earlier section (section 2). Among various mechanisms, the resistive based gas sensors are more popular due to their many advantages but have limited applications in mobile and portable devices because of their high operation temperature, high energy consumption, and sensitivity toward contaminants.

The dimensions of nanomaterials used for gas sensing devices influence their performance. For instance, delocalization of electrons may occur along the axial direction for 1D nanomaterials, but in case of 2D nanomaterials electrons remain restricted within and conduction occurs across their thickness. However, whatever the dimensions may be, the homogeneous surfaces of the nanomaterials cause the development of electron depletion layer. The nanomaterials with higher volume-to-surface area generally performed better as gas sensors. Again, the crystalline structures fared better compared to the amorphous structures. For this reason, nanostructures with rougher surfaces are preferred over those with smoother surfaces for better response.

In addition, it was observed that the sensitivity of the nanomatrerial-based gas sensors is dependent on their morphology. Large surface area, greater sensitivity and selectivity, stability, low weight, lower power consumption, and quick response are some of the merits of NWs and useful

in detecting a wide range of gases. However, the higher temperature condition for synthesis processes of NWs, compared to that for NRs, is one of its drawbacks. Similarly, NRs are also found to be good candidates for gas sensing devices because of their large surface area with a highly active surface for adsorption and powerful charge carrying capacity. Among 1D nanomaterials, NTs benefit from their hollow tubular structures with large surface area (both inner and outer) and small grain sizes. The reactivity of various NTs varies toward target gases as they withdraw or supply electrons to the adsorbed gas molecules depending on their nature. However, this behavior is not quite reliable. On the other hand, 0D NPs having distinctive optical and electrochemical properties are usually preferred for the modification of the surface of the substrates to increase the surface area and to alter the electronic properties for adsorption and interaction with the analyte. Similarly, 2D nanomaterials like graphene sheets and MoS_2 nanosheets benefit as better performing gas sensors from their exceptional conductive path and thickness that can be controlled easily.

From the reported literature, it is very much clear that the sensing performance of gas sensors based on nanomaterials toward a given gas can be improved by modifying their surface states and/or bulk properties. This modification can be achieved by metal doping, coating, or functionalizing their surfaces with other materials. This enhancement in the sensor's performance is attributed to the electrical conductance modulation and/or alternation in the adsorption process obtained after modifications.

The sensing performance of litchi-like In_2O_3 toward NO_2 increased significantly after being combined with CDs. Similarly, high NO response was observed for flower-like microspheres of the ZnO/CDs composite in comparison to bare ZnO microspheres. Functionalization of GaN submicrometer wires with TiO_2 and TeO_2 NWs with ZnO produced improved selectivity and sensitivity toward NO_2. However, in the later case, the response and response time were found to be significantly better, which may be attributed to the fabrication process of the materials (Table 1). Among different metal NPs, Au NPs, due to their biocompatibility, high density, high conductivity, and high dielectric constant, were preferred for preparing composites with conducting polymers (PAni), metal oxide (ZnO NWs), and metal sulfide (PbS NCs) to achieve improved sensing results at RT for toxic gases like CO, NO_2, and CH_4 gas, respectively. The amount of Au NPs has an impact on the sensor's performance. Enhanced sensing behavior toward CO was also exhibited by Ga_2O_3 NWs when modified with Au-NPs. In addition, the composites of metal NWs (Si NWs) and metal oxide NWs (V_2O_5 NWs), respectively, with ZnO and TiO_2 NPs were found to exhibit better gas sensing behavior due to the formation of heterojunctions. Furthermore, the gas sensing characteristics of CNTs with surface modification, combined with their superior electrical conductivity, large surface area, and hollow structure, were found to be exciting compared to the bare CNTs. The core−shell structure of SnO_2 NWs-Cu_2O exhibited very good response toward benzene, but its operating temperature was quite high (300 °C). The gas sensors consisting of 2D nanomaterials like graphene have shown good sensing behavior because of their ability to lower the working temperature and enhance recovery. However, their sensing capacities toward NH_3 are improved upon surface modification with MTA or PAni. 2D TMD MoS_2 nanosheets

were also used to form composites with metal oxides (SnO_2 and CuO), which exhibited good sensing ability toward NH_3 compared to bare MoS_2.

Graphene like 2D MXene nanomaterials are another type of promising materials for gas sensing applications due to their high electronegativity and surface area, which helps improve their surface reaction with gas analyte, leading to changes in their resistivity or conductivity. An adsorption/desorption-type charge transfer mechanism is followed for the sensing process. Other advantages of MXene-based gas sensors are their higher selectivity and sensitivity. Further, the layer spacing and resistivity of MXenes can be manipulated because of their hydrophilic nature, which makes them mix easily with other substances. Using MXenes, it is possible to make a composite membrane on any rigid or flexible surfaces. The beauty of the MXenes is they can react with both oxidizing gas molecules by giving electrons and with VOCs by accepting electrons. Similar to other nanomaterials, MXene-based gas sensors demonstrated higher selectivity and sensitivity upon surface functionalization or metal implantation. MXenes and their composite can be used for detection of a wide range of gases including VOCs, NH_3, and NO_2. For example, titanium carbide-based MXenes can detect acetone, ethanol, and ammonia. However, its overall sensing behavior improved upon surface functionalization/modification. Compared to titanium carbide-based MXenes, vanadium carbide-based MXenes can sense lower concentrations of acetone under the same environmental conditions (Table 1).

MOFs have advantages like porosity-assisted high surface area and coordinative active metal sites with terminated functional groups for greater gas uptake and transportation. The other benefits of possible manipulation of pore size or geometry and their nature in MOFs provides them with higher sensitivity and selectivity toward specific target molecules. In addition, some MOFs have excellent thermal and chemical stability along with reproducibility. The MOF-based gas sensors discussed showed remarkable sensing behavior toward a wide range of gases like ammonia, acetone, methanol, HCHO, H_2, CO_2, NO_2, etc. The MOFs have also been used as coating materials on metal oxide to fabricate a sensor device, where they mainly act as molecular sieves, thereby increasing the selectivity toward a particular gas. On the other hand, COFs have merits like layered structures with weak out-of-plane van der Waals force, high stability, porosity, conductivity, and crystallinity. However, in contrast to MOF-based chemiresistive gas sensors, the application of COFs as gas sensors are limited by their complicated synthesis process and difficulty in generating a stable electrode contact and controlling the crystallinity.

In conclusion, compared to conventional sensors, using gas sensors made of nanostructured materials has a number of benefits. Future generations of gas sensors may take a new turn thanks to the multiple functional properties of nanomaterial-based gas sensors, such as high sensitivity, superior gas detection capability, and high selectivity. In order to address the problem of gas sensors' sensitivity and gas detection capability, this might be helpful. As a result, nanomaterials' applications in gas sensing have recently caught the attention of researchers all over the world. The performances of some gas sensors, in terms of sensitivity and selectivity to test gases at RT, were found to be excellent for practical use. In the field of nanomaterial-based gas sensors, we are hopeful that this Review article will contribute to better advancement.

6.1. Future Scope of Work. In spite of the remarkable progress that is achieved in the field of nanomaterial-based gas sensors, there are still many questions and challenges that need to be addressed for the fabrication of devices for real life applications under different environmental conditions. First, the responses of some of the gas sensors toward very low analyte concentration are found to be not very exciting, which may be due to the influence of temperature and humidity factors. Therefore, the study of the influence of moisture on adsorption and desorption process of analyte molecules under humid conditions may be one of the future scope of research in this field. Second, as little attention is given to 2D TMD materials compared to graphene-based gas sensors, the fabrication and the synergistic electronic and chemical effects of 2D TMD and metal oxide hybrid systems on the gas sensing performance needs thorough investigation. Moreover, there is also scope to design 2D hybrid materials for the detection of VOCs and nonpolar gas molecules with larger size. Third, in spite of having many advantages and better performance, MXene based gas sensors have challenges like oxidation and stability issues in the presence of oxygen and moisture, which need further research attention. Fourth, more efforts are required to address the challenges like long-term stability of MOF-based gas sensors under real life conditions. Finally, extensive research efforts require to be directed toward the innovative design of high performance gas sensor devices with better stability for applications under different environmental conditions, such as in industries. Manipulation of the dimension and the morphology of the gas sensing materials may be a key feature in achieving these aspects of the gas sensors.

■ ASSOCIATED CONTENT

Data Availability Statement

The article itself, the associated supporting materials, or getting in touch with the relevant author can all provide access to the data utilized in this investigation.

■ AUTHOR INFORMATION

Corresponding Authors

Pravas Kumar Panigrahi — *Department of Basic Science, Government College of Engineering, Kalahandi, Odisha 766003, India*; Email: pkp@gcekbpatna.ac.in, pravas.iit@gmail.com

Nagaprasad Puvvada — *Department of Chemistry, School of Advanced Sciences, VIT-AP University, Vijayawada, Andhra Pradesh 522237, India*; ⊙ orcid.org/0000-0001-6444-1348; Email: nagaprasad.p@vitap.ac.in, nagaprasadiitkgp@gmail.com

Author

Basavaiah Chandu — *Department of Nanotechnology, Acharya Nagarjuna University, Guntur, Andhra Pradesh 522510, India*

Complete contact information is available at:
https://pubs.acs.org/10.1021/acsomega.3c06533

Notes

The authors declare no competing financial interest.

■ ACKNOWLEDGMENTS

◾ REFERENCES

(1) Nandy, T.; Coutu, R. A.; Ababei, C. Carbon Monoxide Sensing Technologies for Next-Generation Cyber-Physical Systems. *Sensors* **2018**, *18*, 3443.

(2) Kamal, M. S.; Razzak, S. A.; Hossain, M. M. Catalytic Oxidation of Volatile Organic Compounds (VOCs) - A Review. *Atmos. Environ.* **2016**, *140*, 117−134.

(3) Jung, S. J.; Mehta, J. S.; Tong, L. Effects of Environment Pollution on the Ocular Surface. *Ocul. Surf.* **2018**, *16*, 198−205.

(4) Brugha, R.; Edmondson, C.; Davies, J. C. Outdoor Air Pollution and Cystic Fibrosis. *Paedi. Respir. Rev.* **2018**, *28*, 80−86.

(5) Bernstein, J. A.; Alexis, N.; Bacchus, H.; Bernstein, I. L.; Fritz, P.; Horner, E.; Li, N.; Mason, S.; Nel, A.; Oullette, J.; Reijula, K.; Reponen, T.; Seltzer, J.; Smith, A.; Tarlo, S. M. The Health Effects of Nonindustrial Indoor Air Pollution. *J. Allergy Clin. Immunol.* **2008**, *121*, 585−591.

(6) Beaubien, S. E.; Ciotoli, G.; Lombardi, S. Carbon Dioxide and Radon Gas Hazard in the Alban Hills Area (Central Italy). *J. Volcanol. Geotherm. Res.* **2003**, *123*, 63−80.

(7) Gao, X.; Sun, Y.; Zhu, C.; Li, C.; Ouyang, Q.; Chen, Y. Highly Sensitive and Selective H2S Sensor Based on Porous $ZnFe_2O_4$ Nanosheets. *Sens. Actuators, B* **2017**, *246*, 662−672.

(8) Van Dang, T.; Duc Hoa, N.; Van Duy, N.; Van Hieu, N. Chlorine Gas Sensing Performance of On-Chip Grown ZnO, WO_3, and SnO_2 Nanowire Sensors. *ACS Appl. Mater. Interfaces* **2016**, *8*, 4828−4837.

(9) Yadav, A.; Indurkar, P. D. Gas Sensor Applications in Water Quality Monitoring and Maintenance. *Water Conserv. Sci. Eng.* **2021**, *6*, 175−190.

(10) Sharma, S.; Madou, M. A New Approach to Gas Sensing with Nanotechnology. *Philosophical Transactions of the Royal Society A: Mathematical, Phys. Eng. Sci.* **2012**, *370*, 2448−2473.

(11) Patra, M.; Manzoor, K.; Manoth, M.; Negi, S.; Vadera, S.; Kumar, N. Nanotechnology Applications for Chemical and Biological Sensors. *Def. Sci. J.* **2008**, *58*, 636−649.

(12) Jiménez-Cadena, G.; Riu, J.; Rius, F. X. Gas Sensors Based on Nanostructured Materials. *Analyst* **2007**, *132*, 1083−1099.

(13) Jeevanandam, J.; Barhoum, A.; Chan, Y. S.; Dufresne, A.; Danquah, M. K. Review on Nanoparticles and Nanostructured Materials: History, Sources, Toxicity and Regulations. *Beilstein J. Nanotechnol.* **2018**, *9*, 1050−1074.

(14) Xu, K.; Fu, C.; Gao, Z.; Wei, F.; Ying, Y.; Xu, C.; Fu, G. Nanomaterial-Based Gas Sensors: A Review. *Instrument. Sci. Technol.* **2018**, *46*, 115−145.

(15) Zhu, G.; Guo, L.; Shen, X.; Ji, Z.; Chen, K.; Zhou, H. Monodispersed In2O3Mesoporous Nanospheres: One-Step Facile Synthesis and the Improved Gas-Sensing Performance. *Sens. Actuators, B* **2015**, *220*, 977−985.

(16) Rai, P.; Kim, Y.-S.; Song, H. M.; Song, M. K.; Yu, Y. T. The Role of Gold Catalyst on the Sensing Behavior of ZnO Nanorods for CO and NO2 Gases. *Sens. Actuators, B* **2012**, *165*, 133−142.

(17) Oh, E.; Choi, H. Y.; Jung, S. H.; Cho, S.; Kim, J. C.; Lee, K. H.; Kang, S. W.; Kim, J.; Yun, J. Y.; Jeong, S. H. High-Performance NO2 Gas Sensor Based on ZnO Nanorod Grown by Ultrasonic Irradiation. *Sens. Actuators, B* **2009**, *141*, 239−243.

(18) Majhi, S. M.; Rai, P.; Raj, S.; Chon, B.-S.; Park, K. K.; Yu, Y. T. Effect of Au Nanorods on Potential Barrier Modulation in Morphologically Controlled $Au@Cu_2O$ Core-Shell Nanoreactors for Gas Sensor Applications. *ACS Appl. Mater. Interfaces* **2014**, *6*, 7491−7497.

(19) Han, D.; Ji, Y.; Gu, F.; Wang, Z. Cobalt Oxide Nanorods with Special Pore Structure for Enhanced Ethanol Sensing Performance. *J. Colloid Interface Sci.* **2018**, *531*, 320−330.

(20) Lyson-Sypien, B.; Radecka, M.; Rekas, M.; Swierczek, K.; Michalow-Mauke, K.; Graule, T.; Zakrzewska, K. Grain-Size-Dependent Gas-Sensing Properties of TiO_2 Nanomaterials. *Sens. Actuators, B* **2015**, *211*, 67−76.

(21) Ayesh, A. I. Metal/Metal-Oxide Nanoclusters for Gas Sensor Applications. *J. Nanomater.* **2016**, *2016*, 2359019.

(22) Hoa, N. D.; Duy, N. V.; El-Safty, S. A.; Hieu, N. V. Meso-/Nanoporous Semiconducting Metal Oxides for Gas Sensor Applications. *J. Nanomater.* **2015**, *2015*, 972025.

(23) Sinha, N.; Ma, J.; Yeow, J. T. W. Carbon Nanotube-Based Sensors. *J. Nanosci. Nanotechnol.* **2006**, *6*, 573−590.

(24) Tian, Z. R.; Voigt, J. A.; Liu, J.; Mckenzie, B.; Mcdermott, M. J.; Rodriguez, M. A.; Konishi, H.; Xu, H. Complex and Oriented ZnO Nanostructures. *Nat. Mater.* **2003**, *2*, 821−826.

(25) Torres, I.; Mehdi Aghaei, S.; Rabiei Baboukani, A.; Wang, C.; Bhansali, S. Individual Gas Molecules Detection Using Zinc Oxide-Graphene Hybrid Nanosensor: A DFT Study. *C* **2018**, *4*, 44.

(26) Pippara, R. K.; Chauhan, P. S.; Yadav, A.; Kishnani, V.; Gupta, A. Room Temperature Hydrogen Sensing with Polyaniline/SnO_2/Pd Nanocomposites. *Micro Nano Eng.* **2021**, *12*, 100086.

(27) Biswal, H. J.; Yadav, A.; Vundavilli, P. R.; Gupta, A. High Aspect ZnO Nanorod Growth over Electrodeposited Tubes for Photocatalytic Degradation of EtBr Dye. *RSC Adv.* **2021**, *11*, 1623−1634.

(28) Bhati, V. S.; Ranwa, S.; Fanetti, M.; Valant, M.; Kumar, M. Efficient Hydrogen Sensor Based on Ni-Doped ZnO Nanostructures by RF Sputtering. *Sens. Actuators, B* **2018**, *255*, 588−597.

(29) Krishnan, S. K.; Singh, E.; Singh, P.; Meyyappan, M.; Nalwa, H. S. A Review on Graphene-Based Nanocomposites for Electrochemical and Fluorescent Biosensors. *RSC Adv.* **2019**, *9*, 8778−8881.

(30) Singh, E.; Meyyappan, M.; Nalwa, H. S. Flexible Graphene-Based Wearable Gas and Chemical Sensors. *ACS Appl. Mater. Interfaces* **2017**, *9*, 34544−34586.

(31) Pal, P.; Yadav, A.; Chauhan, P. S.; Parida, P. K.; Gupta, A. Reduced Graphene Oxide Based Hybrid Functionalized Films for Hydrogen Detection: Theoretical and Experimental Studies. *Sens. Inter.* **2021**, *2*, 100072.

(32) Zhang, J.; Qin, Z.; Zeng, D.; Xie, C. Metal-Oxide-Semi-conductor Based Gas Sensors: Screening, Preparation, and Integration. *Phys. Chem. Chem. Phys.* **2017**, *19*, 6313−6329.

(33) Choi, K. J.; Jang, H. W. One-Dimensional Oxide Nanostructures as Gas-Sensing Materials: Review and Issues. *Sensors* **2010**, *10*, 4083−4099.

(34) Shingange, K.; Tshabalala, Z. P.; Ntwaeaborwa, O. M.; Motaung, D. E.; Mhlongo, G. H. Highly Selective NH3 Gas Sensor Based on Au Loaded ZnO Nanostructures Prepared Using Microwave-Assisted Method. *J. Colloid Interface Sci.* **2016**, *479*, 127−138.

(35) Wang, Z.; Zhang, T.; Zhao, C.; Han, T.; Fei, T.; Liu, S.; Lu, G. Anchoring Ultrafine Pd Nanoparticles and SnO_2 Nanoparticles on Reduced Graphene Oxide for High-Performance Room Temperature NO2 Sensing. *J. Colloid Interface Sci.* **2018**, *514*, 599−608.

(36) Majhi, S. M.; Naik, G. K.; Lee, H. J.; Song, H. G.; Lee, C. R.; Lee, I. H.; Yu, Y. T. Au@NiO Core-Shell Nanoparticles as a p-Type Gas Sensor: Novel Synthesis, Characterization, and Their Gas Sensing Properties with Sensing Mechanism. *Sens. Actuators, B* **2018**, *268*, 223−231.

(37) Gomes, J. B. A.; Rodrigues, J. J. P. C.; Rabêlo, R. A. L.; Kumar, N.; Kozlov, S. IoT-Enabled Gas Sensors: Technologies, Applications, and Opportunities. *Journal of Sensor and Actuator Networks* **2019**, *8* (4), 57.

(38) Dickinson, T. A.; White, J.; Kauer, J. S.; Walt, D. R. Current Trends in`artificial-Nose' Technology. *Trends Biotechnol.* **1998**, *16*, 250−258.

(39) Kohl, D. Function and Applications of Gas Sensors. *J. Phys. D: Appl. Phys.* **2001**, *34*, R125.

(40) Panneerselvam, G.; Thirumal, V.; Pandya, H. M. Review of Surface Acoustic Wave Sensors for the Detection and Identification of Toxic Environmental Gases/Vapours. *Arch. Acoust.* **2018**, *43*, 357−367.

(41) Lahrmann, A.; Tschulena, G. R. The Increasing Importance of Sensors in Household Appliances. In *Sensors in Household Appliances*; Sensors Applications, Vol. *5*; John Wiley & Sons, Ltd, 2003; pp 1−8.

(42) Azad, A. M.; Akbar, S. A.; Mhaisalkar, S. G.; Birkefeld, L. D.; Goto, K. S. Solid-State Gas Sensors: A Review. *J. Electrochem. Soc.* **1992**, *139*, 3690.

(43) Fonollosa, J.; Solórzano, A.; Marco, S. Chemical Sensor Systems and Associated Algorithms for Fire Detection: A Review. *Sensors* **2018**, *18*, 553.

(44) Bhati, V. S.; Hojamberdiev, M.; Kumar, M. Enhanced Sensing Performance of ZnO Nanostructures-Based Gas Sensors: A Review. *Energy Rep.* **2020**, *6*, 46−62.

(45) Alenezi, M. R.; Henley, S. J.; Emerson, N. G.; Silva, S. R. P. From 1D and 2D ZnO Nanostructures to 3D Hierarchical Structures with Enhanced Gas Sensing Properties. *Nanoscale* **2014**, *6*, 235−247.

(46) Nasiri, N.; Clarke, C. Nanostructured Gas Sensors for Medical and Health Applications: Low to High Dimensional Materials. *Biosensors* **2019**, *9*, 43.

(47) Tian, X.; Cui, X.; Lai, T.; Ren, J.; Yang, Z.; Xiao, M.; Wang, B.; Xiao, X.; Wang, Y. Gas Sensors Based on TiO₂ Nanostructured Materials for the Detection of Hazardous Gases: A Review. *Nano Mater. Sci.* **2021**, *3*, 390−403.

(48) Chowdhury, N. K.; Bhowmik, B. Micro/Nanostructured Gas Sensors: The Physics behind the Nanostructure Growth, Sensing and Selectivity Mechanisms. *Nanoscale Adv.* **2021**, *3*, 73−93.

(49) Sun, Y. F.; Liu, S. B.; Meng, F. L.; Liu, J. Y.; Jin, Z.; Kong, L. T.; Liu, J. H. Metal Oxide Nanostructures and Their Gas Sensing Properties: A Review. *Sensors (Basel)* **2012**, *12*, 2610−2631.

(50) Xue, S.; Cao, S.; Huang, Z.; Yang, D.; Zhang, G. Improving Gas-Sensing Performance Based on MOS Nanomaterials: A Review. *Materials* **2021**, *14*, 4263.

(51) Zhang, H.; Chen, W.-G.; Li, Y.-Q.; Song, Z.-H. Gas Sensing Performances of ZnO Hierarchical Structures for Detecting Dissolved Gases in Transformer Oil: A Mini Review. *Front. Chem.* **2018**, *6*, 508.

(52) Zhou, T.; Zhang, T. Insights into the Gas Sensor Materials: Synthesis, Performances and Devices. *Sens. Actuators, B* **2022**, *371*, 132565.

(53) Zhang, H.; Guo, Y.; Meng, F. Gas-Sensing Characteristics of Metal Oxide Semiconductor Sensors. *Encyclopedia*, June 20, 2022. https://encyclopedia.pub/entry/24585 (accessed 2023-11-10).

(54) Nakate, U. T.; Singh, V. K.; Yu, Y. T.; Park, S. WO3 Nanorods Structures for High-Performance Gas Sensing Application. *Mater. Lett.* **2021**, *299*, 130092.

(55) Yuan, Z.; Yang, C.; Meng, F. Strategies for Improving the Sensing Performance of Semiconductor Gas Sensors for High-Performance Formaldehyde Detection: A Review. *Chemosensors* **2021**, *9*, 179.

(56) Song, R.; Wang, Z.; Zhou, X.; Huang, L.; Chi, L. Gas-Sensing Performance and Operation Mechanism of Organic π-Conjugated Materials. *Chem. Plus. Chem.* **2019**, *84*, 1222−1234.

(57) Tian, F.; Jiang, A.; Yang, T.; Qian, J.; Liu, R.; Jiang, M. Application of Fractal Geometry in Gas Sensor: A Review. *IEEE Sensors Journal* **2021**, *21*, 14587−14600.

(58) Firth, J. G.; Jones, A.; Jones, T. A. The Principles of the Detection of Flammable Atmospheres by Catalytic Devices. *Combust. Flame* **1973**, *20*, 303−311.

(59) Yunusa, Z.; Hamidon, M. N.; Kaiser, A.; Awang, Z. Gas Sensors: A Review. *Sens. Transducers* **2014**, *168*, 61−75.

(60) Grattan, K. T. V.; Sun, T. Fiber Optic Sensor Technology: An Overview. *Sens. Actuators,A* **2000**, *82*, 40−61.

(61) Ji, H.; Zeng, W.; Li, Y. Gas Sensing Mechanisms of Metal Oxide Semiconductors: A Focus Review. *Nanoscale* **2019**, *11*, 22664−22684.

(62) Caliendo, C.; Verardi, P.; Verona, E.; D'Amico, A.; Natale, C. D.; Saggio, G.; Serafini, M.; Paolesse, R.; Huq, S. E. Advances in SAW-Based Gas Sensors. *Smart Mater. Struct.* **1997**, *6*, 689−699.

(63) Khlebarov, Z. P.; Stoyanova, A. I.; Topalova, D. I. Surface Acoustic Wave Gas Sensors. *Sens. Actuators, B* **1992**, *8*, 33−40.

(64) Yang, H.; Zhou, B.; Zhang, Y.; Liu, H.; Liu, Y.; He, Y.; Xia, S. Valorization of Expired Passion Fruit Shell by Hydrothermal Conversion into Carbon Quantum Dot: Physical and Optical Properties. *Waste Biomass Valor.* **2021**, *12*, 2109−2117.

(65) Hu, J.; Zou, C.; Su, Y.; Li, M.; Hu, N.; Ni, H.; Yang, Z.; Zhang, Y. Enhanced NO₂ Sensing Performance of Reduced Graphene Oxide by in Situ Anchoring Carbon Dots. *J. Mater. Chem. C* **2017**, *5*, 6862−6871.

(66) Miller, D. R.; Akbar, S. A.; Morris, P. A. Nanoscale Metal Oxide-Based Heterojunctions for Gas Sensing: A Review. *Sens. Actuators, B* **2014**, *204*, 250−272.

(67) Cheng, M.; Wu, Z.; Liu, G.; Zhao, L.; Gao, Y.; Li, S.; Zhang, B.; Yan, X.; Geyu, L. Carbon Dots Decorated Hierarchical Litchi-like In₂O₃ Nanospheres for Highly Sensitive and Selective NO₂ Detection. *Sens. Actuators, B* **2020**, *304*, 127272.

(68) Kou, X.; Wang, C.; Ding, M.; Feng, C.; Li, X.; Ma, J.; Zhang, H.; Sun, Y.; Lu, G. Synthesis of Co-Doped SnO₂ Nanofibers and Their Enhanced Gas-Sensing Properties. *Sens. Actuators, B* **2016**, *236*, 425−432.

(69) Wang, Y.; Zhang, B.; Liu, J.; Yang, Q.; Cui, X.; Gao, Y.; Chuai, X.; Liu, F.; Sun, P.; Liang, X.; Sun, Y.; Lu, G. Au-Loaded Mesoporous WO3: Preparation and n-Butanol Sensing Performances. *Sens. Actuators, B* **2016**, *236*, 67−76.

(70) Yu, Z.; Zhang, L.; Wang, X.; He, D.; Suo, H.; Zhao, C. Fabrication of ZnO/Carbon Quantum Dots Composite Sensor for Detecting NO Gas. *Sensors* **2020**, *20*, 4961.

(71) Khan, M. A. H.; Thomson, B.; Debnath, R.; Rani, A.; Motayed, A.; Rao, M. V. Reliable Anatase-Titania Nanoclusters Functionalized GaN Sensor Devices for UV Assisted NO₂ Gas-Sensing in Ppb Level. *Nanotechnol.* **2020**, *31*, 155504.

(72) Henderson, M. A.; Epling, W. S.; Perkins, C. L.; Peden, C. H. F.; Diebold, U. Interaction of Molecular Oxygen with the Vacuum-Annealed TiO₂(110) Surface: Molecular and Dissociative Channels. *J. Phys. Chem. B* **1999**, *103*, 5328−5337.

(73) Lee, F. K.; Andreatta, G.; Benattar, J.-J. Role of Water Adsorption in Photoinduced Superhydrophilicity on TiO₂ Thin Films. *Appl. Phys. Lett.* **2007**, *90*, 181928.

(74) Wang, M.; Li, L.; Zhao, G.; Xu, Z.; Hussain, S.; Wang, M.; Qiao, G.; Liu, G. Influence of the Surface Decoration of Phosphorene with Ag Nanoclusters on Gas Sensing Properties. *Appl. Surf. Sci.* **2020**, *504*, 144374.

(75) Byoun, Y.; Jin, C.; Choi, S.-W. Strategy for Sensitive and Selective NO₂ Detection at Low Temperatures Utilizing P-Type TeO₂ Nanowire-Based Sensors by Formation of Discrete n-Type ZnO Nanoclusters. *Ceram. Int.* **2020**, *46* (11), 19365−19374.

(76) Nasresfahani, Sh.; Zargarpour, Z.; Sheikhi, M. H.; Nami Ana, S. F. Improvement of the Carbon Monoxide Gas Sensing Properties of Polyaniline in the Presence of Gold Nanoparticles at Room Temperature. *Synth. Met.* **2020**, *265*, 116404.

(77) Zhou, Z. Y.; Tian, N.; Li, J. T.; Broadwell, I.; Sun, S. G. Nanomaterials of High Surface Energy with Exceptional Properties in Catalysis and Energy Storage. *Chem. Soc. Rev.* **2011**, *40*, 4167−4185.

(78) Widmann, D.; Behm, R. J. Activation of Molecular Oxygen and the Nature of the Active Oxygen Species for CO Oxidation on Oxide Supported Au Catalysts. *Acc. Chem. Res.* **2014**, *47*, 740−749.

(79) Kim, D. W.; Park, K. H.; Lee, S. H.; Fàbrega, C.; Prades, J. D.; Jang, J. W. Plasmon Expedited Response Time and Enhanced Response in Gold Nanoparticles-Decorated Zinc Oxide Nanowire-Based Nitrogen Dioxide Gas Sensor at Room Temperature. *J. Colloid Interface Sci.* **2021**, *582*, 658−668.

(80) Asgar, H.; Jacob, L.; Hoang, T. B. Fast Spontaneous Emission and High Förster Resonance Energy Transfer Rate in Hybrid Organic/Inorganic Plasmonic Nanostructures. *J. Appl. Phys.* **2018**, *124*, 103105.

(81) Pescaglini, A.; Martín, A.; Cammi, D.; Juska, G.; Ronning, C.; Pelucchi, E.; Iacopino, D. Hot-Electron Injection in Au Nanorod-ZnO Nanowire Hybrid Device for Near-Infrared Photodetection. *Nano Lett.* **2014**, *14*, 6202−6209.

(82) Li, P.; Xia, H.; Dai, Y.-Z.; Yang, H.; Liu, T. Microsensor Based on Gold Nanoparticles for Fast and Sensitive Ortho-Xylene Detection. *IEEE Sens. J.* **2020**, *20*, 12552−12557.

(83) Yang, F.; Kung, S.-C.; Cheng, M.; Hemminger, J. C.; Penner, R. M. Smaller Is Faster and More Sensitive: The Effect of Wire Size on the Detection of Hydrogen by Single Palladium Nanowires. *ACS Nano* **2010**, *4*, 5233−5244.

(84) Steinecker, W. H.; Rowe, M. P.; Zellers, E. T. Model of Vapor-Induced Resistivity Changes in Gold-Thiolate Monolayer-Protected Nanoparticle Sensor Films. *Anal. Chem.* **2007**, *79*, 4977−4986.

(85) Mosahebfard, A.; Dehdashti Jahromi, H.; Sheikhi, M. H. Highly Sensitive, Room Temperature Methane Gas Sensor Based on Lead Sulfide Colloidal Nanocrystals. *IEEE Sens. J.* **2016**, *16*, 4174−4179.

(86) Roshan, H.; Mosahebfard, A.; Sheikhi, M. H. Effect of Gold Nanoparticles Incorporation on Electrical Conductivity and Methane Gas Sensing Characteristics of Lead Sulfide Colloidal Nanocrystals. *IEEE Sens. J.* **2018**, *18*, 1940−1945.

(87) Lin, J. Y.; He, X. L.; Zhang, A. J.; Huang, S. H.; Chen, Z. X. A Hall Effect Hydrogen-Selective Gas Sensor Based on SnO2 Nanowires Operating at Low Temperature. *J. Mater. Sci: Mater. Electron* **2019**, *30*, 20696−20702.

(88) Baraton, M. I.; Merhari, L.; Ferkel, H.; Castagnet, J. F. Comparison of the Gas Sensing Properties of Tin, Indium and Tungsten Oxides Nanopowders: Carbon Monoxide and Oxygen Detection. *Mater. Sci. Eng., C* **2002**, *19*, 315−321.

(89) Cai, Z.; Park, S. Synthesis of Pd Nanoparticle-Decorated SnO_2 Nanowires and Determination of the Optimum Quantity of Pd Nanoparticles for Highly Sensitive and Selective Hydrogen Gas Sensor. *Sens. Actuators, B* **2020**, *322*, 128651.

(90) Kim, J.-H.; Mirzaei, A.; Kim, H. W.; Kim, S. S. Pd Functionalization on ZnO Nanowires for Enhanced Sensitivity and Selectivity to Hydrogen Gas. *Sens. Actuators, B* **2019**, *297*, 126693.

(91) Weng, T. F.; Ho, M. S.; Sivakumar, C.; Balraj, B.; Chung, P. F. VLS Growth of Pure and Au Decorated β-Ga2O3 Nanowires for Room Temperature CO Gas Sensor and Resistive Memory Applications. *Appl. Surf. Sci.* **2020**, *533*, 147476.

(92) Nallagatla, V. R.; Jo, J.; Acharya, S. K.; Kim, M.; Jung, C. U. Confining Vertical Conducting Filament for Reliable Resistive Switching by Using a Au-Probe Tip as the Top Electrode for Epitaxial Brownmillerite Oxide Memristive Device. *Sci. Rep.* **2019**, *9*, 1188.

(93) Samanta, C.; Ghatak, A.; Raychaudhuri, A. K.; Ghosh, B. ZnO/Si Nanowires Heterojunction Array-Based Nitric Oxide (NO) Gas Sensor with Noise-Limited Detectivity Approaching 10 Ppb. *Nanotechnol.* **2019**, *30*, 305501.

(94) Avansi, W., Jr.; Catto, A. C.; da Silva, L. F.; Fiorido, T.; Bernardini, S.; Mastelaro, V. R.; Aguir, K.; Arenal, R. One-Dimensional V_2O_5/TiO2 Heterostructures for Chemiresistive Ozone Sensors. *ACS Appl. Nano Mater.* **2019**, *2*, 4756−4764.

(95) Wang, Y.; Zhou, Y.; Meng, C.; Gao, Z.; Cao, X.; Li, X.; Xu, L.; Zhu, W.; Peng, X.; Zhang, B.; Lin, Y.; Liu, L. A High-Response Ethanol Gas Sensor Based on One-Dimensional TiO_2/V_2O_5 Branched Nanoheterostructures. *Nanotechnol.* **2016**, *27*, 425503.

(96) Fu, H.; Yang, X.; An, X.; Fan, W.; Jiang, X.; Yu, A. Experimental and Theoretical Studies of V_2O_5@TiO2 Core-Shell Hybrid Composites with High Gas Sensing Performance towards Ammonia. *Sens. Actuators, B* **2017**, *252*, 103−115.

(97) Li, Z.; Xu, K.; Pan, Y. Recent Development of Supercapacitor Electrode Based on Carbon Materials. *Nanotechnol. Rev.* **2019**, *8*, 35−49.

(98) Kumar, S.; Pavelyev, V.; Mishra, P.; Tripathi, N. Thin Film Chemiresistive Gas Sensor on Single-Walled Carbon Nanotubes-Functionalized with Polyethylenimine (PEI) for NO_2gas Sensing. *Bull. Mater. Sci.* **2020**, *43*, 61.

(99) Abdulla, S.; Mathew, T. L.; Pullithadathil, B. Highly Sensitive, Room Temperature Gas Sensor Based on Polyaniline-Multiwalled Carbon Nanotubes (PANI/MWCNTs) Nanocomposite for Trace-Level Ammonia Detection. *Sens. Actuators, B* **2015**, *221*, 1523−1534.

(100) Ding, M.; Tang, Y.; Gou, P.; Reber, M. J.; Star, A. Chemical Sensing with Polyaniline Coated Single-Walled Carbon Nanotubes. *Adva. Mater.* **2011**, *23*, 536−540.

(101) Loghin, F. C.; Falco, A.; Salmeron, J. F.; Lugli, P.; Abdellah, A.; Rivadeneyra, A. Fully Transparent Gas Sensor Based on Carbon Nanotubes. *Sensors* **2019**, *19*, 4591.

(102) Colasanti, S.; Deep Bhatt, V.; Abdelhalim, A.; Lugli, P. 3D Percolative Model-Based Multiscale Simulation of Randomly Aligned Networks of Carbon Nanotubes. *IEEE Trans. Electron Devices* **2016**, *63*, 1346−1351.

(103) Rong, Q.; Li, K.; Wang, C.; Zhang, Y.; Chen, M.; Zhu, Z.; Zhang, J.; Liu, Q. Enhanced Performance of an Acetone Gas Sensor Based on Ag-LaFeO3 Molecular Imprinted Polymers and Carbon Nanotubes Composite. *Nanotechnology* **2020**, *31*, 405701.

(104) Wang, P.; Wang, D.; Zhang, M.; Zhu, Y.; Xu, Y.; Ma, X.; Wang, X. ZnO Nanosheets/Graphene Oxide Nanocomposites for Highly Effective Acetone Vapor Detection. *Sens. Actuators, B* **2016**, *230*, 477−484.

(105) Struzzi, C.; Scardamaglia, M.; Casanova-Chafer, J.; Calavia, R.; Colomer, J. F.; Kondyurin, A.; Bilek, M.; Britun, N.; Snyders, R.; Llobet, E.; Bittencourt, C. Exploiting Sensor Geometry for Enhanced Gas Sensing Properties of Fluorinated Carbon Nanotubes under Humid Environment. *Sens. Actuators, B* **2019**, *281*, 945−952.

(106) Katkov, M. V.; Sysoev, V. I.; Gusel'nikov, A. V.; Asanov, I. P.; Bulusheva, L. G.; Okotrub, A. V. A Backside Fluorine-Functionalized Graphene Layer for Ammonia Detection. *Phys. Chem. Chem. Phys.* **2015**, *17*, 444−450.

(107) Yang, F.; Zheng, Z.; Lin, Z.; Wang, B.; Liu, P.; Yang, G. Visible-Light-Driven Room-Temperature Gas Sensor Based on Carbyne Nanocrystals. *Sens. Actuators, B* **2020**, *316*, 128200.

(108) Saadi, L.; Lambert-Mauriat, C.; Oison, V.; Ouali, H.; Hayn, R. Mechanism of NO_x Sensing on WO3 Surface: First Principle Calculations. *Appl. Surf. Sci.* **2014**, *293*, 76−79.

(109) Kabcum, S.; Kotchasak, N.; Channei, D.; Tuantranont, A.; Wisitsoraat, A.; Phanichphant, S.; Liewhiran, C. Highly Sensitive and Selective NO_2 Sensor Based on Au-Impregnated WO3 Nanorods. *Sens. Actuators, B* **2017**, *252*, 523−536.

(110) Pytlicek, Z.; Bendova, M.; Prasek, J.; Mozalev, A. On-Chip Sensor Solution for Hydrogen Gas Detection with the Anodic Niobium-Oxide Nanorod Arrays. *Sens. Actuators, B* **2019**, *284*, 723−735.

(111) Kim, J. H.; Katoch, A.; Kim, S. H.; Kim, S. S. Chemiresistive Sensing Behavior of SnO_2 (n)-Cu2O (p) Core-Shell Nanowires. *ACS Appl. Mater. Interfaces* **2015**, *7* (28), 15351−15358.

(112) Zhang, X.; Hou, L.; Ciesielski, A.; Samorì, P. 2D Materials Beyond Graphene for High-Performance Energy Storage Applications. *Adv. Energy Mater.* **2016**, *6*, 1600671.

(113) Shao, Y.; Wang, J.; Wu, H.; Liu, J.; Aksay, I. A.; Lin, Y. Graphene Based Electrochemical Sensors and Biosensors: A Review. *Electroanalysis* **2010**, *22*, 1027−1036.

(114) Liu, X.; Ma, T.; Pinna, N.; Zhang, J. Two-Dimensional Nanostructured Materials for Gas Sensing. *Adv. Funct. Mater.* **2017**, *27*, 1702168.

(115) Huang, S.; Panes-Ruiz, L. A.; Croy, A.; Löffler, M.; Khavrus, V.; Bezugly, V.; Cuniberti, G. Highly Sensitive Room Temperature Ammonia Gas Sensor Using Pristine Graphene: The Role of Biocompatible Stabilizer. *Carbon* **2021**, *173*, 262−270.

(116) Khurshid, F.; Jeyavelan, M.; Takahashi, K.; Hudson, M. S. L.; Nagarajan, S. Aryl Fluoride Functionalized Graphene Oxides for Excellent Room Temperature Ammonia Sensitivity/Selectivity. *RSC Adv.* **2018**, *8*, 20440−20449.

(117) Zhou, J.; Lin, H.; Cheng, X. F.; Shu, J.; He, J. H.; Li, H.; Xu, Q. F.; Li, N. J.; Chen, D.-Y.; Lu, J.-M. Ultrasensitive and Robust Organic Gas Sensors through Dual Hydrogen Bonding. *Mater. Horiz.* **2019**, *6*, 554−562.

(118) Ahmed, M. A.; Monir, H. Q. M.; Al-Keisy, A. Evaluation of the Graphene Nanosheets as Gas Sensor for NH_3 via Electrical Properties. *Surf. Rev. Lett.* **2020**, *27*, 1950215.

(119) Kumar, R.; Kumar, A.; Singh, R.; kashyap, R.; Kumar, R.; Kumar, D.; Sharma, S. K.; Kumar, M. Room Temperature Ammonia Gas Sensor Using Meta Toluic Acid Functionalized Graphene Oxide. *Mater. Chem. Phys.* **2020**, *240*, 121922.

(120) Tang, S.; Cao, Z. Adsorption and Dissociation of Ammonia on Graphene Oxides: A First-Principles Study. *J. Phys. Chem. C* 2012, *116*, 8778−8791.

(121) Van Cat, V.; Dinh, N. X.; Phan, V. N.; Le, A. T.; Nam, M. H.; Lam, V. D.; van Dang, T.; Van Quy, N. Realization of graphene oxide nanosheets as a potential mass-type gas sensor for detecting NO_2, SO_2, CO, and NH_3. *Mater. Today Commun.* 2020, *25*, 101682.

(122) Hoang, N. D.; Van Cat, V.; Nam, M. H.; Phan, V. N.; Le, A. T.; Van Quy, N. Enhanced SO_2 Sensing Characteristics of Multi-Wall Carbon Nanotubes Based Mass-Type Sensor Using Two-Step Purification Process. *Sens. Actuators, A* 2019, *295*, 696−702.

(123) Wu, Z.; Chen, X.; Zhu, S.; Zhou, Z.; Yao, Y.; Quan, W.; Liu, B. Enhanced Sensitivity of Ammonia Sensor Using Graphene/Polyaniline Nanocomposite. *Sens. Actuators, B* 2013, *178*, 485−493.

(124) Tian, Y.; Yang, H.; Li, J.; Hu, S.; Cao, S.; Ren, W.; Wang, Y. A Comprehensive First-Principle Study of Borophene-Based Nano Gas Sensor with Gold Electrodes. *Front. Phys.* 2022, *17*, 13501.

(125) Anasori, B.; Xie, Y.; Beidaghi, M.; Lu, J.; Hosler, B. C.; Hultman, L.; Kent, P. R. C.; Gogotsi, Y.; Barsoum, M. W. Two-Dimensional, Ordered, Double Transition Metals Carbides (MXenes). *ACS Nano* 2015, *9*, 9507−9516.

(126) Wu, Y.; Li, X.; Zhao, H.; Yao, F.; Cao, J.; Chen, Z.; Huang, X.; Wang, D.; Yang, Q. Recent Advances in Transition Metal Carbides and Nitrides (MXenes): Characteristics, Environmental Remediation and Challenges. *Chem. Eng. J.* 2021, *418*, 129296.

(127) Qin, R.; Shan, G.; Hu, M.; Huang, W. Two-Dimensional Transition Metal Carbides and/or Nitrides (MXenes) and Their Applications in Sensors. *Mater. Today Phys.* 2021, *21*, 100527.

(128) Zhu, Z.; Liu, C.; Jiang, F.; Liu, J.; Ma, X.; Liu, P.; Xu, J.; Wang, L.; Huang, R. Flexible and Lightweight $Ti_3C_2T_x$ MXene@Pd Colloidal Nanoclusters Paper Film as Novel H_2 Sensor. *J. Hazard. Mater.* 2020, *399*, 123054.

(129) Liu, M.; Wang, Z.; Song, P.; Yang, Z.; Wang, Q. In_2O_3 Nanocubes/Ti_3C_2Tx MXene Composites for Enhanced Methanol Gas Sensing Properties at Room Temperature. *Ceram. Int.* 2021, *47*, 23028−23037.

(130) Wang, Y.; Zhou, Y.; Wang, Y. Humidity Activated Ionic-Conduction Formaldehyde Sensing of Reduced Graphene Oxide Decorated Nitrogen-Doped MXene/Titanium Dioxide Composite Film. *Sens. Actuators, B* 2020, *323*, 128695.

(131) Zhang, D.; Mi, Q.; Wang, D.; Li, T. MXene/Co_3O_4 Composite Based Formaldehyde Sensor Driven by ZnO/MXene Nanowire Arrays Piezoelectric Nanogenerator. *Sens. Actuators, B* 2021, *339*, 129923.

(132) Hermawan, A.; Zhang, B.; Taufik, A.; Asakura, Y.; Hasegawa, T.; Zhu, J.; Shi, P.; Yin, S. CuO Nanoparticles/$Ti_3C_2T_x$ MXene Hybrid Nanocomposites for Detection of Toluene Gas. *ACS Appl. Nano Mater.* 2020, *3*, 4755−4766.

(133) Guo, W.; Surya, S. G.; Babar, V.; Ming, F.; Sharma, S.; Alshareef, H. N.; Schwingenschlögl, U.; Salama, K. N. Selective Toluene Detection with Mo_2CT_x MXene at Room Temperature. *ACS Appl. Mater. Interfaces* 2020, *12*, 57218−57227.

(134) Jin, L.; Wu, C.; Wei, K.; He, L.; Gao, H.; Zhang, H.; Zhang, K.; Asiri, A. M.; Alamry, K. A.; Yang, L.; Chu, X. Polymeric $Ti_3C_2T_x$ MXene Composites for Room Temperature Ammonia Sensing. *ACS Appl. Nano Mater.* 2020, *3*, 12071−12079.

(135) Wang, S.; Liu, B.; Duan, Z.; Zhao, Q.; Zhang, Y.; Xie, G.; Jiang, Y.; Li, S.; Tai, H. PANI Nanofibers-Supported Nb_2CT_x Nanosheets-Enabled Selective NH_3 Detection Driven by TENG at Room Temperature. *Sens. Actuators, B* 2021, *327*, 128923.

(136) He, T.; Liu, W.; Lv, T.; Ma, M.; Liu, Z.; Vasiliev, A.; Li, X. MXene/SnO_2 Heterojunction Based Chemical Gas Sensors. *Sens. Actuators, B* 2021, *329*, 129275.

(137) Guo, X.; Ding, Y.; Kuang, D.; Wu, Z.; Sun, X.; Du, B.; Liang, C.; Wu, Y.; Qu, W.; Xiong, L.; He, Y. Enhanced Ammonia Sensing Performance Based on MXene-$Ti_3C_2T_x$ Multilayer Nanoflakes Functionalized by Tungsten Trioxide Nanoparticles. *J. Colloid Interface Sci.* 2021, *595*, 6−14.

(138) Yang, Z.; Jiang, L.; Wang, J.; Liu, F.; He, J.; Liu, A.; Lv, S.; You, R.; Yan, X.; Sun, P.; Wang, C.; Duan, Y.; Lu, G. Flexible Resistive NO_2 Gas Sensor of Three-Dimensional Crumpled MXene $Ti_3C_2T_x$/ZnO Spheres for Room Temperature Application. *Sens. Actuators B* 2021, *326*, 128828.

(139) Zhang, Y.; Jiang, Y.; Duan, Z.; Huang, Q.; Wu, Y.; Liu, B.; Zhao, Q.; Wang, S.; Yuan, Z.; Tai, H. Highly Sensitive and Selective NO_2 Sensor of Alkalized V_2CT_x MXene Driven by Interlayer Swelling. *Sens. Actuators, B* 2021, *344*, 130150.

(140) Qin, R.; Li, X.; Hu, M.; Shan, G.; Seeram, R.; Yin, M. Preparation of High-Performance MXene/PVA-Based Flexible Pressure Sensors with Adjustable Sensitivity and Sensing Range. *Sens. Actuators, A* 2022, *338*, 113458.

(141) Deshmukh, K.; Kovářík, T.; Khadheer Pasha, S. K. State of the Art Recent Progress in Two Dimensional MXenes Based Gas Sensors and Biosensors: A Comprehensive Review. *Coordin. Chem. Rev.* 2020, *424*, 213514.

(142) Ma, Y.; Yue, Y.; Zhang, H.; Cheng, F.; Zhao, W.; Rao, J.; Luo, S.; Wang, J.; Jiang, X.; Liu, Z.; Liu, N.; Gao, Y. 3D Synergistical MXene/Reduced Graphene Oxide Aerogel for a Piezoresistive Sensor. *ACS Nano* 2018, *12*, 3209−3216.

(143) Boota, M.; Anasori, B.; Voigt, C.; Zhao, M.-Q.; Barsoum, M. W.; Gogotsi, Y. Pseudocapacitive Electrodes Produced by Oxidant-Free Polymerization of Pyrrole between the Layers of 2D Titanium Carbide (MXene). *Adv. Mater.* 2016, *28*, 1517−1522.

(144) Lee, E.; VahidMohammadi, A.; Yoon, Y. S.; Beidaghi, M.; Kim, D.-J. Two-Dimensional Vanadium Carbide MXene for Gas Sensors with Ultrahigh Sensitivity Toward Nonpolar Gases. *ACS Sens.* 2019, *4*, 1603−1611.

(145) Kim, S. J.; Koh, H. J.; Ren, C. E.; Kwon, O.; Maleski, K.; Cho, S. Y.; Anasori, B.; Kim, C. K.; Choi, Y. K.; Kim, J.; Gogotsi, Y.; Jung, H. T. Metallic $Ti_3C_2T_x$ MXene Gas Sensors with Ultrahigh Signal-to-Noise Ratio. *ACS Nano* 2018, *12*, 986−993.

(146) Kim, S. J.; Choi, J.; Maleski, K.; Hantanasirisakul, K.; Jung, H. T.; Gogotsi, Y.; Ahn, C. W. Interfacial Assembly of Ultrathin, Functional MXene Films. *ACS Appl. Mater. Interfaces* 2019, *11*, 32320−32327.

(147) Wu, M.; He, M.; Hu, Q.; Wu, Q.; Sun, G.; Xie, L.; Zhang, Z.; Zhu, Z.; Zhou, A. Ti_3C_2 MXene-Based Sensors with High Selectivity for NH_3 Detection at Room Temperature. *ACS Sens.* 2019, *4*, 2763−2770.

(148) Lee, E.; VahidMohammadi, A.; Prorok, B. C.; Yoon, Y. S.; Beidaghi, M.; Kim, D. J. Room Temperature Gas Sensing of Two-Dimensional Titanium Carbide (MXene). *ACS Appl. Mater. Interfaces* 2017, *9*, 37184−37190.

(149) Shuvo, S. N.; Ulloa Gomez, A. M.; Mishra, A.; Chen, W. Y.; Dongare, A. M.; Stanciu, L. A. Sulfur-Doped Titanium Carbide MXenes for Room-Temperature Gas Sensing. *ACS Sens.* 2020, *5*, 2915−2924.

(150) Ma, H.; Xu, Y.; Rong, Z.; Cheng, X.; Gao, S.; Zhang, X.; Zhao, H.; Huo, L. Highly Toluene Sensing Performance Based on Monodispersed Cr_2O_3 Porous Microspheres. *Sens. Actuators, B* 2012, *174*, 325−331.

(151) Lee, S. H.; Eom, W.; Shin, H.; Ambade, R. B.; Bang, J. H.; Kim, H. W.; Han, T. H. Room-Temperature, Highly Durable $Ti_3C_2T_x$ MXene/Graphene Hybrid Fibers for NH_3 Gas Sensing. *ACS Appl. Mater. Interfaces* 2020, *12*, 10434−10442.

(152) Yang, Z.; Liu, A.; Wang, C.; Liu, F.; He, J.; Li, S.; Wang, J.; You, R.; Yan, X.; Sun, P.; Duan, Y.; Lu, G. Improvement of Gas and Humidity Sensing Properties of Organ-like MXene by Alkaline Treatment. *ACS Sens.* 2019, *4*, 1261−1269.

(153) Sun, S.; Wang, M.; Chang, X.; Jiang, Y.; Zhang, D.; Wang, D.; Zhang, Y.; Lei, Y. $W_{18}O_{49}$/$Ti_3C_2T_x$ Mxene Nanocomposites for Highly Sensitive Acetone Gas Sensor with Low Detection Limit. *Sens. Actuators, B* 2020, *304*, 127274.

(154) Zhao, W. N.; Yun, N.; Dai, Z. H.; Li, Y. F. A High-Performance Trace Level Acetone Sensor Using an Indispensable $V_4C_3T_x$ MXene. *RSC Adva.* 2020, *10*, 1261−1270.

(155) Li, H. Y.; Zhao, S. N.; Zang, S. Q.; Li, J. Functional Metal-Organic Frameworks as Effective Sensors of Gases and Volatile Compounds. *Chem. Soc. Rev.* 2020, 49, 6364−6401.

(156) Chen, E. X.; Yang, H.; Zhang, J. Zeolitic Imidazolate Framework as Formaldehyde Gas Sensor. *Inorg. Chem.* 2014, 53, 5411−5413.

(157) Chen, E. X.; Fu, H. R.; Lin, R.; Tan, Y. X.; Zhang, J. Highly Selective and Sensitive Trimethylamine Gas Sensor Based on Cobalt Imidazolate Framework Material. *ACS Appl. Mater. Interfaces* 2014, 6, 22871−22875.

(158) Yuan, H.; Li, N.; Fan, W.; Cai, H.; Zhao, D. Metal-Organic Framework Based Gas Sensors. *Adv. Sci.* 2022, 9, 2104374.

(159) Campbell, M. G.; Sheberla, D.; Liu, S. F.; Swager, T. M.; Dincă, M. Cu$_3$(Hexaiminotriphenylene)$_2$: An Electrically Conductive 2D Metal-Organic Framework for Chemiresistive Sensing. *Angew. Chem. Inter. Ed.* 2015, 54, 4349−4352.

(160) Campbell, M. G.; Liu, S. F.; Swager, T. M.; Dincă, M. Chemiresistive Sensor Arrays from Conductive 2D Metal-Organic Frameworks. *J. Am. Chem. Soc.* 2015, 137, 13780−13783.

(161) Yao, M. S.; Lv, X. J.; Fu, Z. H.; Li, W. H.; Deng, W. H.; Wu, G. D.; Xu, G. Layer-by-Layer Assembled Conductive Metal-Organic Framework Nanofilms for Room-Temperature Chemiresistive Sensing. *Angew. Chem. Inter. Ed.* 2017, 56, 16510−16514.

(162) Smith, M. K.; Jensen, K. E.; Pivak, P. A.; Mirica, K. A. Direct Self-Assembly of Conductive Nanorods of Metal-Organic Frameworks into Chemiresistive Devices on Shrinkable Polymer Films. *Chem. Mater.* 2016, 28, 5264−5268.

(163) Hoppe, B.; Hindricks, K. D. J.; Warwas, D. P.; Schulze, H. A.; Mohmeyer, A.; Pinkvos, T. J.; Zailskas, S.; Krey, M. R.; Belke, C.; König, S.; Fröba, M.; Haug, R. J.; Behrens, P. Graphene-like Metal-Organic Frameworks: Morphology Control, Optimization of Thin Film Electrical Conductivity and Fast Sensing Applications. *CrystEngComm* 2018, 20, 6458−6471.

(164) DMello, M. E.; Sundaram, N. G.; Singh, A.; Singh, A. K.; Kalidindi, S. B. An Amine Functionalized Zirconium Metal-Organic Framework as an Effective Chemiresistive Sensor for Acidic Gases. *Chem. Commun.* 2019, 55, 349−352.

(165) Musho, T.; Wu, N. Ab Initio Calculation of Electronic Charge Mobility in Metal-Organic Frameworks. *Phys. Chem. Chem. Phys.* 2015, 17, 26160−26165.

(166) Allendorf, M. D.; Dong, R.; Feng, X.; Kaskel, S.; Matoga, D.; Stavila, V. Electronic Devices Using Open Framework Materials. *Chem. Rev.* 2020, 120, 8581−8640.

(167) Yao, M. S.; Tang, W. X.; Wang, G. E.; Nath, B.; Xu, G. MOF Thin Film-Coated Metal Oxide Nanowire Array: Significantly Improved Chemiresistor Sensor Performance. *Adv. Mater.* 2016, 28, 5229−5234.

(168) Tian, H.; Fan, H.; Li, M.; Ma, L. Zeolitic Imidazolate Framework Coated ZnO Nanorods as Molecular Sieving to Improve Selectivity of Formaldehyde Gas Sensor. *ACS Sens.* 2016, 1, 243−250.

(169) Drobek, M.; Kim, J.-H.; Bechelany, M.; Vallicari, C.; Julbe, A.; Kim, S. S. MOF-Based Membrane Encapsulated ZnO Nanowires for Enhanced Gas Sensor Selectivity. *ACS Appl. Mater. Interfaces* 2016, 8, 8323−8328.

(170) Wu, X.; Xiong, S.; Mao, Z.; Hu, S.; Long, X. A Designed ZnO@ZIF-8 Core-Shell Nanorod Film as a Gas Sensor with Excellent Selectivity for H$_2$ over CO. *Chem. - Eur. J.* 2017, 23, 7969−7975.

(171) Zhou, T.; Sang, Y.; Wang, X.; Wu, C.; Zeng, D.; Xie, C. Pore Size Dependent Gas-Sensing Selectivity Based on ZnO@ZIF Nanorod Arrays. *Sens. Actuators B* 2018, 258, 1099−1106.

(172) Liu, Y.; Wang, R.; Zhang, T.; Liu, S.; Fei, T. Zeolitic Imidazolate Framework-8 (ZIF-8)-Coated In$_2$O$_3$ Nanofibers as an Efficient Sensing Material for Ppb-Level NO$_2$ Detection. *J. Colloid Interface Sci.* 2019, 541, 249−257.

(173) DMello, M. E.; Sundaram, N. G.; Kalidindi, S. B. Assembly of ZIF-67 Metal-Organic Framework over Tin Oxide Nanoparticles for Synergistic Chemiresistive CO$_2$ Gas Sensing. *Chem. Eur. J.* 2018, 24, 9220−9223.

(174) Ren, G.; Li, Z.; Yang, W.; Faheem, M.; Xing, J.; Zou, X.; Pan, Q.; Zhu, G.; Du, Y. ZnO@ZIF-8 Core-Shell Microspheres for Improved Ethanol Gas Sensing. *Sens. Actuators B: Chemical* 2019, 284, 421−427.

(175) Weber, M.; Kim, J.-H.; Lee, J.-H.; Kim, J.-Y.; Iatsunskyi, I.; Coy, E.; Drobek, M.; Julbe, A.; Bechelany, M.; Kim, S. S. High-Performance Nanowire Hydrogen Sensors by Exploiting the Synergistic Effect of Pd Nanoparticles and Metal-Organic Framework Membranes. *ACS Appl. Mater. Interfaces* 2018, 10, 34765−34773.

(176) Wang, D.; Li, Z.; Zhou, J.; Fang, H.; He, X.; Jena, P.; Zeng, J.-B.; Wang, W.-N. Simultaneous Detection and Removal of Formaldehyde at Room Temperature: Janus Au@ZnO@ZIF-8 Nanoparticles. *Nano-Micro Lett.* 2018, 10, 4.

(177) Wang, P.; Zou, X.; Tan, H.; Wu, S.; Jiang, L.; Zhu, G. Ultrathin ZIF-8 Film Containing Polyoxometalate as an Enhancer for Selective Formaldehyde Sensing. *J. Mater. Chem. C* 2018, 6, 5412−5419.

(178) Travlou, N. A.; Singh, K.; Rodríguez-Castellón, E.; Bandosz, T. J. Cu-BTC MOF-Graphene-Based Hybrid Materials as Low Concentration Ammonia Sensors. *J. Mater. Chem. A* 2015, 3, 11417−11429.

(179) Ko, M.; Aykanat, A.; Smith, M. K.; Mirica, K. A. Drawing Sensors with Ball-Milled Blends of Metal-Organic Frameworks and Graphite. *Sensors* 2017, 17, 2192.

(180) Freund, P.; Senkovska, I.; Kaskel, S. Switchable Conductive MOF-Nanocarbon Composite Coatings as Threshold Sensing Architectures. *ACS Appl. Mater. Interfaces* 2017, 9, 43782−43789.

(181) Freund, P.; Mielewczyk, L.; Rauche, M.; Senkovska, I.; Ehrling, S.; Brunner, E.; Kaskel, S. MIL-53(Al)/Carbon Films for CO$_2$-Sensing at High Pressure. *ACS Sustainable Chem. Eng.* 2019, 7, 4012−4018.

(182) Roztocki, K.; Formalik, F.; Krawczuk, A.; Senkovska, I.; Kuchta, B.; Kaskel, S.; Matoga, D. Collective Breathing in an Eightfold Interpenetrated Metal-Organic Framework: From Mechanistic Understanding towards Threshold Sensing Architectures. *Angew. Chem. Inter. Ed.* 2020, 59, 4491−4497.

(183) Lohse, M. S.; Bein, T. Covalent Organic Frameworks: Structures, Synthesis, and Applications. *Adv. Funct. Mater.* 2018, 28, 1705553.

(184) Medina, D. D.; Sick, T.; Bein, T. Photoactive and Conducting Covalent Organic Frameworks. *Adv. Energy Mater.* 2017, 7, 1700387.

(185) Wang, H.; Zeng, Z.; Xu, P.; Li, L.; Zeng, G.; Xiao, R.; Tang, Z.; Huang, D.; Tang, L.; Lai, C.; Jiang, D.; Liu, Y.; Yi, H.; Qin, L.; Ye, S.; Ren, X.; Tang, W. Recent Progress in Covalent Organic Framework Thin Films: Fabrications, Applications and Perspectives. *Chem. Soc. Rev.* 2019, 48, 488−516.

(186) Sharma, N.; Sharma, N.; Srinivasan, P.; Kumar, S.; Rayappan, J. B. B.; Kailasam, K. Heptazine Based Organic Framework as a Chemiresistive Sensor for Ammonia Detection at Room Temperature. *J. Mater. Chem. A* 2018, 6, 18389−18395.

(187) Meng, Z.; Stolz, R. M.; Mirica, K. A. Two-Dimensional Chemiresistive Covalent Organic Framework with High Intrinsic Conductivity. *J. Am. Chem. Soc.* 2019, 141, 11929−11937.

(188) Lee, E.; Yoon, Y. S.; Kim, D. J. Two-Dimensional Transition Metal Dichalcogenides and Metal Oxide Hybrids for Gas Sensing. *ACS Sens.* 2018, 3, 2045−2060.

(189) Wang, W.; Zhen, Y.; Zhang, J.; Li, Y.; Zhong, H.; Jia, Z.; Xiong, Y.; Xue, Q.; Yan, Y.; Alharbi, N. S.; Hayat, T. SnO$_2$ Nanoparticles-Modified 3D-Multilayer MoS$_2$ Nanosheets for Ammonia Gas Sensing at Room Temperature. *Sens. Actuators, B* 2020, 321, 128471.

(190) Sharma, S.; Kumar, A.; Singh, N.; Kaur, D. Excellent Room Temperature Ammonia Gas Sensing Properties of N-MoS$_2$/p-CuO Heterojunction Nanoworms. *Sens. Actuators, B* 2018, 275, 499−507.

(191) Wang, B.; Yu, J.; Li, X.; Yin, J.; Chen, M. Synthesis and High Formaldehyde Sensing Properties of Quasi Two-Dimensional Mesoporous ZnSnO$_3$ Nanomaterials. *RSC Adv.* 2019, 9, 14809−14816.

(192) Barsan, N.; Weimar, U. Conduction Model of Metal Oxide Gas Sensors. *J. Electroceram.* **2001**, *7*, 143−167.

(193) Wang, L.; Jackman, J. A.; Ng, W. B.; Cho, N. J. Flexible, Graphene-Coated Biocomposite for Highly Sensitive, Real-Time Molecular Detection. *Adv. Funct. Mater.* **2016**, *26*, 8623−8630.

(194) Hashtroudi, H.; Mackinnon, I. D. R.; Shafiei, M. Emerging 2D Hybrid Nanomaterials: Towards Enhanced Sensitive and Selective Conductometric Gas Sensors at Room Temperature. *J. Mater. Chem. C* **2020**, *8*, 13108−13126.